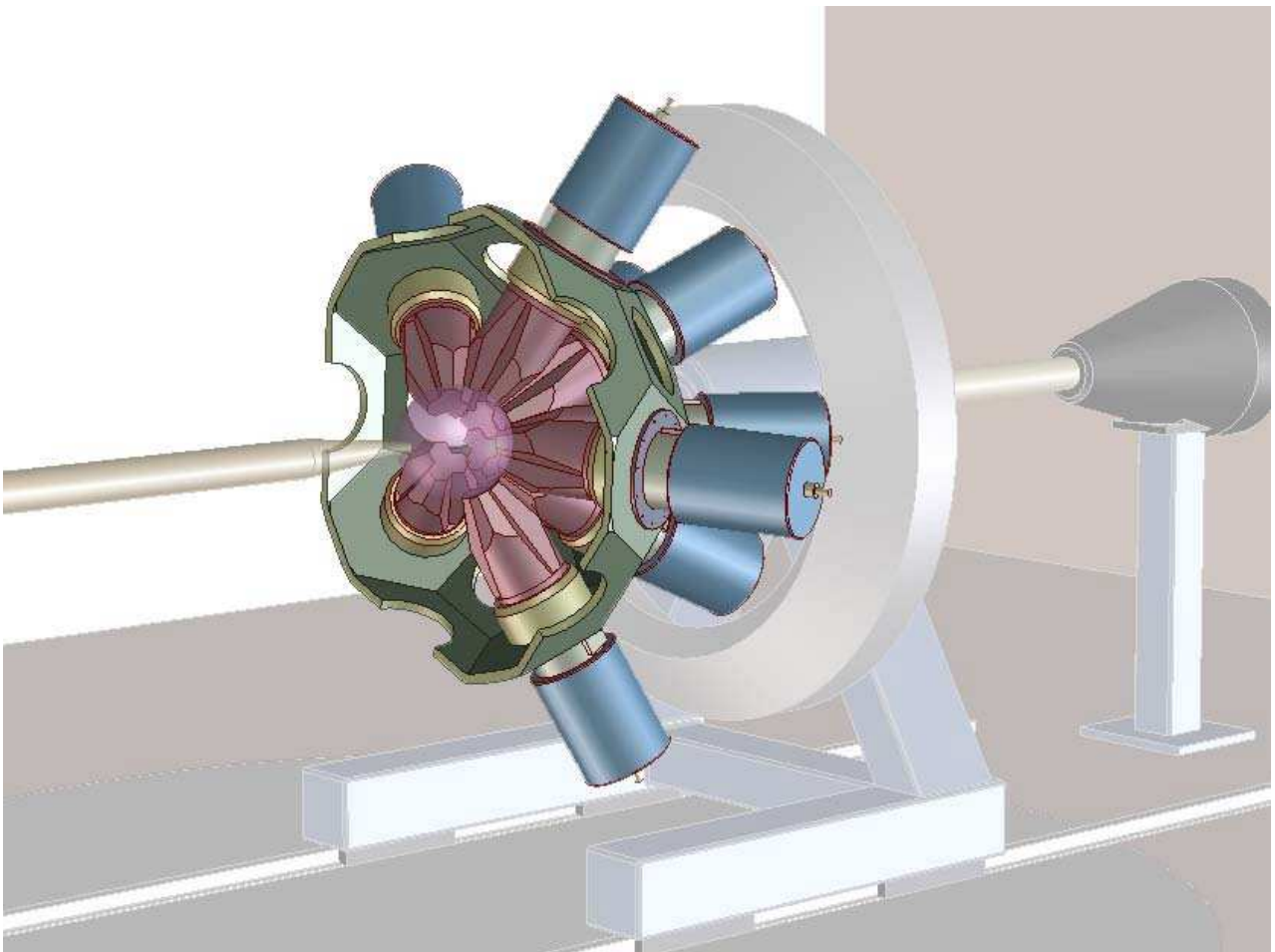# Proposal for Gretina

June 2003

Executive Summary

Gamma-ray detector systems play a key role in a broad range of science and technology. The development of gamma-ray detection systems capable of tracking the location and energy deposition at every gamma-ray interaction point in a detector is a major advance in detector technology. This advance could be of comparable importance to that seen when germanium detectors were first developed four decades ago. The tracking concept will allow construction of gamma-ray detector systems with tremendous improvement in sensitivity and resolution, providing new opportunities for a broad range of science. Such major advances in detector technology, coupled with existing and future facilities, such as RIA, are crucial to further the scientific goals of this nation.

Evidence of the strong support within the community for a new generation of tracking arrays can be found in, for example, (i) the 2002 Long Range Plan for Nuclear Science [LRP02], which identified a 4π γ-ray tracking array as a major initiative for nuclear science, (ii) the Gamma-Ray Tracking Coordinating Committee report of July 2002 [GRTCC02], and (iii) the recent NSAC Facilities Subcommittee.

The present proposal concerns Gretina, which will consist of 30 highly segmented coaxial germanium crystals (10 triple-crystal modules). It will be able to determine the energy (with high-resolution) and position (within 1-2mm) of each gamma-ray interaction point and to track multiple gamma-ray interactions using the energy-angle relationship given by the Compton scattering formula. Gretina will be a unique and extremely powerful detector system, easily surpassing the capabilities of existing detector arrays in many critical areas.

In the 2002 NSAC Long Range Plan for Nuclear Science a number of key themes and questions were selected for special discussion and which outlined future priorities of investigation for our field. They included,

(i) *What are the limits of nuclear existence?*

(ii) *How do weak binding and extreme proton-to-neutron asymmetries affect nuclear properties?*

(iii) *How do the properties of nuclei evolve with changes in proton and neutron number, excitation energy, and angular momentum?*

It is now accepted that a gamma-ray energy tracking detector will be needed to address these questions and to fully capitalize on the science opportunities at existing, and future facilities, such as RIA. Gretina will provide significant gains in sensitivity for a large number of experiments particularly those aimed at nuclei far from beta stability, and will be an important step towards answering these crucial questions in our field.

For example, efforts to improve our understanding of the structure of marginally bound systems near the driplines will face experimental difficulties very different to those encountered before. Tracking detectors are perfectly suited to face these challenges. Many experiments will involve studies in "inverse kinematics", in which beams of exotic nuclei near the dripline produced from fission, fragmentation, or spallation are investigated. In such situations, a highly segmented detector is needed to minimize Doppler effects. In addition, the most interesting nuclei are often those furthest from stability, which are most difficult to produce. Thus, in all cases, the experiments must be as efficient as possible, and be highly selective to clearly differentiate between the states of interest and copious decays from other

sources. Also, the ability to track will result in a greater sensitivity for gamma-gamma angular correlation and polarization measurements, which yield important spin and parity information.
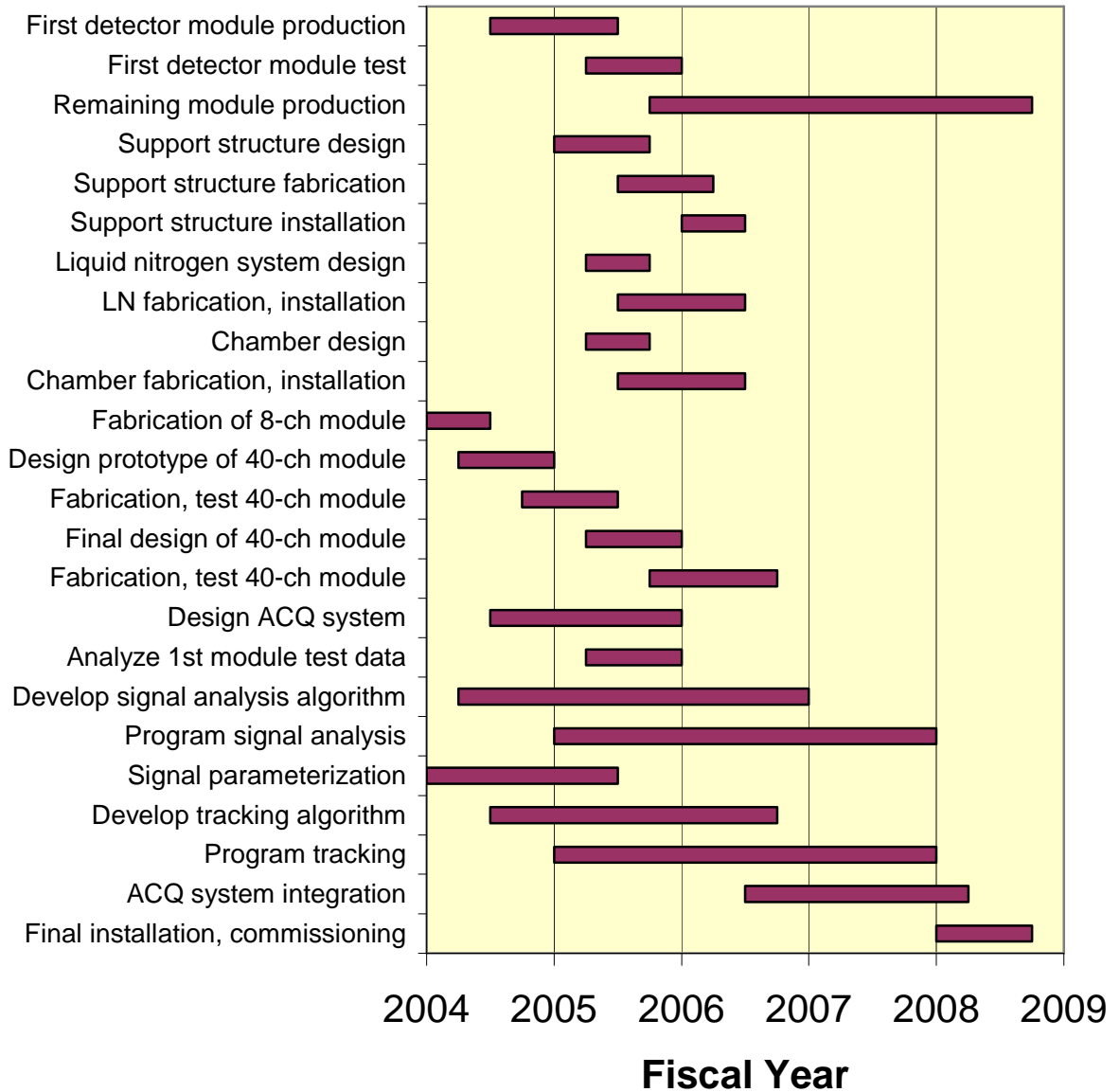
Experiments carried out with Gretina will include studies aimed at understanding many important specific questions fully consistent with those mentioned previously from the NSAC Long Range Plan. For example,

(i)   How does nuclear shell structure evolve in exotic n-rich nuclei, and what are the detailed wave-functions for these nuclei populated using fast rare isotope beams? Here the high efficiency, high resolution, and high segmentation of Gretina, which enables the measurement of photon emission angles of better than 1 degree, will allow huge advances to be made by making possible the detailed study of extremely exotic nuclei.

(ii)   How does the collectivity, and the characteristics of single-particle levels, as well, as pairing correlations, change with particle number using n-rich ISOL beams? Here again the high efficiency, high resolution, and high segmentation of Gretina will be enormously important but so too its very high count rate ability in the hostile radioactive beam environment will pay great dividends in the study of n-rich nuclei.

(iii)   What is the influence on increasing charge on the quantum aspects of nuclear dynamics and structure for the heaviest nuclei? As well as the above mentioned enhanced abilities of Gretina, its compact nature will allow better packing, and thus much higher overall efficiency experiments to be performed with recoil detector charged particle devices for the investigation of very heavy nuclei.

(iv)   What happens to the collective degrees of freedom as the excitation energy and angular momentum increases? Here it is the high segmentation and the order of magnitude improvement in angular resolution, resulting in greatly reduced Doppler broadening, that will give Gretina such an advantage in heavy-ion Coulomb excitation experiments. It will allow the study of odd-A nuclei and transuranic nuclei; all cases of considerable interest where the gamma-ray transition density challenges the resolution of current gamma-ray detectors.

(v)   What are the characteristics of the Giant Dipole Resonances built on superdeformed states and loosely bound nuclei? It is the unique ability of Gretina to combine high resolution at low energies for very selected gating options, with high efficiency at high energies (more than an order of magnitude more than Gammasphere at 15 MeV) to see GDR decays that will allow a new class of experiments to be performed.

A more detailed summary of these advances in physics made possible by Gretina may be found in section 2.3.

Over the past 7 years substantial R&D has been carried out and the technology needed to realize a gamma-ray tracking array has been identified and developed leading to a demonstration of the "proof of principle" in the key areas of (i) detector manufacturing, (ii) signal processing, and (iii) tracking. This extensive R&D has continued and culminated in the recent order for a Gretina module. A Gretina module consists of three germanium crystals, each with 36 segments, in a common cryostat and is the basic building block of the Gretina array.

Table. Optimal schedule for major components of Gretina

	2004	2005	2006	2007	2008	2009
First detector module production						
First detector module test						
Remaining module production						
Support structure design						
Support structure fabrication						
Support structure installation						
Liquid nitrogen system design						
LN fabrication, installation						
Chamber design						
Chamber fabrication, installation						
Fabrication of 8-ch module						
Design prototype of 40-ch module						
Fabrication, test 40-ch module						
Final design of 40-ch module						
Fabrication, test 40-ch module						
Design ACQ system						
Analyze 1st module test data						
Develop signal analysis algorithm						
Program signal analysis						
Signal parameterization						
Develop tracking algorithm						
Program tracking						
ACQ system integration						
Final installation, commissioning						

Fiscal Year

Gretina will be a national instrument, moveable between several major accelerators in the US and available to the entire nuclear science community, in order to capitalize on the broad variety of scientific opportunities this significant detector system can bring. As has proved successful with Gammasphere, the specific order of rotation and duration at any particular laboratory will be decided at the appropriate time by the community of users and funding agencies.

To summarize, it is becoming increasingly clear that segmented germanium detectors and tracking are the future of gamma-ray detection systems. Numerous workshops have been held to discuss the physics opportunities gamma-ray tracking detector systems would bring, as well as technical workshops from which working groups have been formed. The importance of segmented gamma-ray detectors and tracking is further illustrated by the increasing number of projects employing this new technology

around the world. Gretina will allow us to capitalize on a number of unique science opportunities now, and a gamma-ray tracking will be required for a future RIA facility.

Further information on gamma-ray tracking detectors can be found at http://greta.lbl.gov, and at http://www.pas.rochester.edu/~cline/grtcc/grtcc_webpage.htm.

Table of Contents

1. INTRODUCTION

The nucleus is a complex system constructed from *two basic constituents*, protons and neutrons. Like many complex systems it displays remarkably regular and often simple excitation modes. Nuclei concentrate into a single body many types of behavior, almost all of which are found individually in other systems but which, in nuclei, interact with one another. It is this property that makes the nucleus unique. The questions being addressed by nuclear physics reflect major challenges facing many areas of modern science; namely, how do complex systems evolve from basic elements and what governs the emergence of regularity and symmetry? Nuclei, their reactions and their structure, are also central to our understanding of the physical universe. They provide a mechanism for the generation of energy within stars, they impact the evolution of the stars, and their properties play a decisive role in the synthesis of all the elements. The goal to achieve a fundamental understanding of the many-body physics of nuclei that applies equally well in all mass and N-Z regions will require the study of nuclei at the extremes of mass, charge and isospin, as well as angular momentum and temperature. In all these areas gamma-ray spectroscopy detector is an essential tool.

In nuclear physics the typical energy range for gamma radiation is between 0.1 and 20 MeV and over the decades there have been major developments in gamma-ray detector technology that have culminated in the state-of-the-art large multidetector gamma-ray arrays, Gammasphere in the US and Euroball in Europe. The influence of these arrays has been enormous. Gammasphere was the first national gamma-ray facility in the US. It continues to have a profound impact on nuclear structure research, and acts as a focal point for the US and worldwide community. However, today's 4π arrays, with their large volume germanium crystals surrounded by a suppression shield, have pushed this particular detector technology to near its limit and it is apparent that significant further gains in sensitivity will require innovative and new designs.

In this proposal we present the science and technical case for Gretina, which has 30 highly-segmented coaxial germanium crystals and uses the new concept of gamma-ray energy tracking. It will have the capability to determine the energy (with high-resolution) and position (within 1-2mm) of each gamma-ray interaction point and to track multiple gamma-ray interactions using the energy-angle relationship given by the Compton scattering formula. Gretina will supercede the capabilities of many existing state-of-the-art arrays. It's high angular resolution for gamma-ray interactions and the large number of crystals arranged in a compact and close-packed geometry make it a unique and powerful instrument that will greatly enhance our ability to carry out high resolution studies of the most exotic nuclei far from stability.

Over the past 7 years substantial R&D has been carried out, and the technology needed to realize a gamma-ray tracking array has been identified and developed leading to a demonstration of the "proof of principle" in the key areas of (i) detector manufacturing, (ii) signal processing, and (iii) tracking. This extensive R&D has continued and culminated in the recent order for a Gretina module. A Gretina module consists of three germanium crystals, each with 36 segments, in a common cryostat and is the basic building block of Gretina. An 8-channel digital signal processing board has also been fabricated.

---

[1] More generally, electromagnetic radiation is important for a broad range of science; including atomic and molecular physics, nuclear physics, weak-interaction physics, astrophysics, and particle physics among others, and while the energy ranges of interest differ there is a common need to develop new detectors in order to answer the most compelling scientific questions.

It is becoming increasingly clear that segmented germanium detectors and tracking are the future of gamma-ray detection systems. Numerous workshops have been held to discuss the physics opportunities gamma-ray tracking detector systems would bring, as well as technical workshops from which working groups have been formed. The importance of segmented gamma-ray detectors and tracking is also clearly illustrated by the large (and increasing) number of projects employing this new technology around the world. Specifically, the SeGA array of eighteen 32-fold segmented germanium detectors has just been completed and has begun experiments using fast exotic beams at MSU. There is also a major effort in Europe aimed at developing segmented tracking arrays, and there are advanced plans to build a 4π highly segmented germanium shell, called AGATA. Evidence of the strong community support for a new generation of tracking arrays can be found in, for example, (i) the 2002 Long Range Plan for Nuclear Science [LRP02], which identified a 4π γ-ray tracking array as a major initiative for nuclear science, (ii) the Gamma-Ray Tracking Coordinating Committee report of July 2002 [GRTCC02], and (iii) the recent NSAC Facilities Subcommittee report.

The physics opportunities of Gretina will be outlined in more detail in chapter 2. Past achievements and R&D in gamma-ray tracking as well as an overview of worldwide efforts are discussed in chapter 3. Chapter 4 will contain the details of the Gretina design. Chapter 5 contains the management plan, while the project cost, effort, and schedule are given in chapter 6.

2. ADVANCING THE FRONTIERS: PHYSICS AT THE LIMITS WITH GRETINA

In the 2002 NSAC Long Range Plan (LRP) for Nuclear Science [LRP02] a major chapter was devoted to "Atomic Nuclei: Structure and Stability". A number of key themes and questions were selected for special discussion, which outlined future priorities of investigation for our field. These included

(i) *What are the limits of nuclear existence?*
(ii) *How do weak binding and extreme proton-to-neutron asymmetries affect nuclear properties?*
(iii) *How do the properties of nuclei evolve with changes in proton and neutron number, excitation energy, and angular momentum?*

A gamma-ray energy tracking detector will be needed to address these questions and to fully capitalize on the science opportunities at existing facilities as well the proposed Rare Isotope Accelerator, RIA. Gretina will provide a unique and powerful detector system with large gains in sensitivity for a large number of experiments, particularly those aimed at nuclei far from beta stability, and will be an important step towards answering the questions in our field.

The sections below discuss a brief selection from the wide range of physics topics which can be addressed with Gretina at a variety of facilities and illustrate the significant benefits that Gretina and gamma-ray tracking can bring. In addition one should mention that significant interest in this detector system and its related technology is also present in other fields such as astrophysics and fundamental interaction physics [GRTCC02].

2.1. How Do Weak Binding and Extreme Proton-to-Neutron Asymmetries Affect Nuclear Properties? Nuclei Far from Stability

A forefront challenge in nuclear structure physics today is to broaden our understanding of nuclei to encompass the full range of bound systems of protons and neutrons. As we move away from the valley of stability towards the driplines our overall view of the nuclear landscape is improving and the important underlying physics is gradually becoming clearer. However, gamma-ray spectroscopy of the nuclear landscape far from stability is always difficult. Cross-sections for producing the most interesting nuclei are always low and there are many backgrounds. In these hostile environments all approaches that glean new information and all methods to increase efficiency and sensitivity will be useful. In recent years, we have made great progress in moving away from stability towards proton rich nuclei. This has been possible by fusing or fragmenting stable heavy ions and developing sophisticated experimental techniques that can pick out the interesting new isotopes that lie farthest from stability. By these means we can now reach and even pass the proton dripline for many elements. However much important work remains at the proton dripline.

Other major future challenges lie near the neutron dripline. Here, as illustrated in Fig. 2.1, there are several reasons to expect that many features of nuclear structure are quite different from the stable and proton-rich isotopes. Access to nuclei near the neutron dripline will not only enhance our overall picture of nuclear structure, but will provide vital data on nuclei along the r-process nucleosynthesis path, the route through which we believe most heavy elements were synthesized. In the last decade novel experimental techniques have been developed for in-beam gamma-ray measurements with low rare-

isotope beam rates. New techniques developed for fast exotic beams can measure energy levels, transition rates, and absolute occupation numbers with rates as low as a few particles/second. A recent key breakthrough has been the convincing demonstration that important information on n-rich nuclei may be obtained using rare isotope beams of 10^4 particles per second or less using transfer, Coulomb excitation and fusion reactions with gamma-ray spectroscopy. The success of these extremely sensitive techniques bodes well for the future.
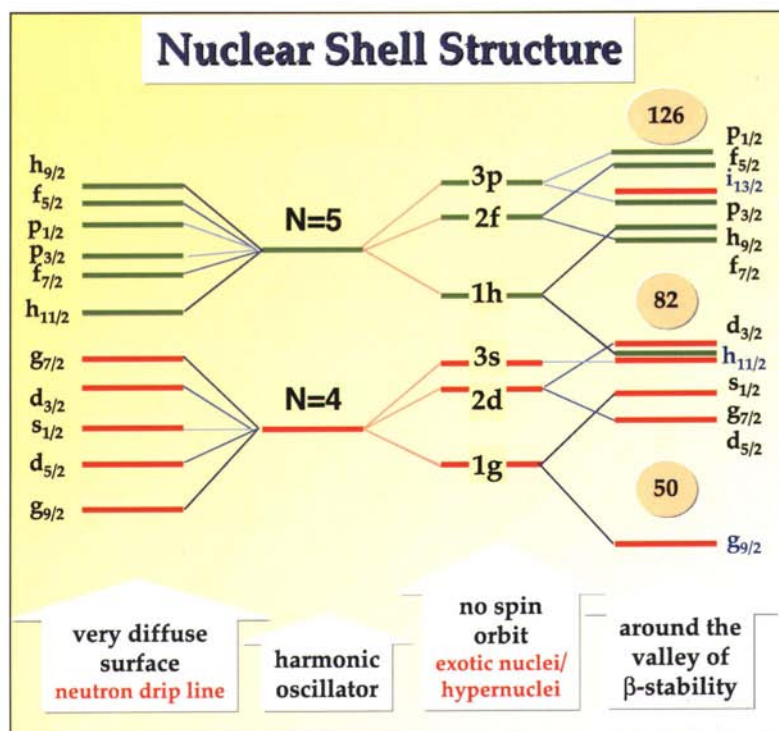
Figure 2.1. Calculated sequences of nuclear single-particle levels for various potentials [Do96]. The levels on the far right correspond to nuclei close to stability; those to the left correspond to a system with a very diffuse surface close to the neutron dripline.

Efforts to improve our understanding of the structure of marginally bound systems near the driplines will focus on obtaining a detailed picture of the wave functions of low-lying states, and the ground states themselves. It is clear that the experimental difficulties will be different to those that have been encountered before. However, there is no doubt that gamma-ray spectroscopy will play a key role in these investigations, and tracking detectors are perfectly suited to face these challenges. Many of the experiments will involve studies in "inverse kinematics", in which a beam of exotic nuclei from near the dripline, produced from fission, fragmentation, or spallation will be utilized. In such situations, a highly segmented detector is needed to minimize Doppler effects. In addition, the most interesting nuclei are often those furthest from stability, which are most difficult to produce. Thus, in all cases, the experiments must be as efficient as possible and be highly selective to clearly differentiate between the states of interest and copious decays from other sources. Also with the ability to track, more sensitive measurements of gamma-gamma angular correlations and polarization, which yield important spin and parity information, become possible.

Some key themes related to studies of far-from-stability nuclei are mentioned below.

2.1.1. Experiments with fast rare Isotope beams

Fast beams of exotic nuclei, typically in the energy range of 30 to 300 MeV/nucleon, are made via the separation of fragmentation products by a combination of magnetic, electric, and energy-loss methods. This technique of projectile fragmentation provides a powerful and universal method of separation by physical means, which is equally applicable to all elements lighter than uranium. The NSCL Coupled Cyclotron Facility presently provides such fast exotic beams reaching the neutron-dripline up to sulfur (Z=16), although ultimately the envisioned Rare Isotope Accelerator will provide experimental access to even more neutron-rich nuclei reaching the neutron-dripline up to Z=40.

Experiments with fast exotic beams using gamma-rays to tag inelastic scattering extend the scientific reach of any fast-beam facility by several orders of magnitude. Experiments with standard luminosities can be carried out with thick secondary targets (order of g/cm^2) and very low incident beam rates (order of particle/s or less). Photons traverse targets with little and known attenuation and with the availability of position-sensitive gamma-ray detectors it has become possible to measure the energies and directions of photons emitted in-flight. This allows the accurate reconstruction of the photon energy in the frame of the moving exotic projectile. Thus Gretina will greatly enhance the scientific reach of any fast-beam rare isotope facility. Several experimental techniques have been developed in the last decade. Coulomb excitation [Gl98] and proton scattering measure transition matrix elements in exotic nuclei in response to electromagnetic and hadronic excitations. In-beam fragmentation reactions populate a variety of excited states [Yo01], and nucleon knockout reactions [Ha01] allow for precision wavefunction spectroscopy through the measurement of cross sections, which can be converted into spectroscopic factors.

The instrument crucial to realizing these physics opportunities is a high solid-angle gamma-ray detector, which can detect photons with energies up to 10 MeV with a resolution of 0.5% or better and which can measure photon-emission angles with an accuracy of better than 1°. Gretina will provide these capabilities needed to understand the evolution of nuclear structure with isospin. Specifically, Gretina will help answer the following questions:

(a) How does nuclear shell structure evolve in n-rich nuclei?

New physics is predicted close to the nuclear driplines, where the binding energies for protons and neutrons become zero. For example, as the outer regions of very neutron-rich nuclei approach pure low-density neutron matter, mean field calculations suggest that the nuclear potentials will diverge from those encountered close to stability (see [Do96]). This could lead to a change in single-particle orbit ordering and shell structure as illustrated for heavy nuclei in Fig. 2.1. In spite of the theoretical excitement, experimental data on the structure of very neutron-rich nuclei, apart from the very lightest ones (Z ≤6), is sparse. The first experimental evidence for a possible reordering of nuclear shells for light neutron-rich nuclei in the $\pi(sd)$-shell has been achieved with the measurements of the disappearance of the *N=8* shell closure in ^{11}Be [Mi83,Na00], the high degree of collectivity in the low lying $\nu(f_{7/2})$ intruder state in N=20 ^{32}Mg [Mo95], the experimental discovery of the weakening of the N=28 shell closure for neutron-rich ^{44}S [Gl97], and the emergence of N=16 as a shell closure near the neutron dripline.

The goal of the proposed research activities is to gain experimental information on isotopic chains of nuclei, including the most exotic nuclei possible, using a set of complementary techniques to provide comprehensive measurements from the proton dripline to the neutron dripline. The results will form the experimental foundation for a detailed theoretical understanding of the evolution of nuclear shell structure. In particular, the structure of exotic nuclei will be investigated via intermediate energy Coulomb excitation to probe the electromagnetic degrees of collectivity, via proton scattering to isolate hadronic degrees of collectivity, with in-beam fragmentation to establish higher-lying states and their spins and parities via angular distribution measurements [Ol03], and we will measure the spectroscopic factors for particular states of interest to investigate their single-particle character.
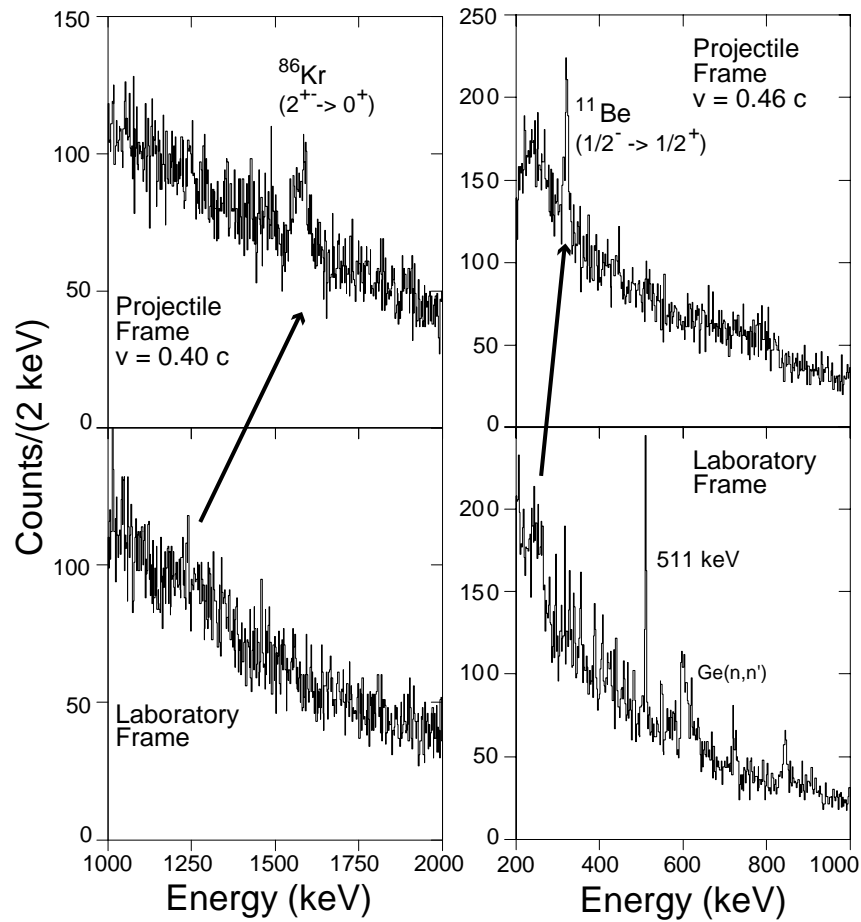
Figure 2.2. Online spectra from SeGA's first in-beam test experiments with a heavy nucleus (^{86}Kr) and a light nucleus (^{11}Be) impinging on a gold target at intermediate beam energies. The bottom panels show the energy spectra as they are measured in the laboratory and the top panels show the same spectra after an event-by-event Doppler-reconstruction has been applied. The gamma-rays from the first excited states to the ground states become visible as peaks.

Intermediate-energy Coulomb excitation experiments have shown that it is possible to measure the excitation energy of the first excited state and the degree of quadrupole collectivity (B(E2↑) value) in a moderately deformed nucleus with secondary beam intensities of as little as 3 particles/seconds in a three day long experiment with the position sensitive NSCL NaI(Tl) detector array [Pr01]. However,

the energy resolution in this detector array is limited to about $\Delta E/E=6\%$, which is insufficient to resolve the fragmented transition strength in odd and odd-odd nuclei. For better energy resolution the SeGA array of 18 highly-segmented germanium detectors can be used. Energy spectra measured in commissioning experiments on light and heavy secondary beams are shown in figure 2.2. SeGA can run in different configurations and has a photopeak efficiency of 2% (at 1.3 MeV) for an angular uncertainty of 0.6^o. Gretina will have nearly 4 times greater efficiency for similar angular resolution. For a recoil velocity of v/c=0.5, this angular resolution will give an average energy resolution $\Delta E/E=0.7\%$ for the 30 Gretina detectors mounted around 0°. This will enable us to measure transition matrix elements in odd nuclei, which are more sensitive to changes in single-particle states than their even-even neighbors.

Gretina will be used to study the evolution of nuclear shell structure in the $\pi(fp)$-shell via intermediate-energy Coulomb excitation. In particular, we will fragment primary beams of ^{64}Ni, ^{70}Zn, ^{76}Ge, and ^{86}Kr to study isotopic chains of nuclei out to, for example, ^{60}Cr, ^{68}Fe, ^{74}Ni, and ^{78}Zn. The low predicted secondary beam rates in these experiments and the lower expected excitation energies and higher level densities compared to the $\pi(sd)$-shell necessitate the use of a very efficient, high-resolution device such as Gretina.

(b) What is the detailed wave function for exotic nuclei?

The properties of a quantal system are fully described by means of its wave function. However, direct measurements of wave functions cannot be made easily. The measurement of the momentum distribution of particles from knock-out reactions is one of the techniques that can be used to determine the wave function in the momentum representation. This method was introduced in nuclear physics to measure proton wave functions via the *(p,2p)* reaction and then was widely applied in atomic physics to map the electron wave function in atomic and molecular systems. Recently the technique has been applied in nuclear physics to determine the momentum distribution of the valence neutron(s) in halo nuclei. Halo nuclei are unique in that the one or two valence neutrons are much less tightly bound compared with "normal" nuclei and their wave functions extend out to large distances. The experiments, using beam break-up reactions, have been applied to single-neutron halo nuclei such as ^{11,12}Be, ^{14}B and ^{15}C [Au00,Na00], neutron-rich carbon isotopes [Ma01], nuclei in the vicinity of *N*=20 [En02], and proton-rich nickel isotopes [Mi03]. An illustration of the method is shown in Fig 2.3. Although very useful, momentum measurements alone cannot determine all the components of the valence-nucleon wave function. The complex parentage of the neutron wave function leaves the residual nucleus in a variety of excited states which require a high-resolution gamma-ray detector to identify and classify them from their gamma decay. With the currently available NaI arrays it is not possible to resolve the complex energy spectra resulting from the knockout of deeply bound nucleons. The SeGA array does not have enough efficiency to reliably extract feeding to excited states. Gretina will have the ability to measure spectroscopic factors for specific excited states, complementing the measurements of ground state spectroscopic factors possible with current detectors.

The superior energy resolution and position sensitivity of Gretina will be used to extend the measurement of spectroscopic factors for specific excited states in exotic medium-mass nuclei (A=40-80). By combining the radioactive beams and the S800 spectrometer at the NSCL with Gretina the evolution of single-particle parentage will be studied in exotic nuclei. The nature of the neutron single-particle structure of exotic nuclei is vital for the determination of the actual location of the neutron drip-line. In addition, single-particle ground-state structures will be measured for nuclei which lie on the

astrophysical r-process path. This information will provide important benchmarks for the theoretical description of r-process nuclei.
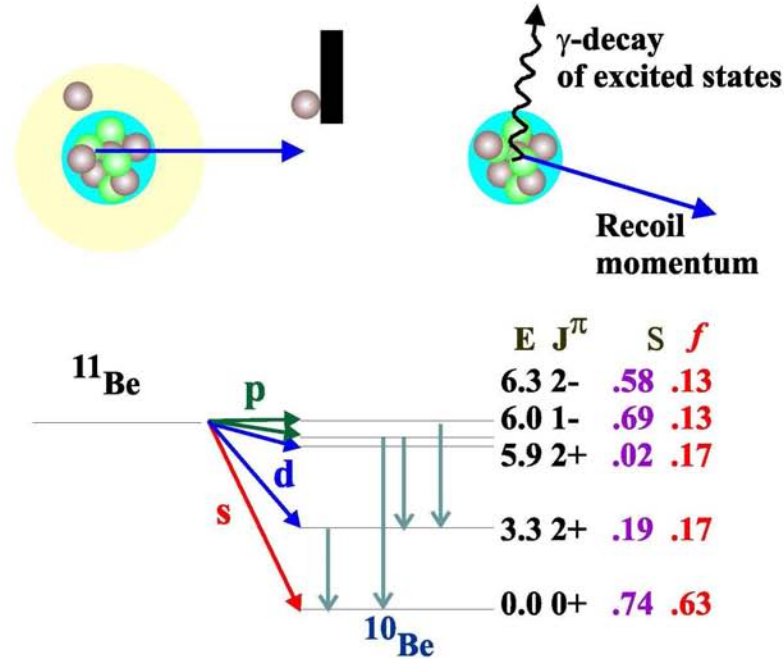
Figure 2.3 The momentum wave function of the halo neutron in ^{11}Be is measured using break-up reactions. The recoil moment of 11Be is measured in coincidence with gamma rays from excited states which represent different parentages of neutron wave functions (i.e. s, p, and d orbitals).

(c) How do nuclear properties evolve with spin in n-rich nuclei

As was discussed in previous sections, low spin properties of n-rich nuclei are providing new insights into nuclei near the neutron drip-line. These nuclei were produced via fragmentation reactions, and studied using Coulomb excitation, knockout reactions, and beta-decays. These methods only propulate nuclei at low spin states. Higher spin states can provide additional important information on the physics of n-rich nuclei. For example, in even-even collective nuclei, the ratio of the 4^+ to the 2^+ energy, R_{42}, gives a clear indication of whether the nuclei are rotational (R_{42}=3.33), or vibrational (R_{42}=2). In nuclei near closed shells the energy of the multiplets arising from two-particle coupling gives a measure of the strength of residual reactions. One of the most interesting properties of nuclei near the neutron drip-line is whether the extended neutron distribution could produce new collective modes in which the protons and neutrons exhibit different motions. For example, if the neutron halo rotates, but the core of protons and neutrons makes no contribution, the evolution of such rotation as a function of spin will give important information on the rotational properties of pure neutron matter.

It has been demonstrated recently that fragmentation reactions produce fragments with a spin as high as 10ħ and in-beam spectroscopy studies have been carried out successfully on nuclei produced with a rate as low as one per second. Obviously, the most n-rich nuclei that can be studied in these experiments were limited by the sensitivity of the gamma-ray detector array. Gretina will provide far better Doppler correction and thus the detector can be placed closer to the target to produce a higher efficiency, allowing nuclei closer to the neutron drip-line to be studied. The high efficiency of Gretina for high-

energy gamma rays is equally important because relatively light nuclei are produced near the neutron drip-line and these nuclei have larger level spacing.

2.1.2. Experiments with ISOL beams

Isotope Separation Online (ISOL) radioactive ion beams also are opening exciting possibilities for a wide range of new spectroscopic studies, including B(E2) measurements through Coulomb excitation in inverse kinematics, gamma-ray spectroscopy following fusion-evaporation reactions, and neutron- and proton-transfer reactions to investigate single-particle states. As for experiments utilizing fast beams, these experiments, involve significant technical and experimental challenges but every possible solution involves the need for a high efficiency, highly segmented Ge array such as Gretina. For example, many experiments involve heavy beams and light targets to produce excited nuclei with high recoil velocities, typically ~0.07c. This generates significant Doppler broadening for gamma-rays, an effect ameliorated by good angular resolution, i.e. segmentation, in the detection system.

(a) How does collectivity change with proton and neutron number?

An important aspect in the understanding of the structure of nuclei far from stability is the evolution of collectivity with proton and neutron number. Of particular interest is the nature of low lying vibrational states near closed shell nuclei. Consider, for example, the recent measurements of B(E2)'s in Te and Sn isotopes around ^{132}Sn. Extracted values for the B(E2) of Te isotopes, and preliminary values for Sn isotopes, are displayed in figure 2.4 together with the B(E2) systematics for this mass region. These results [Ra02] provided a major surprise since the B(E2) value for ^{136}Te was expected to conform to the symmetry around neutron number N=82 exhibited by Ba, Ce and other heavier nuclei, and thus be similar to the value for ^{132}Te. Instead, the ^{136}Te value is almost a factor of two smaller. This unexpected behavior can be associated with a decrease in neutron pairing as one crosses N=82 [Te02], which in turn lowers the neutron quasiparticle energies. As a result the energy of the lowest 2^+ state decreases while the increasing neutron amplitude in the wave functions reduces the B(E2) strength, which is dominated by the proton contribution.

In these Coulomb excitation experiments, the high 2^+ energies and low B(E2) values yield low cross sections for excitation, which in combination with the low intensity beams (~10^5 –10^6 /sec) make these types of measurements challenging. There is much for us to learn as we move towards more neutron rich nuclei. In fact measurements of the ^{132,134}Sn isotopes are currently being performed but with a BaF_2 array of gamma detectors to improve the efficiency for high energy (~4 MeV) gamma-rays. Such experiments performed with a high resolution, high efficiency gamma-ray array such as Gretina will have much greater discovery potential and will ultimately lead to new insights and opportunities in the Coulomb excitation of rare isotope beams.
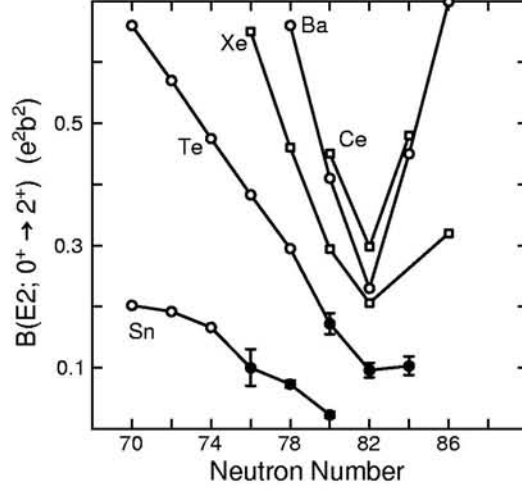
Figure 2.4 Values of B(E2;0+ - 2+1) for even-even Sn, Te, Xe, Ba and Ce isotopes around neutron number N=82. Open symbols are adopted values from Ref.[Ra01] while filled symbols are [Ra02]

(b) How do single-particle levels and pairing correlations change far from stability?

Single-particle and pairing degrees of freedom play a central role in nuclear structure. While single-nucleon transfer reactions are the most direct and unambiguous probe of single-particle structure, pair transfer is a direct and unambiguous probe of pairing correlations. Shell structure in nuclei is expected to change dramatically when approaching the extremes of isospin far from stability. This should be manifested by large changes in single-nucleon and pair transfer cross sections to individual nuclear states. For example, the valence single particle orbitals will be different in nuclei at extreme isospin, and these orbitals can be probed by studying single-nucleon transfer reactions with rare isotope beams. Similarly, extreme neutron-rich nuclei should exhibit unusual neutron pairing behavior in the tail of the nuclear wavefunction that will lead to fascinating nuclear Josephson effects such as strongly enhanced pair transfer cross sections and diabolical pair transfer.

Gretina used in conjunction with scattered ion detection will provide the sensitivity to measure the transfer angular momentum and spectroscopic factors to individual states in nuclei both far from stability as well as to closely spaced states at higher excitation energy in deformed nuclei or in very heavy nuclei where standard particle spectroscopy techniques do not provide enough resolution. Studies of transfer using heavy ions can simultaneously probe the interplay of single-particle, pairing, and collective degrees of freedom.

As an illustration of these experiments figure 2.5 shows gamma-ray spectra from a series of recent neutron transfer reactions ^{9}Be(^{134}Te, ^{8}Be) ^{135}Te and ^{13}C(^{134}Te, ^{12}C)^{135}Te in inverse kinematics. The lower half shows the spectrum using the Clarion array from the ^{nat}Be target, gated by pairs of alpha-particles, and the upper half shows the similar spectrum gated by carbon ions from the ^{13}C target. Transitions from the previously-assigned [Ho89] single-neutron states at 659, 1084 and 1127 keV ($p_{3/2}$, $p_{1/2}$ and $f_{5/2}$, respectively) are clearly visible in the Be spectrum. Also visible are the 11/2⁻ state at 1180 keV, and several new transitions, such as the 1400 keV peak. The C spectrum has very few counts, but

the $p_{3/2}$ state is clearly populated, and probably also the $p_{1/2}$ and $11/2^-$ states. Inelastic excitation to the 2^+ and proton stripping to [133]Te are the dominant contaminants.

Obviously Gretina with its high efficiency, high resolution, and high segmentation provides the next step in gamma-ray detection for use in this class of experiments.
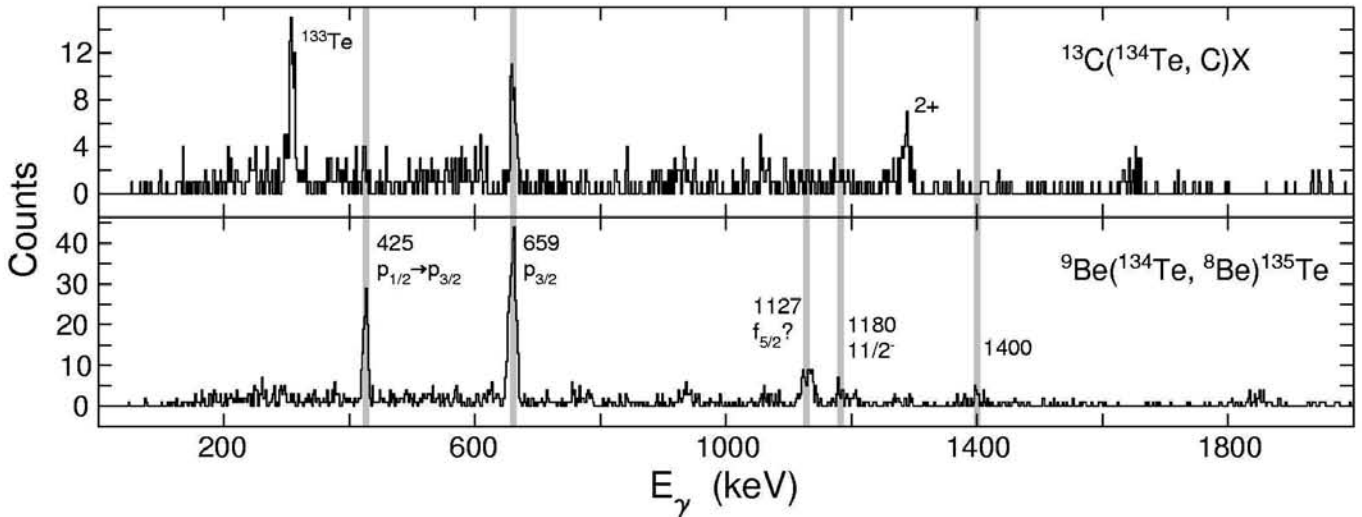
Figure 2.5 Gamma-ray spectra from the neutron transfer experiment with [134]Te on natBe and ^{13}C targets. The spectra are gated by coincidence with alpha-particle pairs (Be target, lower part) or carbon ions (^{13}C target, upper part) detected in the HyBall array.

2.2. How Do the Properties of Nuclei Evolve with Changes in Proton and Neutron Number, Excitation Energy, and Angular Momentum? Some Experiments with Stable Beams

In-beam experiments using Coulomb excitation, transfer reactions, strongly-damped reactions, and fusion evaporation reactions at beam energies close to the Coulomb barrier have played an important role in the development of nuclear structure. In this energy domain the recoil velocities typically range from v/c= 5 to 10%. This limits the gamma-ray energy resolution for recoiling ions to $\geq 1\%$ due to the finite solid angle of individual gamma-ray detectors for modern gamma-ray arrays such as Gammasphere. Use of thick targets to stop the recoils does improve the energy resolution for the lowest states that have lifetimes exceeding the stopping time; but it results in badly Doppler-broadened line shapes for shorter-lived states. Use of thin targets is necessary to observe the recoiling ions in coincidence with de-excitation gamma-rays to study higher angular momentum states as well as to measure the impact parameter dependence and accurate cross sections, both of which are crucial to determine electromagnetic or transfer matrix elements. The order of magnitude improvement in angular resolution provided by Gretina will lead to a reduction in Doppler broadening giving improved gamma-ray energy resolution for thin target experiments. Gretina will have a factor of about eight improvement in resolving power relative to Gammasphere for lower multiplicity processes, such as Coulomb excitation and transfer reactions. The improved energy resolution will greatly expand the opportunities

for advancing nuclear structure studies to higher spin, heavier mass, and to odd-A nuclei; all cases where the density of gamma-ray transitions exceeds the energy resolution achieved using present day gamma-ray detectors for in-beam spectroscopy. Gretina marks the next step for this field of study and opens new avenues of study at stable beam facilities. Some of these opportunities are mentioned below.

2.2.1. What new information can we learn about collective shape degrees of freedom in nuclei?

Collective rotational and vibrational shape degrees of freedom are a dominant and ubiquitous feature of nuclear structure. Studies of coexistence of states with very different collectivity in individual nuclei as well as the evolution of collective correlations with isospin and temperature are required to better understand the role of collective correlations in nuclear structure. Coulomb excitation is the preeminent probe of collective shape degrees of freedom in that it selectively populates collective states with cross sections that are a direct measure of the collective matrix elements. The efficiency and resolving power of Gretina, when coupled with detection of scattered heavy ions, provides the opportunity to measure both the excitation energies and collective matrix elements coupling these states.

The completeness of such data adds a new dimension to the study of quadrupole and octupole collective shapes degrees of freedom in nuclei. For example, one can directly measure the magnitude and distribution widths for both quadrupole deformation and triaxiality. The far superior resolving power and efficiency provided by Gretina will make it feasible to study collective modes in odd-A nuclei, transuranic nuclei, as well as at higher excitation energies, all cases where the gamma-ray transition density challenges the energy resolution of current gamma-ray detectors. Studies of odd-A nuclei are especially sensitive probes of nuclear structure. Unfortunately, the gamma-ray transition density becomes very large in heavy odd-A nuclei; for example, ~300 gamma-ray peaks were observed in the energy range 150-1700 keV in ^{235}U. The resolution of Gretina is crucial to extract the physics from studies of such odd-A nuclei.

2.2.2. Do unusual configurations coexist at low excitation energy in nuclear structure?

A small proportion of nuclei exhibit highly-excited metastable (isomeric) states coexisting at low excitation energy. Isomeric states in nuclei have unique and unusual properties that can provide new insights into nuclear shell structure and nuclear shapes. Three classes of isomers are observed, shape isomers, spin isomers, and K isomers. In contrast to shape isomers, which are due to a large change in deformation as seen in fission isomerism, spin and K isomers result from the angular momentum coupling of a few valence nucleons. Studies of collective bands based on isomeric states are of considerable interest in order to investigate the breakdown of approximate symmetries with increasing angular momentum. A recent breakthrough has been the observation and identification of the Coulomb excitation paths populating collective bands based on several K-isomers in ^{178}Hf including the 31 year half life K=16$^+$ isomer. The much improved energy resolution plus higher efficiency of Gretina will provide opportunities to greatly exploit isomeric states to probe nuclear structure in both stable and exotic nuclei.

2.2.3. What is the influence of increasing charge on the quantum aspects of nuclear dynamics and structure?

Exploring the structure and properties of nuclei in the region above Z~100 has just begun and our long term goal is to understand these nuclei as well as we understand those closer to stability. These heavy nuclei would fission instantly if it were not for the stabilizing effects of nuclear shell structure. By studying both the decays of nuclei collected at the focal plane of a high efficiency separator and the prompt gamma-ray decays emitted at the production target it will be possible to obtain important information on the excited states in these nuclei. These studies enable us to identify and place single-particle levels, to determine the nuclear deformation, and study the reaction dynamics, all of which are needed to further test the models which calculate where the most stable super-heavy elements should exist. Gretina can play a significant role in these investigating due its physical compactness, high efficiency, high count rate capability, and segmentation properties.

The compact size of the Gretina array and the geometry of the detectors allows the target position to be placed very close to the entrance to the first focusing element of the recoil separator, with a corresponding large improvement in the transmission efficiency of the separator. For example, the ideal target position for the Argonne FMA is ~30 cm from the entrance to the FMA. However when used in conjunction with Gammasphere, the target to FMA distance must be increased to ~90 cm. With Gretina the closer optimal target position could be utilized, which will greatly benefit the study of high-spin structures of some of the heaviest elements, particularly ^{254}No and surrounding nuclei [Re99, Bu02, He02, Le99]. Overall the increased transmission and the higher count rate capability of Gretina will give about an order of magnitude increase in sensitivity over Gammasphere plus the FMA, and coupling Gretina with a gas filled separator can give a factor of 30 improvement.

Such gains can be extremely significant when one considers the very low cross sections involved in these experiments and will extend their reach in studying odd-A nuclei, such as ^{255}Lr, which are important for extracting the correct placement of single particle orbitals at these high particle numbers. Measuring the lifetimes of nuclear levels provides a very sensitive probe and test of nuclear models. The Gretina array, with excellent position resolution, excellent energy resolution, excellent peak-to-total, and with high detection efficiency will be an ideal spectrometer for precision lifetime measurements using Doppler shift techniques. Lifetime measurements in very weakly populated nuclear species either very far from stability or in very heavy nuclei will be possible by selecting gamma-rays in coincidence with recoils at the focal plane, possibly tagged by their subsequent alpha, proton, or beta-decay.

2.2.4. What are the characteristics of the Giant Dipole Resonances built on superdeformed states and loosely bound nuclei?

Giant Resonances are fundamental collective excitations of nuclei and they play an important role in the understanding of basic nuclear structure properties. The gamma-ray decay of the giant dipole resonance for example is sensitive to the size and shape of nuclei. It would be very exciting to discover and study the giant dipole resonance built on a superdeformed shape. The N and Z dependence of giant resonances is predicted to change dramatically near the neutron dripline and can be studied with Coulomb excitation of fast beams from rare isotope accelerators. The large Doppler broadening due to the high-energy

beams requires the excellent position resolution available with Gretina. These two physics examples are discussed in more detail below.

Giant resonances in superdeformed nuclei: A very interesting experiment would be to find the giant dipole resonance (GDR) built on a superdeformed nucleus [Ca98]. To do this, one could select the rotational transitions in a superdeformed band and look for the (preceding) GDR decays, which in this case should consist of two peaks, corresponding to oscillations along the two different-length nuclear radii. Gretina combines excellent energy resolution at low energy with high efficiency at high energy (more than an order of magnitude greater than Gammasphere at 15 MeV). Because of the large deformation, these two peaks would be widely separated in energy, the lower of which might well fall below 10 MeV for nuclei in the mass-150 region. The intensity of the two peaks will give the shape of the superdeformed nucleus, and the width of each peak is related to the damping of the GDR. It might be possible to find fine structure on the low-energy side of the lower peak and thereby learn about the damping mechanism of giant resonances.

Giant resonances in neutron-rich nuclei: Neutron-rich nuclei obtained from primary beam fragmentation are ideal to study the population and decay of giant resonances (GRs) [Au99,Va99]. To excite GRs with appreciable cross section, a beam energy greater than 100 MeV/A (v/c > 0.4) is required. Here the Doppler broadening is an even more serious problem than in the Coulomb-excitation experiments. The excitation energy and shape of the GR is expected to change dramatically near the drip-line. This will give us a chance to study the N and Z dependence of the properties of GRs, while traditional studies are limited to the mass dependence along the line of stability.

In many nuclei the isoscalar giant quadrupole resonance has a fine structure on the low-energy side which could contain information on its damping into the single-particle states. This can be studied by looking at gamma-ray decays to the ground state and low-lying isoscalar surface vibrational states (e.g., 3^- states). Such a study involves detecting a high-energy gamma-ray from the GR in coincidence with the cascade gamma-ray from low-lying states. Currently, due to poor energy resolution, these types of study are limited to closed shell nuclei (e.g., ^{208}Pb) with widely spaced excited states [Be89].

In heavy nuclei, the giant resonances decay almost entirely by evaporation of one neutron followed by γ decay of the low-lying states in the nucleus with one less neutron. These gamma rays can be used to tag the decay pathways of the GR. They also provide a unique method to study the structure of the populated low-lying states, which can be in very exotic nuclei produced with both stable and radioactive beams. In addition Gretina could be partnered with a BaF_2 array to create an even more versatile device for studying giant resonances.

2.3. Summary and Selected Physics Highlights

Experiments carried out with Gretina will include studies aimed at understanding many important specific questions, for example,

(i) How does nuclear shell structure evolve in exotic n-rich nuclei, and what are the detailed wave-functions for these nuclei populated using fast rare isotope beams? Here the high efficiency, high resolution, and high segmentation of Gretina, which enables the measurement of

photon emission angles of better than 1°, will allow huge advances to be made by making possible the detailed study of extremely exotic nuclei.

For example, it will allow the study, for the first time of the evolution of nuclear shell structure in the proton (fp)-shell via intermediate-energy Coulomb excitation. These experiments will give data for determining the new magic numbers of neutron-rich nuclei, from the study of nuclei such as ^{60}Cr, ^{68}Fe, ^{74}Ni, and ^{78}Zn. This will provide a better understanding of the nuclear force, especially the neutron-proton interaction between orbitals with large energy separation.

(ii) How does the collectivity, and the characteristics of single-particle levels, as well as pairing correlations, change with particle number using n-rich ISOL beams? Here again the high efficiency, high resolution, and high segmentation of Gretina will be enormously important but also its very high count rate ability in the hostile radioactive beam environment will pay great dividends.

For example, unexpected behavior was observed from the recent measurements of B(E2)'s in Te and Sn isotopes around ^{132}Sn. This was interpreted as a decrease in neutron pairing as one crosses the N=82 shell, which in turn lowers the neutron quasi-particle energies. As a result the energy of the lowest 2^+ state decreases while the increasing neutron amplitude in the wave functions reduces the B(E2) strength. Gretina will extend these study to regions further away from the lines of stability, and to other regions of closed-shell nuclei. These studies can give unique information on the separate contribution of protons and neutrons to the nuclear collectivity, which cannot be obtained from nuclei close to the valley of stability.

(iii) What is the influence on increasing charge on the quantum aspects of nuclear dynamics and structure for the heaviest nuclei? As well as the above mentioned enhanced abilities of Gretina, its compact nature will allow better packing, and thus much higher overall efficiency experiments to be performed with recoil detector charged particle devices.

Such gains can be extremely significant when one considers the very low cross sections involved in these experiments and will extend their reach to the study of odd-A nuclei, such as ^{255}Lr, which are important for extracting the correct placement of single particle orbitals at these high particle numbers. In addition Gretina will make possible measurements of the lifetimes of nuclear levels which will provide a very sensitive determination of the nuclear deformation. This information is very important for an accurate description of heavy nuclei. Especially, these measurements are crucial for better predictions of the shell structure of super heavy nuclei.

(iv) How do the collective degrees of freedom and shell structure evolve as the excitation energy and angular momentum increases? Studies of the evolution of collectivity and shell structure with spin and excitation energy play a key role in probing the underlying structure of nuclei. The high segmentation, plus the great reduction in Doppler broadening due to the order of magnitude improvement in angular resolution, are the crucial technical advances for addressing such studies.

The far superior resolving power provided by Gretina in heavy-ion Coulomb excitation studies will make it feasible to greatly extend the investigation of collective modes and shell structure, as well as to

the study of odd-A nuclei and transuranic nuclei; all cases of considerable interest where the gamma-ray transition density challenges the energy resolution of current gamma-ray detectors.

(v) What are the characteristics of the Giant Dipole Resonances built on superdeformed states and loosely bound nuclei? It is the unique ability of Gretina to combine high resolution at low energies for very selected gating options, with high efficiency at high energies (more than an order of magnitude more than Gammasphere at 15 MeV) to observe GDR decays that will allow a new class of experiments to be performed.

For example, it is expected, due to the large deformation, that the two GDR peaks built on SD states would be widely separated in energy, the lower of which might well fall below 10 MeV for nuclei in the mass-150 region. The energy and intensity of the two peaks will give the shape of the superdeformed nucleus, and the width of each peak is related to the damping of the GDR. Gretina will have the unique ability to resolve the possible fine structure on the low-energy side of the lower peak and thereby provide a better understanding of the damping mechanism of giant resonances. It will thus open up a whole new avenue of study in nuclei at high temperature.

3. TECHNICAL DEVELOPMENTS

The current generation of 4π gamma-ray detector arrays, for example Gammasphere, are based on modules of Compton suppressed Ge detectors. They use high-purity Ge crystals, which have intrinsically good energy resolution. Although the largest available crystals are used most of the gamma rays do not deposit all their energy in a single crystal. Such partial-energy events contribute to a background, which can be rejected by detecting the gamma rays that scatter out of the Ge crystal into a "Compton shield" (made with a high density scintillator such as BGO) surrounding the Ge detector. While this improves the peak-to-total ratio it does not improve the efficiency. Furthermore, the suppressors occupy about the same solid angle coverage as the germanium detectors. This limits the full-energy peak efficiency in Gammasphere, for example, to 10% (at 1 MeV) and the peak-to-total ratio is 60%. To explore new scientific regions, as identified in the 2002 Long Range Plan for Nuclear Science and discussed in Chapter 2, new technologies and capabilities are required that go beyond those provided by arrays of Compton-suppressed detectors.

The efficiency limit reached in current arrays can be overcome by eliminating the Compton shields and by closely packing the Ge crystals. Rather than suppressing events that scatter out of individual crystals, the gamma rays can be tracked across crystal boundaries by determining the location of the scattering points (a 1 MeV gamma ray has typically 3 to 4 interactions within the Ge before depositing its full energy). This can be achieved by using the new technology of highly segmented Ge detectors (Fig 3.1). These detectors have their outer electrical contact divided into a number of individual segments. By analyzing the direct and induced charges from these segments the interaction locations of gamma-rays can be determined to better than a few millimeters. The pathways through the crystals can then be followed and the gamma-ray energies reconstructed by using suitable algorithms. This is the new concept underpinning a gamma-ray energy tracking array, such as Gretina.

To date considerable progress has been made towards the R&D necessary to design and build a tracking array. This includes 1) the manufacture of segmented detectors and pre-amplifiers that can provide high quality signals needed to resolve and locate individual interaction points, 2) the use of signal processing methods to determine energy, time, and position based on pulse shape digitization and digital signal processing, 3) the development of a tracking algorithm that uses the energy and position information to identify interaction points belonging to a particular gamma ray, and 4) the design and packing schemes for a close-packed array of segmented coaxial germanium detectors.

In this section we present an overview of the technical developments that demonstrate the "proof-of-principle" for the gamma-ray tracking concept, and which include results from measurements and simulations, primarily carried out on the 36 segment Ge detector (the Gretina single-detector prototype), as well as R&D in the areas of computation and electronics. Many of these results are given in more detail in [De99, Ku02, Sc99a, Sc99b, Ve00a, Ve00b]. A summary of the developments and achievements is given in section 3.9.

3.1. Prototype Detector

The ability to manufacture coaxial Ge detectors with a high degree of two-dimensional segmentation is an essential component of the technology of a gamma-ray tracking array. Two two-dimensionally

segmented closed-ended HPGe detectors have been built by Eurisys Mesures and tested at LBNL. Both detectors have a regular hexagonal shape and are tapered by 10º. They are 9 cm long with a maximum diameter of 7 cm at the back. The first prototype was 12-fold segmented (6 azimuthal x 2 longitudinal) and the second prototype, shown in Fig. 4.1, was 36-fold segmented (6 azimuthal x 6 longitudinal).
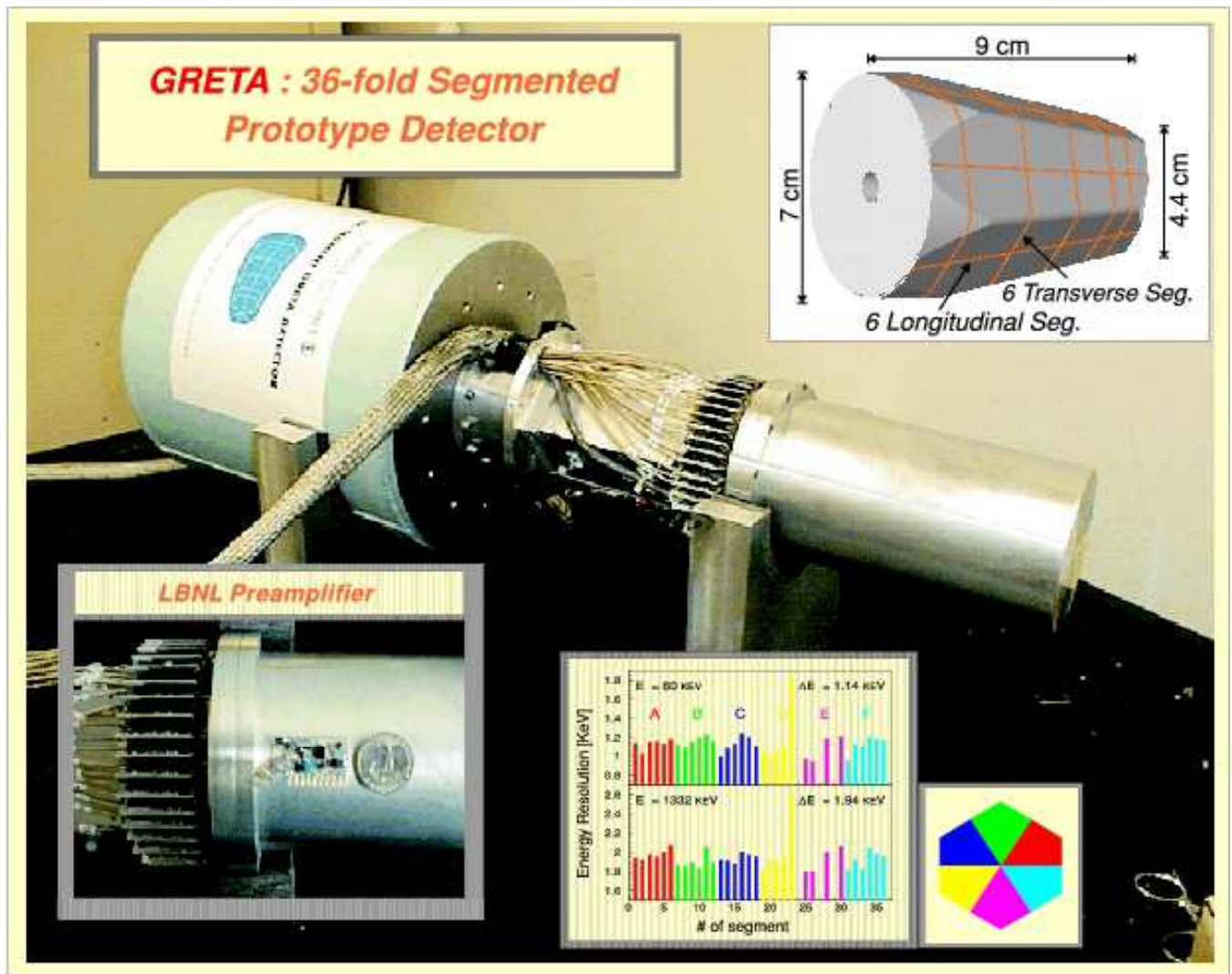
Figure 3.1 Picture of the 36-segment detector prototype. The insets show the preamplifier configuration, the crystal segmentation, and the energy resolution for each segment.

The 6 longitudinal boundaries are located in the middle of the flat surfaces of the hexagonal sides. The widths of the transverse segments starting at the front (the narrow end) are 7.5 mm, 7.5 mm, 15 mm, 20 mm, 25 mm, and 15 mm, and were chosen to distribute the number of the interactions more equally among the segments for gamma rays coming from the front. Varying the segmentation widths also allowed us to study the effects of different thicknesses on the transient-signal sensitivity. The Ge crystal resides in a 1 mm thick aluminum can of the same shape as the crystal. The can is separated from the crystal by 1 mm to simulate the close packed geometry of individually encapsulated detectors. The 37

FETs (36 segments + 1 central contact) are located and cooled in the same vacuum as the crystal. Cold FETs provide low noise, which is important for optimizing the energy and position resolution.

Preamplifiers were designed and built at LBNL and mounted on the 36-fold segmented prototype detector. They are characterized by their low noise, excellent response properties, and small size, which made it possible to mount all 37 preamplifiers radially on a cylindrical motherboard close to the feed-throughs on the back of the detector. The preamplifiers have an energy resolution, obtained with a pulser, of about 900 eV, which is dominated by the FET noise. No overshoot is observed down to rise times as low as 10 ns. This was measured with an input capacitance of 10 pF and translates into a bandwidth of 35 MHz.

Extensive measurements have been performed to determine basic properties, such as energy resolution, noise characteristics, three-dimensional position sensitivity and position resolution, and crystal orientation effects. The 36-fold segmented prototype was found to have excellent signal properties demonstrating it can be used as the basic co-axial crystal element in a gamma-ray tracking array.

A) Energy Resolution

The energy resolution reflects the quality of the crystal and its charge collection properties, as well as contributions from both parallel and series noise. Parallel noise depends on the leakage current or transistor base current, series noise depends on the transconductance of the FET and the detector capacitance. While the energy resolution at low energies (e.g. 60 keV from a ^{241}Am source) characterizes the noise contribution, the resolution at a higher energy (e.g. 1332 keV from a ^{60}Co source) reflects the charge collection properties.

The average energy resolution for the 34 working segments of the 36-fold segmented Ge detector was 1.14 keV and 1.94 keV at 60 keV and 1332 keV, respectively, and the spread was 0.08 keV (RMS). The individual values are shown in the insert to fig. 3.1. These excellent values are far superior to the 5 keV segment resolution of the two-fold segmented Gammasphere detectors. This is predominantly due to the small segment size and therefore smaller capacitance, which reduces the series noise contribution. The importance of a small capacitance can be seen by the fact that the pair of shorted segments had energy resolutions of 1.83 keV at 60 keV and 2.61 keV and 1332 keV.

B) Noise Properties

The noise response is used to study properties of the detector electronics (e.g. FET and detector capacitance). The level of noise determines the low energy threshold for the identification of an energy deposition in a segment and is also an important factor in obtaining good energy resolution. Measurements of the noise spectrum, its power spectrum, and integrated power spectrum indicate it is possible to set a threshold of ~5 keV. For a tracking array a low energy threshold of about 10 keV is needed.

C) Relative Efficiencies of the Segments

The relative efficiencies of the individual segments reflect the charge collection properties for a specific volume in the detector, which in turn depend on the crystal properties and the geometry of the crystal boundaries and segmentation lines.

Relative efficiencies for the different segments have been measured and calculated (using GEANT) as a function of depth, z, for a gamma-ray energy of 662 keV and 1332 keV. In a closed-ended and tapered detector many more field lines terminate on the first segment compared with the next segment in the second layer, and to reproduce the intensity profile one has to take into account the fact that the electric field is not always perpendicular to the detector axis. There is good agreement between measurement and calculation, particularly for the shape of the distributions, indicating that the segments perform as expected. The geometry of the electric field and its impact on the charge carrier pathways has to be taken into account in the design of segmented detectors.

D) Cross-talk

Due to the relatively high density of electronics in the 36-fold segmented prototype, shielding of the individual channels against cross-talk is crucial. This applies to the FETs, the wiring, the feed-throughs, and the preamplifiers. Although care was taken to minimize the cross-talk we did observe a coupling between some of the segments. Two types of cross-talk were found. The first occurs only between adjacent channels on the FET board. The main characteristic of this cross-talk is a net charge in both adjacent channels with opposite polarity to the original net charge signal. This cross-talk can be compensated by adding a fraction (about 3%) of the original net charge signal to the two adjacent channels. It can be explained by an insufficient decoupling of the power supply for the FETs. The second type of cross-talk only affects one of the neighboring segments and is based on an inductive coupling. It indicates an insufficient shielding between the input and output of adjacent FETs and can be compensated by subtracting a fraction of the derivative of the original net charge signal. In summary, the origin of both types of cross-talk is understood and can be removed by changing the electronic (FET) lay-out (the manufacturer has already implemented this change in later production detectors).

3.2. Three-Dimensional Position Sensitivity

Pulse shape analysis provides the three dimensional position resolution and energy of individual gamma-ray interactions. It relies on the fact that the shapes of the measured signals vary according to the location of the gamma-ray interaction within the detector volume. It is this difference that allows the interaction location to be determined to an accuracy better than the segment size. The amount by which the two signals differ relative to the noise is called the position sensitivity and is one of the essential performance measures of a gamma-ray tracking array. It is important to note that the position sensitivity alone does not give the final measured position resolution. Other effects will contribute, such as the range of the Compton electrons, the broadening of the distribution of charge carriers traveling towards the electrodes due to diffusion, and the uncertainties associated with the use of algorithms designed to analyze the pulse shapes (see discussion on signal decomposition).

In the following we will briefly describe the methods used to study the position sensitivity for both one and two interactions in a segment. It includes the calculation and measurement of both the net and transient signals as a function of the location of the primary gamma-ray interaction.

3.2.1. Calculation of charge signals in a segmented Ge detector

Electric field and pulse-shape calculations as well as Monte-Carlo simulations have been performed to understand the measured properties and to parameterize measured signals in terms of calculated signals.

These signals are necessary for the signal decomposition process, which requires knowledge of the expected pulse shapes as a function of location. It is not feasible to measure all the necessary pulse shapes throughout the detector volume and having accurate calculated pulses will be essential for a tracking array employing pulse shape analysis.
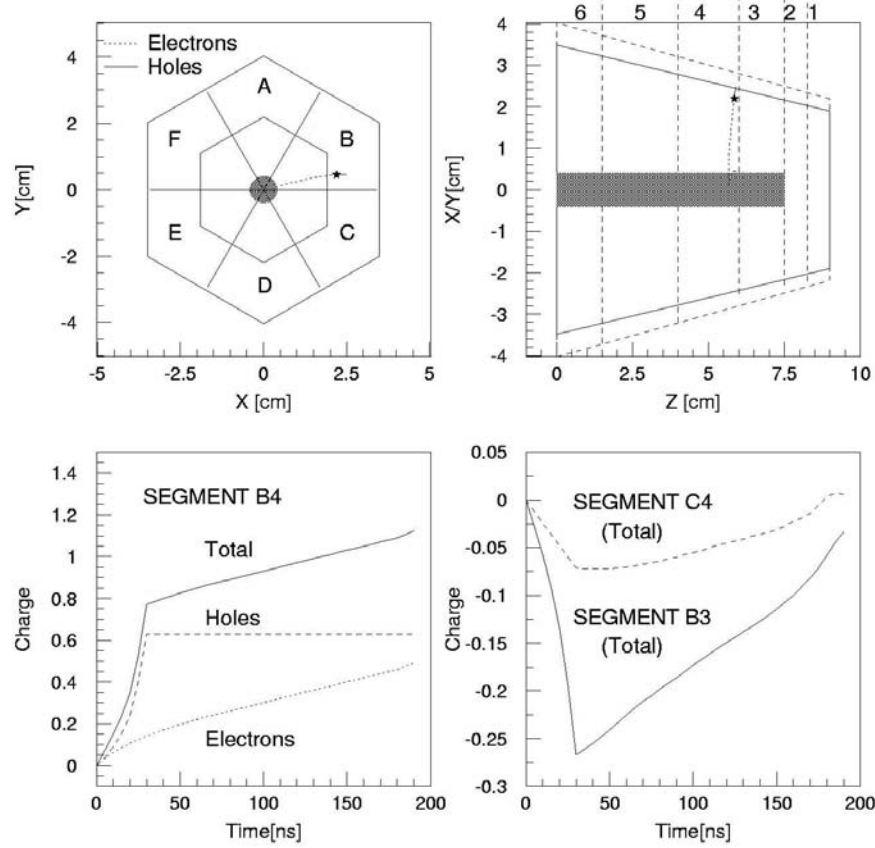
Figure 3.2. The upper part shows the calculated path of electrons and holes in the 36-segment prototype detector. The geometry as well as the arrangement of segment boundaries is shown. The interaction at x=22 mm, y=4.5 mm and z=58.5 mm is marked with a star in segment B4. Calculated signals for B4 and the nearest neighbors B3 and C4 are plotted in the lower part.

Calculated charge signals are obtained by first calculating the pathway of the charge carrier for a given interaction position. The motion of the charge carriers is determined by the electric field, which itself depends on the detector geometry, applied voltage, and intrinsic space charge density and mobility. The electric field is calculated from the potential, which is derived by solving the Poisson equation numerically. Fig. 3.2 shows calculated trajectories for electrons and holes assuming an interaction took place at x=2.2 cm, y=0.45 cm and z=5.85 cm in a coordinate system indicated in the figure.

Finally, to calculate the induced signals in the different segments we use Ramo's theorem [Ra39] for the so-called weighted potential. The lower part of fig. 3.2 shows calculated signals for the indicated starting point of the trajectory in segment B4. The left hand side shows the net charge signal of segment B4 and the different contributions of holes and electrons. The right hand side shows transient charge signals in the azimuthal neighbor (C4) and the segment in front (B3).

3.2.2. Signal measurements

An experimental set-up (fig. 3.3) was designed to measure the net and transient signals that arise from a single gamma-ray interaction at a known point in the 36-fold segmented detector. A single interaction was achieved by using a collimated 1 mCi ^{137}Cs gamma-ray source placed in front of the detector and requiring a coincidence between this detector and one of three collimated 5"x 6" NaI detectors, which were located at 90 degrees to the crystal axis (gamma-ray direction) and at an adjustable depth (z) along the axis. The 1 mm collimators mapped out a cylindrical volume of about 1.7 mm in x and y and about 1.9 mm in z. The ^{137}Cs source was specially built to have all the activity in a 1 mm diameter cylinder.
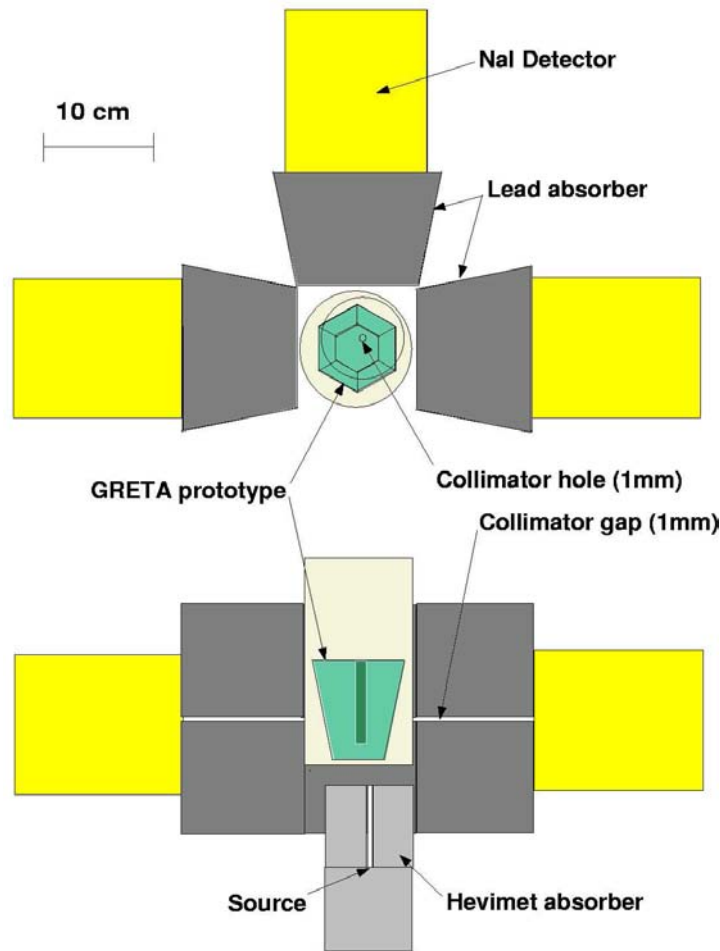
Figure 3.3. Experimental setup used for the measurements. The upper figure shows a top view on the coincidence setup and the lower part illustrates a side view of the vertical arrangement of collimation and detector systems.

The alignment of the collimation system relative to the segmentation of the detector was done by scanning the front face with collimated sources of ^{137}Cs and ^{241}Am.
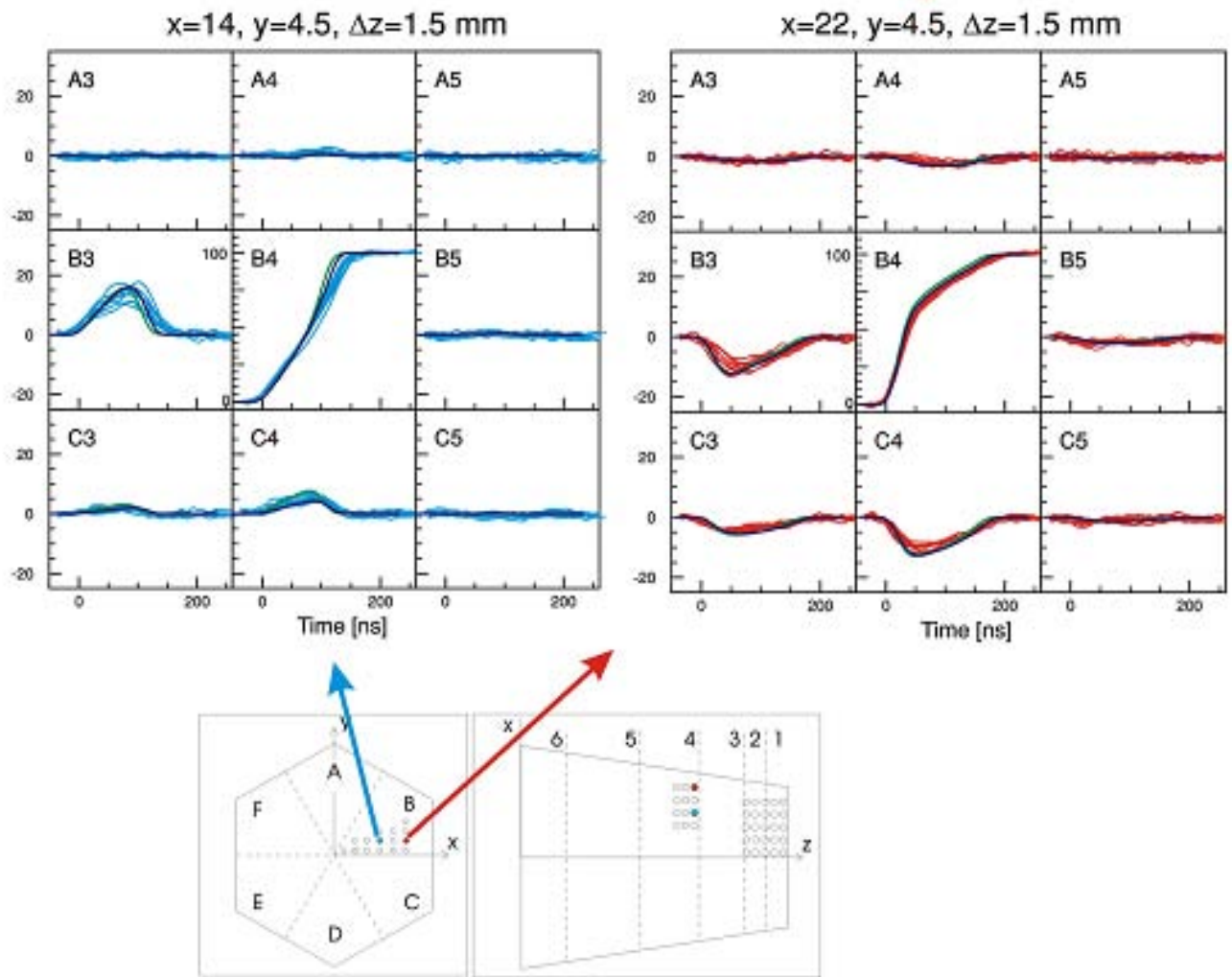
Figure 3.4. Comparison of measured and calculated signals at two positions in a given segment (B4) of the prototype detector, as indicated in the inset. Measurements are the blue or red curves, calculations are given by the dark colored curves. Note the sensitivity of both main and induced signals to the position. The locations are indicated in the lower part of the figure. In total 36 positions were measured, indicated by the circles. The segments are labeled 1-6 in the longitudinal direction and A-F in azimuthal direction.

Pulse shapes from the Ge-NaI coincidence events of the ^{137}Cs source were measured at various locations. Single interactions were selected by setting gates on the energies deposited in the Ge and the NaI detectors: a 90 degree Compton scatter of a 662keV gamma-ray deposits 374 keV in the Ge crystal. Using the 1 mm collimation system and a 1 mCi source we obtained a count rate of about 1 event in 10 to 60 minutes (depending on the radial position of the front collimator at a depth of 4 cm in the Ge). The low event rates meant that a limited number of positions in segments B1, B2, and B4 could be chosen.

Signals from 91 locations (36 in B4 and 55 in segments B1 and B2) were measured. Locations were separated by 4 mm in the x-direction and 3 mm in the y- and z-directions (open circles in the lower part of figure 3.4) and they provided a good variety of pulse shapes to determine the sensitivity and compare with calculations. On average, events were acquired at each location for a period of 1 day. This gave between 10 and 200 events per location. At each location the signals from the segment collecting the

charge and its eight nearest neighbors segments (one "net" and 8 "transient") were recorded using a waveform digitizer operating with a 500 MHz sampling rate and a pulse height resolution of 8 bits. To improve the signal-to-noise ratio in the measured signals, we averaged 16 samples at 500 MHz to give a 32 MHz sampling rate, which is close to the bandwidth of the prototype detector and preamplifier system.

Examples of measured signals in segment B4 are shown in figure 3.4 for two locations (blue and red curves). They clearly demonstrate the sensitivity of both the net and transient signals to the position of the individual interactions. For comparison, calculated signals at the given positions are plotted as dark lines; the agreement between calculation and measurement is very good.

Determining the position sensitivity

The position sensitivity relates the difference in pulse shapes, as a function of the interaction location, to the observed noise and in this way it measures the minimum distance between interactions that produce distinguishable signals. For a single interaction in a segment the position sensitivity S_{ij} is given by

$$S_{ij} = \frac{\Delta r_{ij}}{\chi_{ij}} \; .$$

Δr_{ij} is the distance between the locations i, and j, and χ^2_{ij} quantifies the square of the difference of the signals at positions i and j in terms of the measured noise σ^m

$$\chi^2_{ij} = \sum_{m=1}^{9} \sum_{t=t_{10}}^{t_{90}} \left[\frac{\langle q \rangle_i^m (t) - \langle q \rangle_j^m (t)}{\sqrt{2}\sigma^k} \right]^2$$

The $q^m(t)$'s are the signal amplitudes[2] from a segment m as a function of the time sample for the positions i and j. Since we compare two signals in the same segment the total noise contribution is $\sqrt{2} \, \sigma^m$, assuming the noise does not depend on the position of the interaction. The limits t_{10} and t_{90} are the times for the net charge signal to reach 10% and 90% of its full height, respectively. Using this definition a large value of S_{ij} means a high sensitivity. If the signals in a set differ only by σ_{ij} $(= \sqrt{2} \, \sigma^m$ for two locations i and j), the sensitivity will be just Δr^2_{ij}.

The results of the measurements gave single-interaction position sensitivities of ~0.2 mm in the x-direction, and ~0.5 mm in the y- and z- directions. The x-direction is similar to the radius and the higher sensitivity compared with other directions comes from the larger variation in the signal shape for a given change in radial position. Since the origin of the transient induced signal along the y and z direction is the same, the sensitivity along these directions is comparable. The single-interaction position sensitivity was also derived from calculated pulse shapes. The positions and energies of the interactions were given

---

[2] The finite opening angle of the collimation system meant that interactions could take place in a volume of about 3 mm^3 and it is not possible to determine the signal at a fixed position on an event-by-event basis. It is possible, nevertheless, to use signals averaged over many measurements (i.e. $\langle q \rangle_i^m(t)$) to generate one set of signals, which corresponds to the center (average) position of the collimation system. Another benefit of averaging is that noise is removed, leaving a signal which reflects purely the position variation. The noise level σ^m was determined by extracting the standard deviation of 500 time samples of one of the individual events, excluding the signal region. The average noise level (1σ) for the channels considered was about 5 keV in agreement with the more sophisticated noise analysis above.

by Monte-Carlo simulations that included the geometry of the 36-fold segmented prototype detector as well as the collimation system and using the same energy conditions as in the experiment. A realistic response and noise was folded into the calculated signals. Figure 3.5 shows distributions of all combinations of sensitivities obtained from measurement and simulation. Average values of 0.36 mm and 0.33 mm with an rms width of 0.13 mm and 0.18 mm were found for the measured and simulated distributions, respectively, again showing good agreement between the measured and calculated pulse shapes. These results are for an energy of 374 keV. By scaling signals and comparing them with noise, we found that even for gamma-ray energies as low as 100 keV a sensitivity of about 1 mm can be achieved.
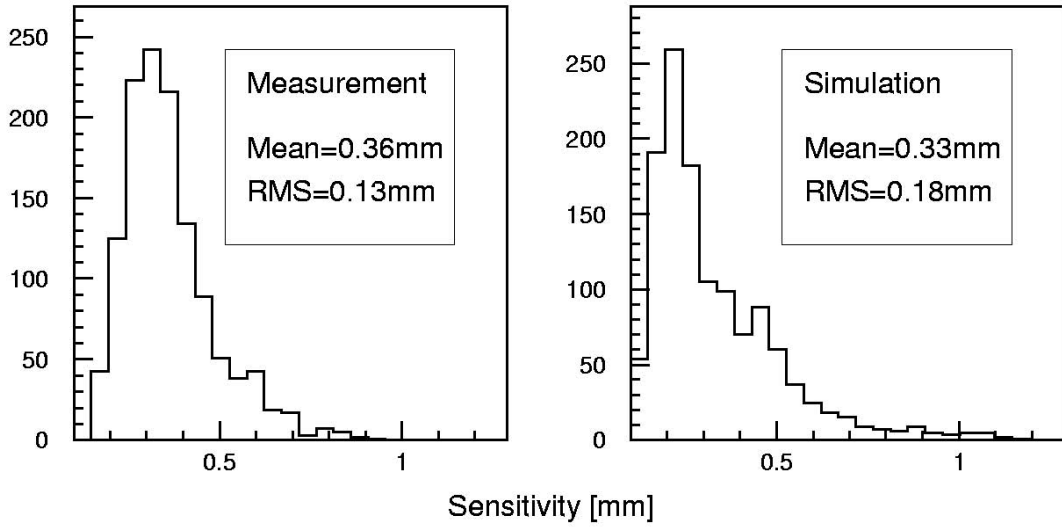
Figure 3.5. (left) Distributions of position sensitivities calculated from the measurement of single interactions with an energy deposition of ~374 keV. (right) Position sensitivities from calculated pulse shapes at the position.

For segment sizes of the order of 1 cm there is a significant probability that two interactions will occur in the same segment. The position sensitivity for two interactions in a segment occurring at locations i and k is complicated by the fact that the observed pulse shape $q_{ik}(t)$ is a superposition of two signals $\alpha q_i(t) + \beta q_k(t)$ and the sensitivity is now given by the ability to distinguish two interactions occurring at i and k from a single interaction at position j midway between i and k.

$$S_{ijk} = \frac{\Delta r^2}{\chi_{ijk}}.$$

Δr is the distance between the locations i and j (it is squared to ensure that when $\chi^2_{ijk} = 1$ there is consistency between the solution for S_{ijk} and the total separation between i and k, which is 2Δr), and

$$\chi^2_{ijk} = \sum_{m=1}^{9} \sum_{t=t_{10}}^{t_{90}} \left[\frac{\frac{1}{2}\left(\langle q \rangle^m_i(t) + \langle q \rangle^m_k(t)\right) - \langle q \rangle^m_j(t)}{\sqrt{\frac{3}{2}}\sigma} \right]^2$$

quantifies the square of the difference of the signals in terms of the noise σ^m in segment m.

The two-interaction position sensitivity was studied using simulated signals derived from locations separated by $\Delta r = 1$ mm in x, y, and z, and noise $\sigma^m = 5$ keV. The pulse shape resulting from two interactions (one at i and one at k) of equal energy deposition (331 keV each) was compared with a single interaction at j of 662 keV. The distribution of two-interaction position sensitivities, $\overline{S}_T$, for all of the segments is illustrated in Figure 3.6. The mean value 1.01 mm^2 indicates that on average the two equal energy interactions from a 662 keV gamma ray must be separated by about 2 mm in order to be distinguished from a single interaction between them. $\overline{S}_T$ increases with increasing segment size and ranges from 0.26 mm^2 in segment 2 to 1.23 mm^2 in segment 5, and in these larger segments there are regions where the separation needed to distinguish two interactions approaches 4 mm. In line with these results, we have tried to minimize the segment size, where possible. The next prototype detector (section 3.7) will have a maximum segment size of 2 cm compared with 2.5 cm for the present detector.
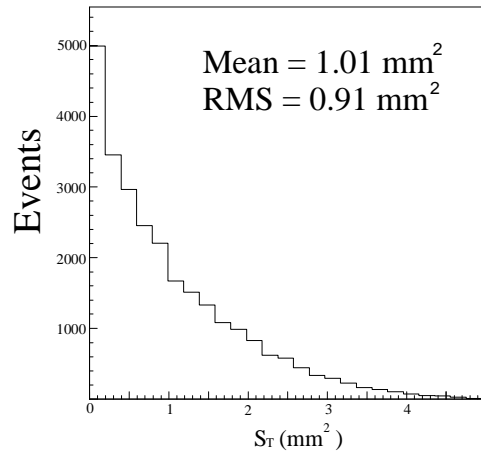
Figure 3.6. Simulated position sensitivity for all segments for two-interactions and a total energy deposition of 662 keV.

Crystal Orientation Effects

The charge mobility is not only a function of the temperature and electric field but depends also on two additional parameters (or angles); (i) the angle between the crystal axis orientation and the charge drift direction, and (ii) the angle between the crystal orientation direction and the electric field direction. We have studied the effects of crystal orientation on the drift velocity in n-type as well as p-type Ge detectors and found that the change in magnitude of the velocity due to different orientations is significant; if not taken into account it introduces an error of up to 3 mm in the position determination based on pulse-shape analysis. Figure 3.7 shows drift times measured in a p-type Ge detector as a function of the angular position of a collimated [241]Am source. Since the energy deposition of the 60 keV gamma ray from [241]Am is localized to the outside surface of the crystal, only one type of charge carrier travels to the inside contact and contributes to the signal, i.e. holes for a p-type detector and electrons for an n-type detector.
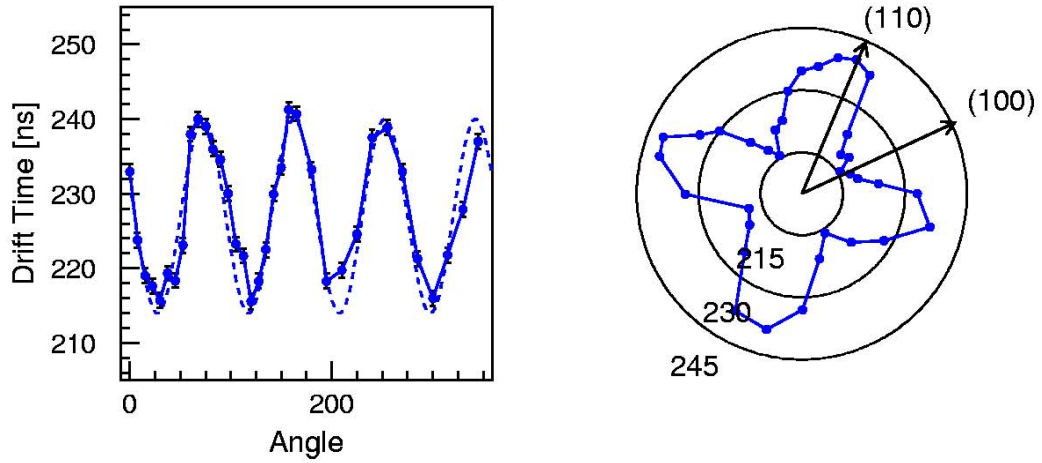
Figure 3.7 Measured drift times in a p-type Ge detector as a function of the angular position of a collimated [241]Am source. The left figure shows the measured drift time of holes as a function of the angle (in deg.) and the right figure shows the same dependency in a polar plot (the drift time scale is offset by 200 ns). The arrows indicate the crystal orientation axes as defined by the measurement.

As seen from figure 3.7 the maximum differences in the drift times correspond to ~10% of the total drift time, depending on the crystal axes, which translates into the mentioned (3%) error in the radius. A similar error is introduced if the directional dependence of the velocity from the crystal orientation is not taken into account. We were able to measure this effect using the segmentation of the 36-fold segmented prototype detector and can correct it in the signal decomposition procedure.

Uncertainties due to the electron range and Compton profile

The range of the Compton electron represents an uncertainty which will limit the accuracy to determine the location of the scattering process. In the current measurements the Compton electron of 374 keV has a range of about 0.2 mm, which is of the same order as the sensitivity obtained for many positions. The reason we were able to achieve a sensitivity sometimes better than the range of the Compton electron was due to the averaging procedure and using a slit in front of the NaI detectors to define the 90 degrees scattering. For a Compton electron of 1 MeV (i.e. 90 degree Compton scattering of a 1.4 MeV gamma ray) the range increases to about 1 mm [Mu76]. On the other hand, the maximum diameter of the distribution of charge carriers can be estimated to be less than 0.1 mm in the present prototype geometry and therefore does not represent a serious limitation.

The Compton profile reflects the initial momentum distribution of the electrons involved in Compton scattering. Generally, a description of Compton scattering neglects the binding energy as well as the momentum of the electron. However, the momentum of the electron has a measurable effect on the angle-energy relation for gamma-ray energies up to several MeV. In contrast to the range of the Compton electron, this effect becomes more important for smaller gamma-ray energies and also depends on the scattering angle. Evidence for the importance of this effect is shown in fig. 3.8 which shows measured and calculated energy spectra obtained in the 36-fold segmented detector mounted in the collimation system with a hole diameter as well as slit size of 1 mm. The momentum distribution of the electrons in germanium [Br75] has to be taken into account to obtain agreement between the measured and the calculated energy profile in the germanium detector. The Compton profile does not effect the position determination of a single interaction, but it does affect the tracking based on events with at least two interactions.
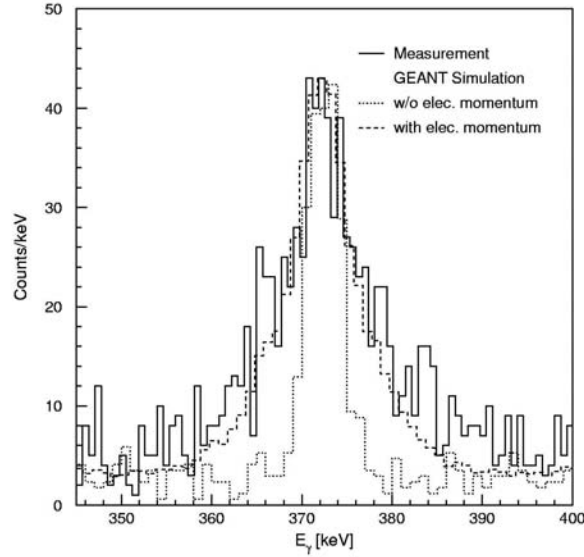
Figure 3.8. Partial energy spectra measured in segment B4 of the 36-segment detector (solid line). The peak at 374 keV reflects the requirement of a coincidence between the Ge and one of the NaI detectors. The dotted and the dashed lines show calculated spectra assuming the same geometry as in the experiment without and with taking into account the electron momentum, respectively.

For higher gamma-ray energies the range of the Compton electrons will be the dominant factor limiting gamma-ray tracking while the uncertainty in the energy-angle relation in the Compton scattering formula due to the momentum distribution of the electrons (Compton profile) will dominate for lower gamma-ray energies.

3.3. Signal Decomposition

The three-dimensional position sensitivity obtained above satisfies an essential condition to enable gamma-tracking and reflects the accuracy for separating gamma-ray interactions based on pulse shape differences. To determine locations and energies of one or more interactions in one or more segments requires algorithms to decompose signals into their individual components. In this section we will describe several methods to extract the positions and energies of multiple interactions in multiple segments from the detector signals. Optimizing these algorithms for both accuracy and speed remains an active area of R&D.

A great deal of effort is being devoted to signal decomposition. This is a major component of the gamma-ray tracking related work being carried out elsewhere (e.g. Europe). We have extensively explored three approaches, an adaptive grid method, a sequential quadratic programming technique, and a method based on solving systems of equations using generalized matrix-inversion. Work is also being pursued using artificial neural networks (ANN), genetic algorithms (GA), and wavelet transformations. All except the ANN approach employ a set of "basis" signals which are used as to determine the number, amplitudes, and positions of interactions. The basis signals have to be derived from calculations and the aim is to find the interaction points by minimizing the difference between the measured signals and signals taken from the basis. The measured signal can be a superposition of basis signals due to multiple interactions.

3.3.1. Adaptive grid search method

The grid search method is a known technique used to reliably find global minima that does not depend on the starting condition. However, the drawback of this method is that it is very slow because it maps out the whole space of parameters, which is large for this problem. The parameters to be determined from the measured signals are the number of interactions, their amplitude, and their three-dimensional positions. Each signal is about 300 ns long and will be sampled every 10 ns (100 MHz), resulting in 270 data points when 9 segments are taken into account. A 1 mm grid spacing gives ~5000 grid points per segment. Assuming an accuracy of 1% for each amplitude we end up with about 10^{23} possible combinations to be checked for up to 4 interactions in one segment. This is obviously prohibitive.

A better approach is to use an adaptive grid search method. The search for the interaction points begins on a grid using a relatively large spacing, e.g. 8 mm, and then the spacing is reduced iteratively down to 1 or 2 mm. Pre-calculated signals corresponding to interactions at each point of a rectangular (or hexagonal) grid (as shown in the upper right plot) are stored in a lookup table and used as "basis" functions. The upper left portion of figure 3.9 shows examples of signals (for an 8 mm grid size) from the segment containing the interaction and from the two nearest neighbors that have a transient charge signal. The deviation from the measured composite signal is minimized by varying the number of interactions, the positions of the interactions, and the corresponding amplitudes. By an iterative method, which improves both the position resolution (from 8 mm to 1 mm) and amplitude resolution (from about 10% to only a few percent) we were able to show that one can resolve the composite signal into its components and determine the positions and energies of the original interactions. This is demonstrated in the lower part of figure 3.9. The left hand side shows the input signals in red and the output signals in green (input refers to the measured signal, output refers to the reconstructed signal from a sum of base signals). The input signals are generated from three interactions at positions indicated by red stars on the upper right plot. The lower right hand side shows the amplitude distribution of interactions found on the grid. Interactions found in neighboring grid points are assumed to correspond to a single "real" interaction. The energy-weighted average between these points then gives the position of this interaction. The deviation in all three positions is less than 1 mm.

This method for the event-by-event decomposition of measured signals using purely calculated signals as a basis gives a position resolution for single interactions of order 1 mm at 374 keV. These results are presented in Fig. 3.10, where position resolutions in 3D (x, y and z) are compared for fitted positions and positions obtained by Monte Carlo calculations.
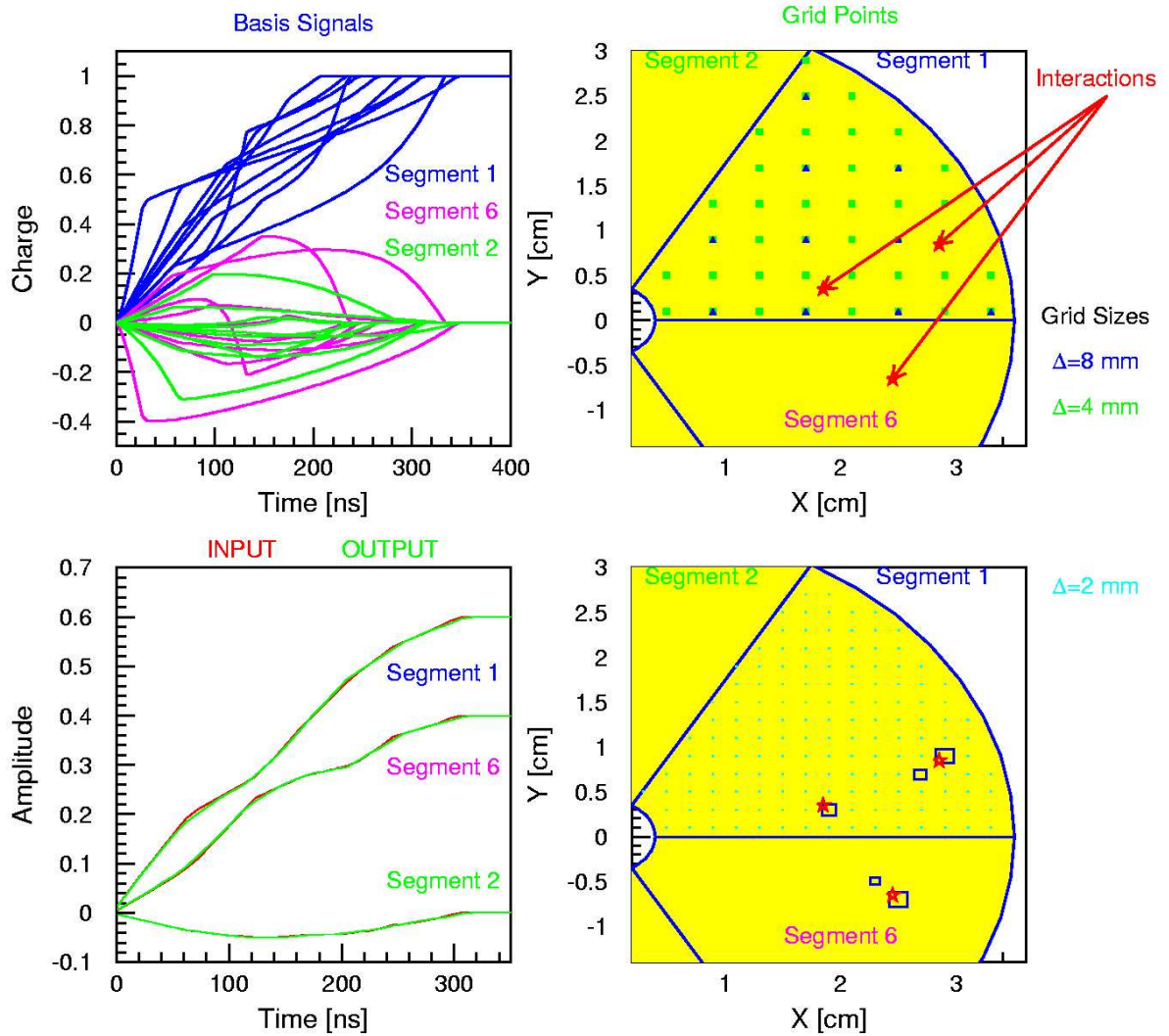
Figure 3.9. Demonstration of the decomposition of signals due to multiple interactions into their individual components in a coaxial detector with 6 fold azimuthal segmentation. The upper right indicates grid positions (green squares: Δ=4 mm) where signals - shown on the left for Δ=8 mm (blue triangle) are calculated. Assuming three interactions (at the locations of the red stars on the upper right figure and which result in the red signals in the lower left figure) the minimization procedure is able to find the closest grid points to the interactions. The resulting signals for three segments are shown in green and can hardly be distinguished from the input red signals. The lower right figure shows the amplitudes (proportional to the area of the squares) obtained for all grid points found to contribute to the signal.

3.3.2. Sequential quadratic programming method

The sequential quadratic programming (SQP) method is an iterative process to minimize an arbitrary function subject to both linear and nonlinear constraints on a set of parameters. The SQP routine was used in the minimization procedure to fit measured pulse shapes to calculated basis signals and was implemented via the NAG fortran library. The algorithm is designed to quickly converge to a minimum without sampling all possible solutions and is an alternative to the adaptive grid search method. The SQP method was used in the signal decomposition code for the full source measurements described in

39
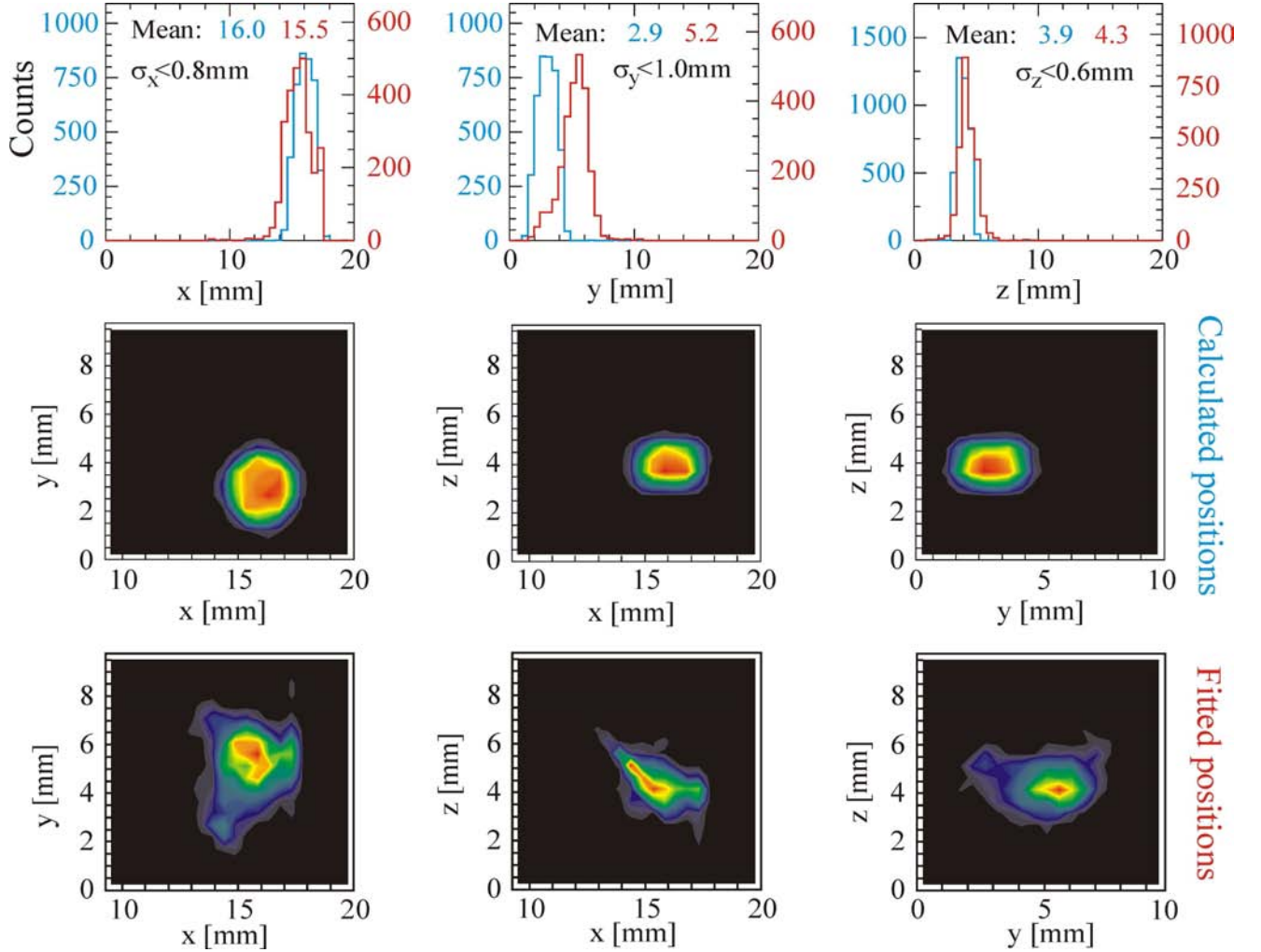
Fig. 3.10. Three dimensional position resolution of the prototype for a single (374 keV) interaction. The larger discrepancy between measurement and simulation for the y-direction is due to the crystal orientation effect, which was not included in the calculations shown here.

section 4.4. On average, simulated single 662 keV events were located to better than 1mm, neglecting such effects as the range of the primary electron. The important development of this study [Ku02] was the extension to the case where two interactions occur in one segment. Considerable improvement in speed of this algorithm has been made recently at ORNL by D. Radford. To date, this version of the decomposition code locates interactions (converges) with a success rate of 85% and can decompose 2 interactions in about 0.025 second (using a 700 MHz CPU) and is one of the current algorithms that can be used in Gretina.

3.3.3. Singular value decomposition

We have also investigated a way to decompose the detector signals by describing the positions and energies of the interaction points using a system of linear equations. Thus, the determination of the

energies and positions becomes a matrix-inversion operation. This approach is potentially very fast since the inverse can be calculated *a priori* and the decomposition is reduced to a multiplication of a matrix with a vector. However, the matrix, which is composed of basis signals for interaction points on a three-dimensional grid, is usually singular and its inverse can not be obtained. A mathematical technique known as singular value decomposition (SVD) is used to separate the matrix into a product of a diagonal and two orthogonal matrices. By taking the inverse of each matrix, we arrive at the Moore-Penrose generalized inverse. When a measured signal is multiplied by the generalized inverse, the optimal positions and energies of the interaction points are obtained.

With the total set of basis signals it appears that due to the linear dependency of the base signals, it is only possible to accurately determine the radius and the depth (z) of the interactions. The azimuthal position can be obtained in a second step by limiting the radius and the depth. These results indicate that for interaction points near a grid point, their positions can be determined with an accuracy of about 1-2 mm. For points away from a grid point, this method gives a distribution with a width of about a 4-5 mm. Although this is worse than the 1-2 mm resolution from the SQP search method, these values represent a good first step in any decomposition method. The advantage of this method is its speed, which is of the order of milliseconds for each gamma-ray decomposition.

Further improvements of this method by constraining the number of basis signals and the number and amplitude of the interaction points should be studied. In addition, a combination of the singular value method with the sequential quadratic programming method can be envisioned, by first defining volumes of about 50 mm^3 containing interactions by the SVD and then to refine the positions by the SQP method.

3.3.4. Other methods

Other methods, which either are just starting to be investigated or are being pursued elsewhere include decomposition based on wavelet transformations, genetic algorithms, and artificial neural networks. The wavelet approach allows the information contained in the basis and measured signals to be stored far more efficiently leading to a faster minimization procedure. Instead of storing the basis signals in the time domain, we store the coefficients of the wavelet expansion and compare these coefficients with the coefficients of the wavelet-transformed measured signals. This approach is also being investigated by the European AGATA collaboration. Two other algorithms are currently under development in Europe which are based on genetic algorithms and artificial neural networks. Currently, the genetic algorithm approach appears more favorable and a position resolution of about 2 mm was achieved for randomly distributed interactions while a resolution of about 5 mm was obtained employing artificial neural networks. Close connections exists between the U.S and European gamma-ray tracking communities, and the results from the respective R&D in all areas, e.g. signal decomposition, tracking algorithms, and detector design, are shared.

3.4. Tracking Algorithms

The goals of a tracking algorithm are to (i) identify sequences of interactions (obtained from signal decomposition) that belong to a given gamma ray, (ii) resolve the tracks of multiple, coincident gamma rays, (iii) distinguish between gamma rays that deposit their full energy from those that deposit a fraction of their energy, and (iv) determine the first and second interactions. The first interaction is

required for proper Doppler correction and together with the second interaction can be used to determine the linear polarization.

Most of our efforts [Sh99a] have focused on the treatment of Compton scattering since this is the dominant interaction process for gamma-ray energies between 150 keV and 5 MeV in germanium. Below 150 keV the photo-electric effect and above 5 MeV the pair production processes dominate respectively. Recently, we developed a tracking algorithm to identify and recover gamma rays interacting by the pair production process.

The following contains a description of the tacking algorithms developed. The performance of the tracking code is discussed for a 4π germanium array and for high multiplicity events, which represent the most challenging demand on a tracking algorithm. A brief overview of the principles behind gamma-ray tracking is given in Appendix A.

3.4.1. Tracking of Compton events

The current algorithm consists of three steps. The first step is cluster identification where the interaction points within a given angular separation (angle parameter), as viewed from the target, are grouped together. In the second step, each cluster is evaluated to determine whether it contains all the interaction points belonging to a single gamma ray. The evaluation process (tracking algorithm) uses the angle-energy relation of Compton scattering to determine the most likely scattering sequence from the position and energy of the interaction points. If the interaction points had infinite position and energy resolution, the tracking would be exact and the properly identified full-energy clusters (i.e. groups of interactions assigned to a single gamma-ray) will show no deviation from the scattering formula ($\chi^2 = 0$). Wrongly identified clusters or partial-energy clusters will deviate from the formula and the separation between good and bad clusters would be easy. However, in reality, with finite position and energy resolution, good clusters also will have a non-zero χ^2 and they cannot be separated cleanly from bad clusters. This causes a lower efficiency and reduced P/T ratio. In the third step, we try to recover some of the wrongly identified gamma rays. For example, a single good gamma ray can be separated into two bad clusters. This gamma ray can be recovered by tracking together all pairs of two bad clusters and recalculating the χ^2. Similarly, the case of two gamma rays wrongly identified as one cluster can also be separated by tracking. The clusters which do not satisfy any of the above criteria are rejected.

Simulations were carried out for a number of different conditions such as the multiplicity and energies of the gamma rays as well as position resolution of the detector. Fig. 3.11 shows the efficiency and peak-to-total ratio achieved for a spherical 4π shell and simulated events assuming 25 1.33 MeV gamma rays and detector position resolutions of 1 and 2 mm. This represents one of the most challenging cases. For a position resolution of 2 mm, which appears to be feasible based on the previous results, and an angle separation parameter of 8 degrees, an efficiency of 25% and a peak-to-total of 65% can be achieved for a 4π shell with realistic dead-layers (aluminum cans etc). Compared with Gammasphere, which has an efficiency of about 8% and a peak-to-total of about 66% under the same conditions, this implies a gain of ~3 in efficiency for each of the 25 emitted gamma rays.

Besides the identification and separation of multiple gamma rays, the tracking algorithm is able to provide the time sequence of the interactions; in particular the first and second interactions, which is an important feature of a tracking array.
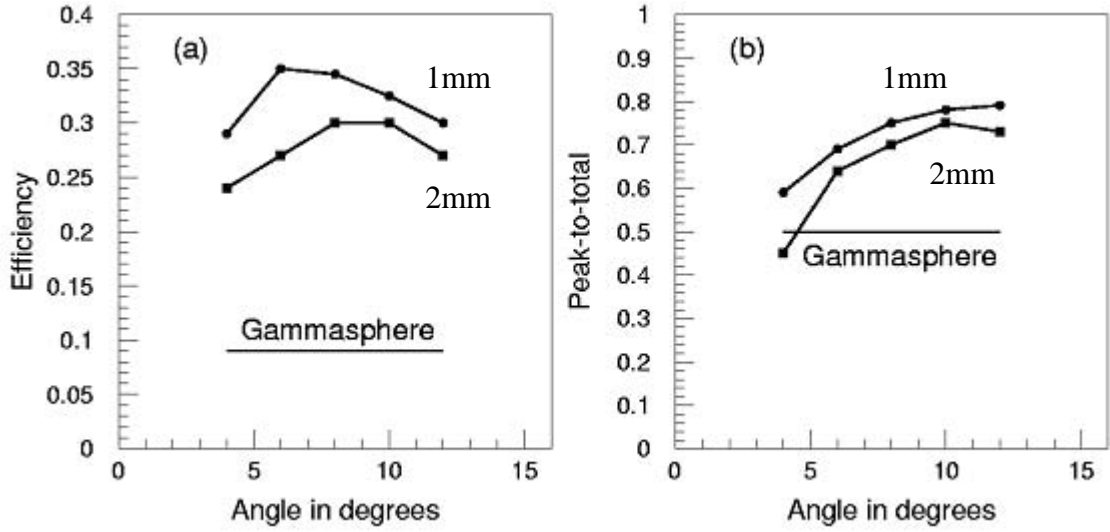
Figure 3.11. Efficiency (a) and peak-to-total (b) achieved with the current tracking algorithm for a 4π shell (see text for details) and for simulated events of 25 gamma rays with energy of 1.33 MeV and a detector position resolution of 1 mm and 2 mm, respectively. The curves are plotted as a function of the angle parameter used in the cluster identification.
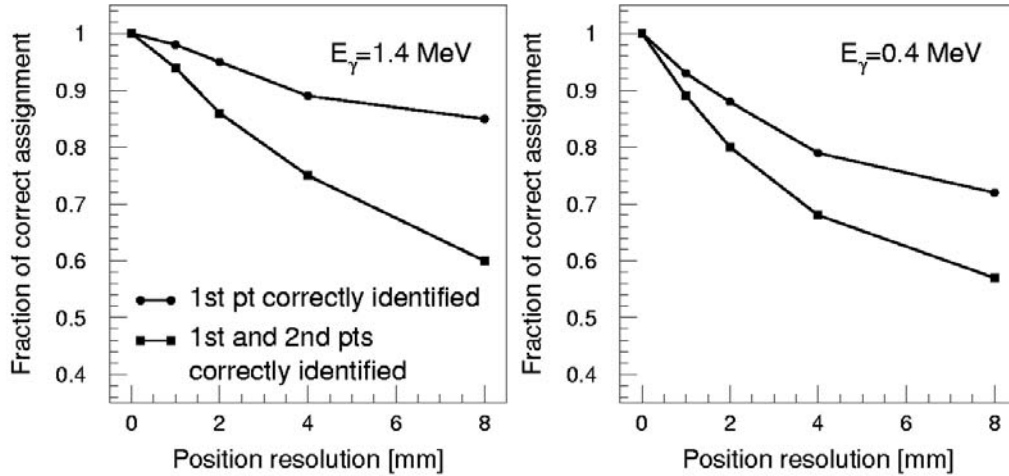
Figure 3.12. Capability of the developed tracking algorithm to identify the first and the second interactions of a gamma-ray track. Shown is the fraction of correctly identified events as a function of the position resolution.

Figure 3.12 shows the probability of finding the first and second interaction for 0.4 MeV and 1.4 MeV. For both energies, and a position resolution of 1 mm, the success rate is larger than 90%. While the efficiency of Gretina will be less than that of a full 4π array, the ability to identify and measure the first interaction will be very similar for both set-ups. This is important for Doppler correcting gamma-rays emitted from fast moving nuclei (velocities up to 50% of c). The high probability of localizing and identifying the first two interactions is also reflected in a high polarization sensitivity. The gain in polarization sensitivity (Q) is between 10 for lower energies and 4 for higher energies.

The ability to separate gamma rays from neutrons emitted in coincidence from a highly excited nucleus was studied. The predominant elastic scattering of neutrons can be efficiently separated by time cuts (of e.g. 15 ns). In this way, the majority of neutron interaction points are eliminated, and those that remain

are tightly clustered, and promptly eliminated during the gamma-ray tracking phase of the algorithm (these small neutron clusters mimic bad gamma-ray clusters, and thus have a poor figure of merit).

Tracking an event of 25 coincident 1.33 MeV gamma rays with a position resolution of 1 mm and an angle separation parameter of 10 degrees takes about 10 ms on a current 700 MHz CPU and is significantly less than the time required to carry out the signal decomposition process. The details of computational needs for Gretina will be discussed in Chapter 5.

Although our algorithm satisfies the requirement for an efficient gamma-ray tracking array, several improvements are being considered. Information such as the energy dependence of the angular distribution of the Compton scattering cross section and the distribution of the distance between two interaction points can be used in the first stage of the algorithm, in particular in combination with the technique of "minimum spanning trees" which is known to be very efficient and fast.

3.4.2. Tracking of pair-production events

Gretina will have an increased photo-peak efficiency for high energy gamma-rays (e.g. E_γ above ~10 MeV), compared with Compton suppressed Ge arrays, e.g. Gammasphere and Euroball. Above the threshold of 1.022 MeV, the probability of pair production increases as energy increases. At 10 MeV, this probability is about 60% and therefore pair-production events need to be identified with a high efficiency.

In most cases pair-production occurs at the first interaction because the gamma-ray energy decreases rapidly as the Compton scattering sequence proceeds. The electron and positron pairs produced by a 10-MeV gamma-ray have short ranges, less than 6 mm in Ge. Therefore, the electron and positron paths could be identified as a single interaction point with a high energy deposit of $E_\gamma - 1.022 \sim 9$ MeV, in our example. The annihilation of the positron produces two 0.511 MeV gamma-rays and each of them creates a cluster of interaction points. Therefore, the pattern of pair-production events can be characterized as a single high-energy point surrounded by low energy points.

A pair-production tracking algorithm has been developed that utilizes these characteristics. The first step is to select candidates of pair-production points based on the high energies deposited. A second step searches for the two 0.511 MeV clusters close to the high-energy point. The search and evaluation of the 0.511 MeV clusters are done using Compton kinematics and placing constraints on the spatial distribution of interaction points.

The algorithm was tested using simulated data of interaction points generated by GEANT3. The detector consisted of a shell of Ge with an outer radius of 21 cm and an inner radius of 12 cm. In each event, a 10 MeV gamma-ray was launched from the center in coincidence with several 1 MeV gamma-rays to simulate background gamma-rays. Fig. 3.13 shows the tracking efficiency ε_t for pair production events as functions of energy and position resolutions (ΔE and ΔR, respectively) and multiplicity of 1 MeV gamma rays (M_γ). It can be seen that the efficiency decreases linearly as ΔR or M_γ increases. A preliminary result gives a value of $\varepsilon_t \sim 0.4$ at 10 MeV for $\Delta E = 2$ keV and $\Delta R = 3$ mm.

The efficiency of the current algorithm can be improved by relaxing some of the requirements such as requiring the complete identification of two 0.511 MeV clusters. This change would allow the acceptance of single-escape events and might even enable the recovery of partial escape events.
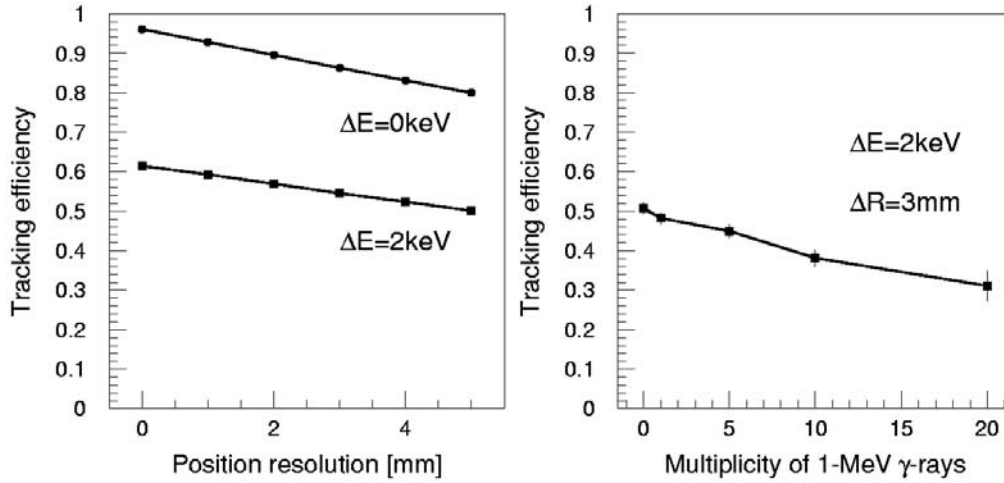
Figure 3.13. Simulated tracking efficiency for 10 MeV pair-production events as functions of energy and position resolutions (left) and as a function of multiplicity of background 1 MeV gamma-rays (right). The photo-peak efficiency for pair events is the product of the tracking efficiency ε_t and full absorption efficiency ε_p.

3.5. Source Measurements with the 36-segment Prototype

Additional end-to-end tests of the 36-fold segmented prototype have been performed using radioactive sources of ^{60}Co, ^{137}Cs and ^{152}Eu. These tests demonstrate that by combining all the separate elements of Gretina the resulting system performs as expected. In these measurements, most of the segments were instrumented with digital electronics and the full analysis procedure of signal decomposition and tracking was applied to the data. A full account of the measurements can be found in A. Kuhn, Ph.D. Thesis, U.C. Berkeley, 2002.

The experimentally measured data were taken with the prototype detector. The sources were placed at a distance of 12 cm from the center of the detector's front face and a 32 channel 40 Mhz 12 bit flash ADC system manufactured by XIA was used to digitally record the signals from 29 segments plus the central contact. The fact that not all segments were instrumented (5 segments were not working) meant that an event was considered if and only if the energy in the central contact matched the summed energy from the 29 segments. This guaranteed that no information (such as the transient signal) was lost.

The pulse shapes were input into the signal decomposition algorithm (section 3.3.2), which had the ability to determine a maximum of two interactions for the segment where energy deposition occurred, and a fit to the basis pulse shapes returned the positions and energies of one or more interactions. With the positions and energies of the interactions determined for each event, the tracking process was implemented to construct a figure of merit for each event and to discriminate between partial and full energy events.

Results for the ^{137}Cs source are presented in Fig. 3.14. The left panel corresponds to a full simulation and the right panel to the real data. The tracking algorithm improves the peak-to-total from ~16% to 31%. As expected for a single crystal, the tracking improves the peak-to-total ratio but does not increase the efficiency. The efficiency can however increase for an array of close-packed crystals. The tracking

45

efficiency ε_t, defined as the fraction of photo-peak events obtained with and without tracking, was 62%. The measured and simulated efficiency and the peak-to-total ratio agree with each other for both the raw spectra and the spectra after the tracking. These results indicate that we have an accurate understanding of the entire system.
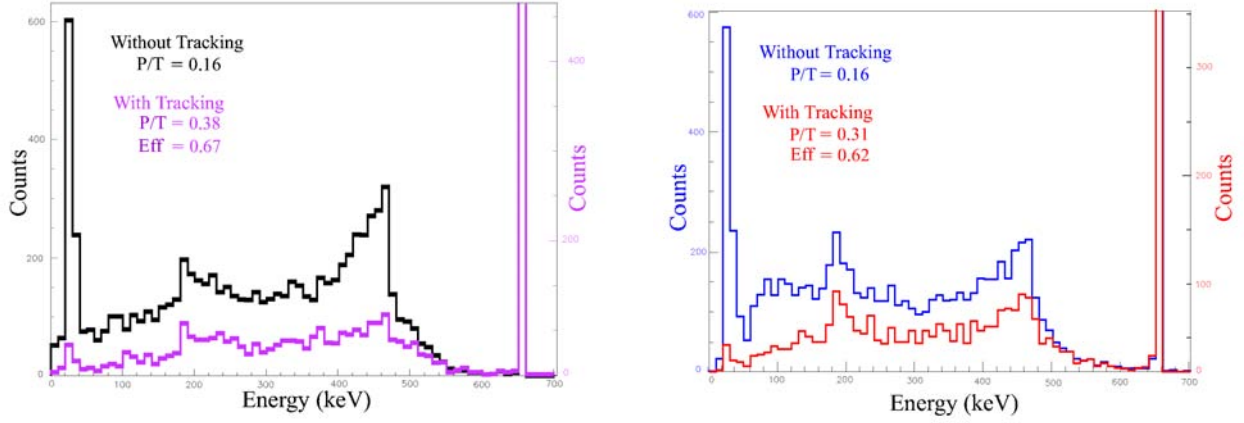
Fig. 3.14. Singles spectrum for the ^{137}Cs source (662.7 keV) obtained with and without tracking. The left panel corresponds to a full simulation while the right panel is for the real data. The low energy [137]Ba conversion x-rays are also seen (32.5 and 36.5 keV) and were considered as part of the background radiation for this measurement.

The results for the [152]Eu source measurement are shown in fig 3.15 and show the relationship between tracking efficiency and peak-to-total for various cuts of the tracking figure of merit as a function of gamma-ray energy.
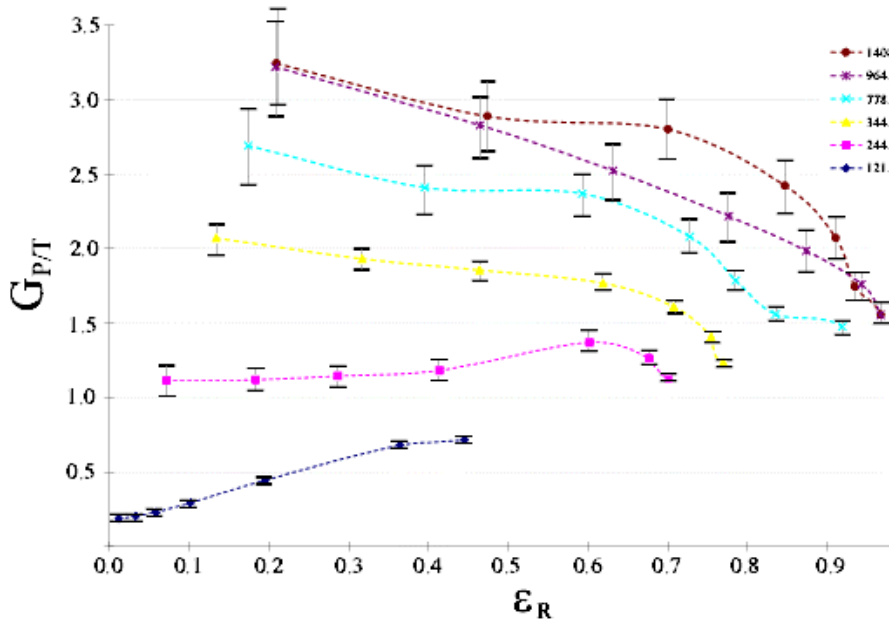
Fig. 3.15 Relationship between the gain in peak-to-total $G_{P/T}$ and the tracking efficieny ε_r in [152]Eu as a function of the threshold placed on the figure of merit from the tracking code. The legend gives the energy of the gamma-ray in keV for each curve. The data point to the far right (1.0, 1.0) marks the gain in P/T prior to tracking at all energies.

3.6. Electronics

There are two challenges to be addressed in the electronics development for Gretina. The first is the production of high-bandwidth, low-noise preamplifiers that are capable of preserving the position information in the transient current signal from each detector segment. These units must be low power and highly miniaturized as 111 such preamplifiers are to be mounted on each 3-crystal cryostat. Such a preamplifier was designed and built at LBNL for the 36-fold segmented prototype detector. Measurements of noise characteristics, position sensitivity, and position resolution were performed with an 8-bit 500 MHz digitizers (Tektronix RTD720, on loan from LLNL) and 12-bit 50 MHz digitizers (XIA DGF-4C, on loan from ORNL). It was found that these preamplifiers meet the bandwidth, noise, and power requirements and improve the energy resolution by 0.1 keV when compared to standard preamplifiers.

The second challenge is to develop fast, inexpensive digitizers capable of performing real-time data reduction, analysis, and triggering. Measurements performed with the 36-segment prototype and unsegmented p-type and n-type detectors have been used to specify the requirements for the signal processing electronics. An amplitude resolution of 12 bits and a sampling rate of 100 MHz are needed to obtain good energy and time resolution based on pulse-shape analysis. Ideally, a 14 bit ADC is desirable to guarantee high resolution over a very large dynamic range (100 keV to 20 MeV).

The amplitude resolution for the ADC was derived from tests using the 12-bit DSP-board from XIA and the 36-fold segmented prototype detector. The energy resolution was comparable to that obtained using an analog processing system. The minimum sampling rate was determined by measurements performed with unsegmented p-type and n-type detectors and a 500 MHz waveform digitizer with 8 bit amplitude resolution. The read-out was triggered by a fast BaF_2 detector which detected a coincident gamma-ray from a ^{22}Na source. We developed several algorithms to define the start of the signal in order to optimize the time resolution. Different sampling rates were studied by averaging adjacent samples. A timing resolution of ~3 ns at 511 keV was obtained with an extended constant-fraction method and averaging 4 samples resulting in an effective sampling rate of 125 MHz.

3.6.1. The 8 channel pulse shape digitizer board

The measurements described above indicate that 12 bit amplitude conversion and sampling rates of 100 MHz are required for good energy resolution and to preserve the position and time resolution required for the ~5000 channels in a 40-module array. To demonstrate the feasibility of such a system an 8-channel, 100 MHz, 12-bit ADC board was designed and constructed in 2002 (figure 3.16). Unlike some commercially available ADC boards, which perform only waveform digitization, the 8-channel prototype board is capable of performing real-time digital signal processing with a functionality equivalent to standard analog electronic systems for Ge detectors. Currently implemented functions include:

- A leading edge discriminator employing a binomial filter to generate internal triggers.
- A constant fraction discriminator to provide energy-independent timing.
- An energy algorithm, which employs a user adjustable trapezoidal filter to optimize S/N for energy determination.
- A user adjustable window to extract relevant parts of the pre-amplifier pulse for subsequent signal decomposition.

Also provided on the board are three trigger modes (internal, external, and combined) for each channel allowing maximum flexibility. Readout of the prototype ADC board is carried out over a VME bus to simplify integration into current data acquisition systems, and is designed for a sustained counting rate of 10 kHz, typical of in-beam experiments. The readout for the final system (section 4.2), which will have a higher channel density, will use a much faster data transfer system.

The design and construction of the 8-channel board (including full simulations of the complex VHDL code required to implement the above functions) has been successful. The ability to carry out the required signal processing on a single large FPGA without the need for a dedicated on-board CPU or DSP has considerably reduced the cost and development time for this project. More 8-channel boards will be fabricated and fifteen of them will be integrated in a 120-channel acquisition system required for the three-crystal Gretina module prototype (described below). This board meets the specifications outlined at the digital electronics workshop held in Argonne (2001) for a general-purpose digital signal processing board for the low-energy nuclear physics community and will serve as the prototype for a more complex 40 channel ADC board required for the Gretina array.
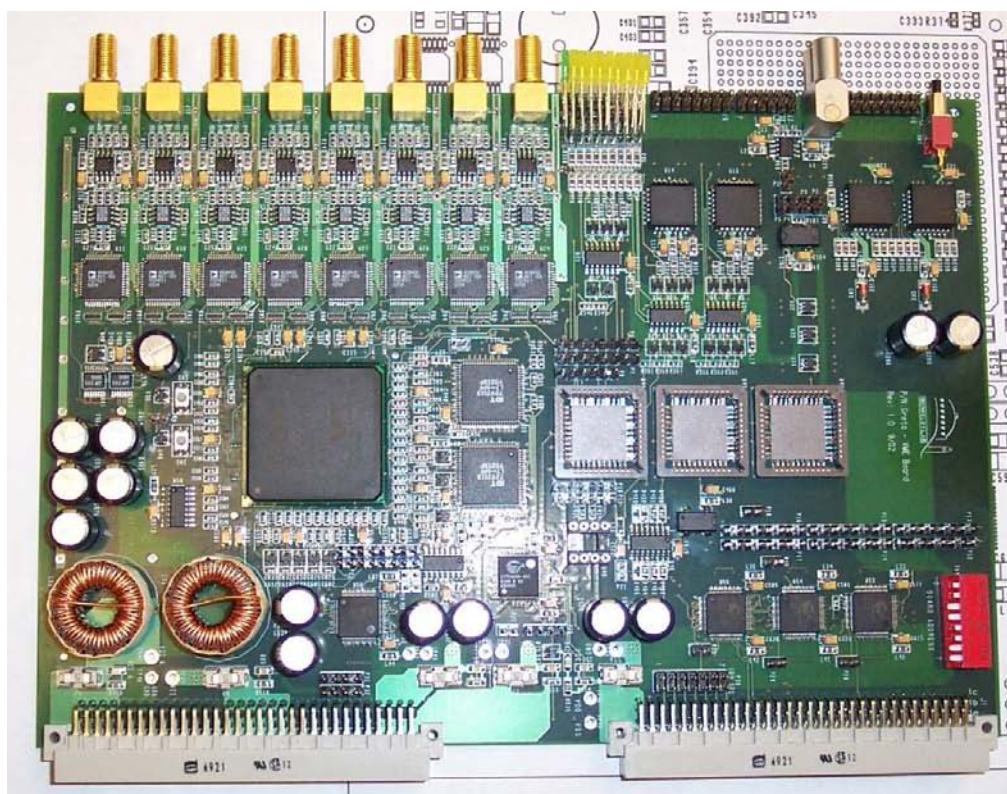
Figure 3.16. The 8 channel prototype digital processing board.

3.7. The Gretina Triple Crystal Module

A triple-crystal detector module was ordered in September 2002, and delivery is expected at the end of 2003. The design of this prototype integrates all the technology needed for a complete Gretina detector module. Such a module consists of three encapsulated Ge detectors, each with 36 segments, placed in a single cryostat. Each crystal gives 37 signals (from the 36 segments and one central electrode) amplified with cold FETs mounted in the cryostat. Since such a module may be regarded as the 'basic unit' from which Gretina will be constructed, by accepting the order the manufacturer has indicated that there are no fundamental fabrication issues for the full array. (It is important to note that the Gretina detector module is also the basic unit for a 4π array and any future scaling to a full array requires no additional detector development.)
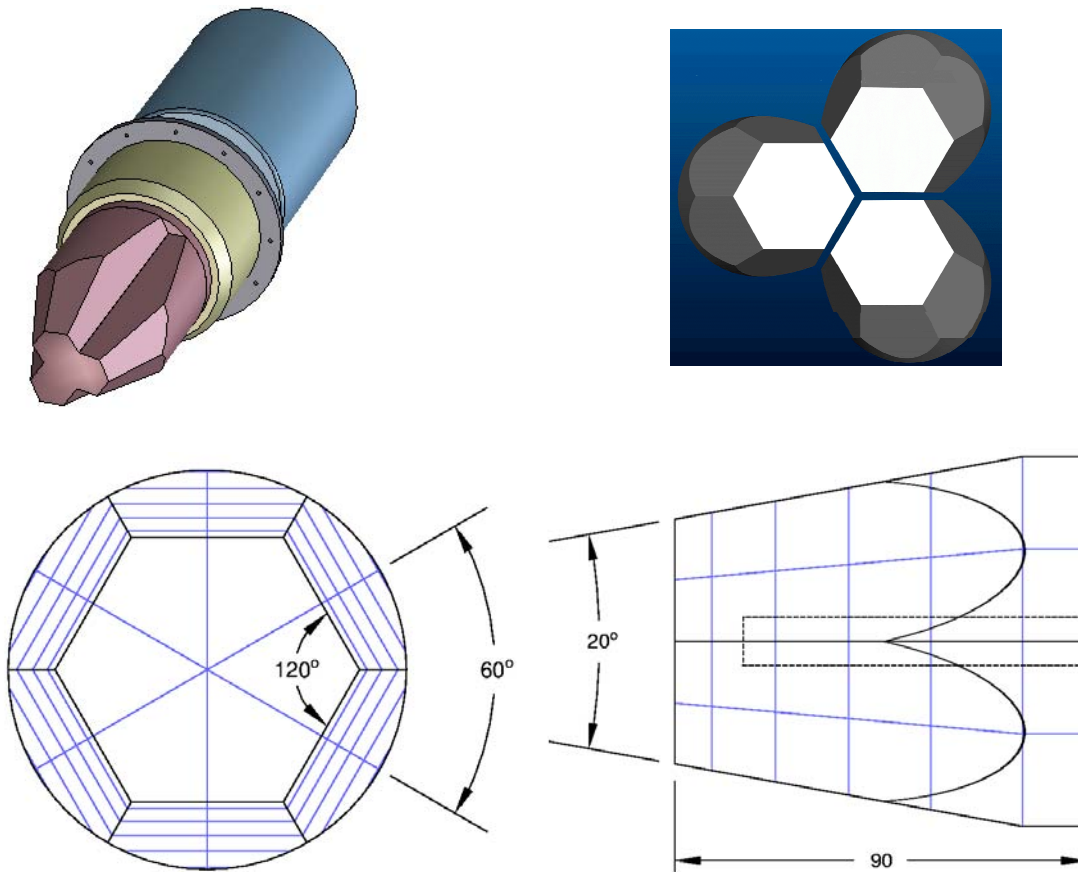
Figure 3.17. Drawings of the 3 crystal Gretina prototype module showing the closed packed geometry of the tapered regular hexagonal crystals. Each crystal has 36 segments. The dimensions of one of the crystals is shown together with the segmentation.

Each crystal, before it is shaped, has a diameter of 8 cm and a length of 9 cm. To simplify the production of this first module, a regular tapered hexagonal shape was chosen. As shown in the figure 3.17 the crystal has a taper angle of 10 degrees between the axis and the center of a flat surface, and the apex of

the extrapolated tapered surface is 15 cm from the front surface of the crystal. The first 5 cm of the crystal is fully tapered, the next 3 cm are partially tapered, and the last 1 cm of the crystal retains the original cylindrical shape of the crystal (not tapered). This shape maximizes the distance from the source to the detector, allows more space for an auxiliary detector in the target chamber, and optimizes the germanium coverage of the shell space between 15 and 26 cm. Six longitudinal segmentation lines are placed at the centers of the flat faces. The transverse segmentation separates the crystal into 6 unequal "layers" with thickness of 1.0, 1.2, 1.6, 1.8, 2.0, and 1.4 cm. The crystals are packed closely in one cryostat with minimal gamma-ray absorbing material. The distance between the crystals is 3.5 mm and the distance between the crystal and the cryostat wall is 4.5 mm.

3.8. Other Developments

Significant effort has gone on worldwide towards the development of highly segmented large volume germanium detectors and the realization of a gamma-ray tracking array. A summary of arrays of segmented detectors (more than 2-fold segmentation) is shown below.

Name	# of crystals	Size[a]	Shape	# of segments[b]	Crystals/cryostat	Status
SeGA[c]	18	7×8	cylinder	4×8	1	operational
EXOGAM[d]	64	6×7	square	4×1	4	operational
MINIBALL[e]	40	7×7.8	reg. hexagon	6×1	3,4	operational
TIGRESS[f]	64	6×9	square	4×2	4	prototype
AGATA[g]	180	8×9	irr. hexagon	6×6	3	prototype

[a]diameter × length in cm before shaping
[b]azimuth × length
[c]Michigan State University, USA
[d]GANIL, France
[e]REX-ISOLDE, CERN
[f]TRIUMF, Canada
[g]Europe

In the following we will briefly describe the AGATA and SeGA arrays, which are most relevant to Gretina

3.8.1. AGATA: The Advanced GAmma-Tracking Array

The European efforts in γ-ray tracking are focused on the AGATA project [Ag03]. AGATA, the Advanced Gamma-Tracking Array, is a 4π array of segmented coaxial detectors. The original design consists of a geodesic tiling of a sphere with 12 regular pentagons and 180 hexagons. To minimize inter-detector space losses while still preserving modularity, 3 hexagonal crystals are arranged in one cryostat (fig 3.18). The pentagonal detectors are individually canned. The inner radius of the array is 17 cm. The total solid angle covered by germanium material is close to 80% and the photo peak efficiency is 50% for an individual 1 MeV γ-ray. The AGATA collaboration includes 38 institutions from Bulgaria, Denmark, Finland, France, Germany, Italy, Poland, Sweden and UK, and the estimated cost for the project is 40MEuros and the manpower 150 FTEs. It could be completed in 8 years.
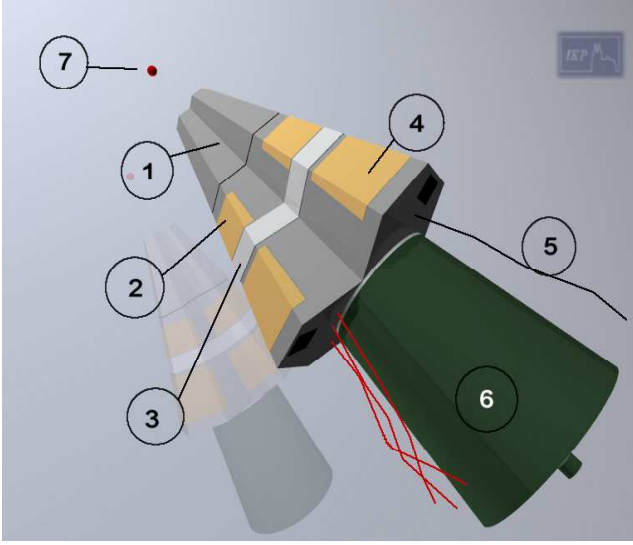
Fig. 3.18. Simulation of the AGATA Detector Module consisting of (1) three 36-fold segmented Ge detectors, (2) preamplifier, (3) frame support, (4) digital pulse processing electronics, (5) fiber-optics read-out, and (6) LN_2 – dewar.
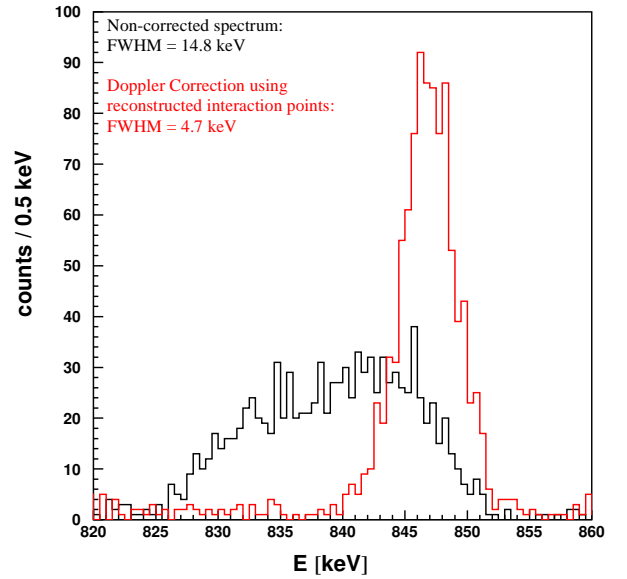
Fig. 3.19 The 2^+ transition in ^{56}Fe before and after Doppler reconstruction using a genetic algorithm. The expected energy resolution is 3.5 keV for perfect tracking and 4.2 keV for a position resolution of 5 mm.

A significant amount of R&D has been supported by the TMR Network project and included work on simulations and tracking, calculations of pulse shapes, signal decomposition, and development of segmented detectors. These efforts resulted in the AGATA proposal. It is important to note that most AGATA results are consistent with those obtained by the Gretina collaboration. A segmented prototype detector with 6 azimuthal and 4 longitudinal segments plus an extra segment in the front was built by Eurisys for the Legnaro-Padova group. Using this detector the collaboration demonstrated that tracking can be used to locate the position of the first interaction point and correct for Doppler broadening. In this measurement a beam of ^{56}Fe at 240 MeV was Coulomb excited by a ^{208}Pb target. The recoils, with v/c ~8%, were detected in an array of 15 tightly collimated particle counters positioned at approximately 90º from the prototype. Figure 3.19 shows the Doppler corrected spectrum generated by the reconstructed points obtained by a tracking using a genetic algorithm. The FWHM of 4.7 keV for the 2^+ transition in ^{56}Fe (846 keV) is very close to the 4.2 keV expected from simulations including a position resolution of 5 mm. This result is an important milestone in the development of a gamma-ray tracking array.

The AGATA and Gretina designs share a great deal of common technology and therefore the two projects have benefited and will continue to benefit from common developments in all areas of R&D.

3.8.2. The SeGA array

The National Superconducting Cyclotron Laboratory (NSCL) at Michigan State University has developed the SeGA [Mu01] 32-fold segmented germanium detector array optimized for in-beam γ-ray spectroscopy experiments with fast (v/c = 0.3-0.5) exotic beams. The SeGA array consists of 18 individual detectors. Each cylindrical crystal is 8 cm long and 7 cm in diameter and made of n-type high-purity germanium. The outer p-type ion-implanted contact of the crystal is vertically segmented into four longitudinal segments and horizontally segmented into eight transverse segments. The detectors are placed "side-on" to the gamma-ray source (target) and the transverse segments provide the angular resolution for Doppler correction.

The array is in operation and the design goals have been achieved. The central contact energy resolution varies between 2.5 keV and 2.8 keV. The average resolution of the 32 side channels is 2.5 keV for all but the four segments at the front where the average resolution is 3.3 keV (all resolutions were measured at 1332 keV). Each crystal is about 75% efficient relative to a 3"x 3" NaI detector. Peak-to-total values range from 0.210 to 0.216. The time resolution ranges from 7.0 ns to 9.0 ns (FWHM) for energies greater than 100 keV from a ^{60}Co source. The flexible design of the array was optimized for fast beam experiments. The detectors can be arranged in several configurations with distances to the target varying from 10 cm to 100 cm.

SeGA demonstrates that it is possible to manufacture a large number of reliable highly segmented coaxial germanium detectors. It also provides an opportunity to develop signal decomposition and tracking algorithms and this future effort will be coordinated with the development of digital signal processing for Gretina.

3.9. Summary and Conclusions of the Technical Development

We have shown that it is possible to manufacture a segmented Ge crystal that can be used as an element of a gamma-ray tracking array and to carry out the signal processing needed to reconstruct gamma-ray energies. This was done by demonstrating "proof-of-principle" in the following key areas; intrinsic detector performance, signal/position sensitivity/resolution, signal decomposition, and gamma-ray interaction tracking.

The results are summarized as follows:

- A 36-fold segmented Ge detector (single-crystal) was extensively tested. Energy resolution as well as noise characteristics have been measured and found to exceed expectations. For example, the segments had an average energy resolution of 1.93 keV for a gamma-ray energy of 1.33 MeV and a noise value of ~ 5 keV for a bandwidth of 35 MHz. This low noise level implies a very low energy threshold for the identification of an energy deposition in a segment.

- The position sensitivity for both one and two interactions in a segment was determined by analyzing measured and simulated pulse-shape differences relative to the noise for different locations.

- Algorithms to extract the location of gamma-ray interactions from the pulse shape were explored. In general these algorithms attempt to fit the observed signal(s) to a pre-calculated set

of "basis" signals. The process is complicated by the fact that the measured pulse can be a superposition of multiple basis signals. An algorithm based on a fast minimization procedure, called the sequential quadratic programming method, gave position resolution of order 1-2 mm, and reached convergence in about 0.025 second. Several other approaches, e.g. singular value decomposition and wavelet analysis, have also been investigated. The results show that it is possible to decompose a signal and extract the interaction locations. The signal decomposition process is a challenging problem and optimizing the signal processing algorithms for both accuracy and speed remains an active area of R&D.

- Tracking algorithms were developed that reconstruct the individual gamma-rays energies from sum of the interaction locations. They take into account Compton scattering, pair-production, and the photo-electric effect, which are the dominant interaction processes for gamma rays with energies between 0.1 MeV and 15 MeV and can resolve multiple gamma rays of different energies. They also accurately identify the first interaction point, which is crucial for proper Doppler correction of gamma-rays emitted from fast moving nuclei (velocities up to 50% of c).

- Comprehensive end-to-end tests of the 36-fold segmented prototype have been performed using radioactive sources of ^{60}Co, ^{137}Cs and ^{152}Eu. These tests demonstrate that by combining all the separate elements of Gretina the resulting system performs as expected.

- A triple-crystal detector module was ordered in September 2002, and delivery is expected towards the end of 2003. The design of this prototype integrates all the technology needed for a complete Gretina detector module and may be regarded as the 'basic unit' from which an array will be constructed. By accepting the order the manufacturer has indicated that there are no fundamental fabrication issues for the full array.

- An 8-channel, 100 MHz, 12-bit ADC board was designed and constructed. It is capable of performing real-time digital signal processing (providing time and energy) and implements a user-defined window to extract relevant parts of the pulse shape for subsequent signal decomposition. The board has three trigger modes (internal, external, and combined) for each channel allowing maximum testing flexibility. The ability to carry out the required signal processing on a single large FPGA without the need for a dedicated on-board CPU or DSP has considerably reduced the cost and development time for this project. More 8-channel boards will be fabricated and fifteen of them will be integrated in a 120-channel acquisition system required for the three-crystal Gretina module prototype.

- Significant worldwide effort has gone towards the development of highly segmented large volume germanium detectors and the realization of a gamma-ray tracking array. This is an ongoing effort and it important to realize that there is opportunity for the major projects such as AGATA in Europe and Gretina in the U.S. to share R&D. To date, the various collaborations have enjoyed frequent and open dialogue and the aim is to maintain these connections in the future.

4. THE GRETINA DETECTOR ARRAY

In this section we describe the design and performance of the Gretina detector system. We begin with a review of the detector packing schemes for the 4π array. This defines the geometry for Gretina, which is ¼ of 4π array. The design of the germanium modules, data acquisition hardware and software, as well as the mechanical support and liquid nitrogen filling system is then discussed. At the end we briefly describe a few examples of the auxiliary detectors planned for use with Gretina. The expected performance of Gretina is listed in Appendix B.

4.1. Gretina Geometry

A spherical shell of germanium is the most symmetric and compact configuration for a 4π array. It provides the best solution in terms of solid angle coverage, spectral response, modularity, free inner space, and germanium usage, as well as being ideally suited to the measurement of angular distributions, angular correlations, and lifetimes from Doppler shifted energies. Two design parameters for such a shell include its inner radius and the thickness of the shell. The inner radius is determined by the space for the target (ranging from 1 cm for re-accelerated beams to several cm for fragmentation beams), and for placing auxiliary detector inside the chamber (see section 4.4). In addition, time-of-flight measurement, for neutron-gamma separation in the germanium detector and mass identification of heavy ions in detectors such as CHICO, requires a target to detector distance of the order of 10 – 20 cm.

The thickness of the shell determines the efficiency of the array and becomes crucial for high-energy gamma rays. The detection efficiency increases logarithmically with the detector thickness. For example, a shell 10 cm thick will give an efficiency of 0.8 for a 1 MeV gamma ray, while a shell of 9 cm thick will give a slightly lower efficiency of 0.76. Gretina will have a target to crystal distance of 15 cm and a thickness of 9 cm.

4.1.1. Geodesic design

A spherical shell of detectors can be designed on the basis of the geodesic dome proposed by the architect Buckminster Fuller. The basic idea is to cover the spherical surface with the 20 triangular faces of the icosahedrons. Each triangle can then be covered with a specific number of hexagons depending on the symmetry requirements, which then tile the spherical surface leaving a given number (12) of pentagon holes. Possible solutions for the total number of hexagons and the number of different hexagonal shapes required to tile a spherical surface are listed in table 4.1[3]. Once the number of elements is fixed, the size and the shape of the detector have to be decided. The goal is to minimize the inter-detector spaces and the inactive material associated with each detector. Currently, the largest Ge detector that can be made with reasonable yield and cost has a diameter of 8 cm and a length of 9 cm. Using this size of crystal and a distance of approximately 15 cm, about 100 detectors are needed to fill a shell. The detectors are cut from cylindrical crystals and the pentagons and hexagons provide the more efficient use of material usage compared with other shapes, such as rectangular detectors. The taper meets at the center of the sphere, so one crystal or a group of crystals can be removed radially.

---

[3] The Gretina geometry will be classified by the number of hexagons. For all geometries there are an additional 12 pentagons, many of which can also contain germanium detector elements.

The Gretina design is based on the 120-hexagon geometry, as shown in figure 4.1, with 120 irregular hexagons and 12 pentagons. In this geometry there are two types of hexagons, 60 of each type, and the angles for these two types are shown in table 4.2. The 120-hexagon design has advantages over the neighboring 110 and 150-hexagon designs. The 110-hexagon geometry uses 3 hexagon types making it difficult to pack them into a few styles of identical modules with 3-4 detectors per module. The 150-hexagon design gives a larger inner radius, but also a larger cost due to the larger number of detectors.
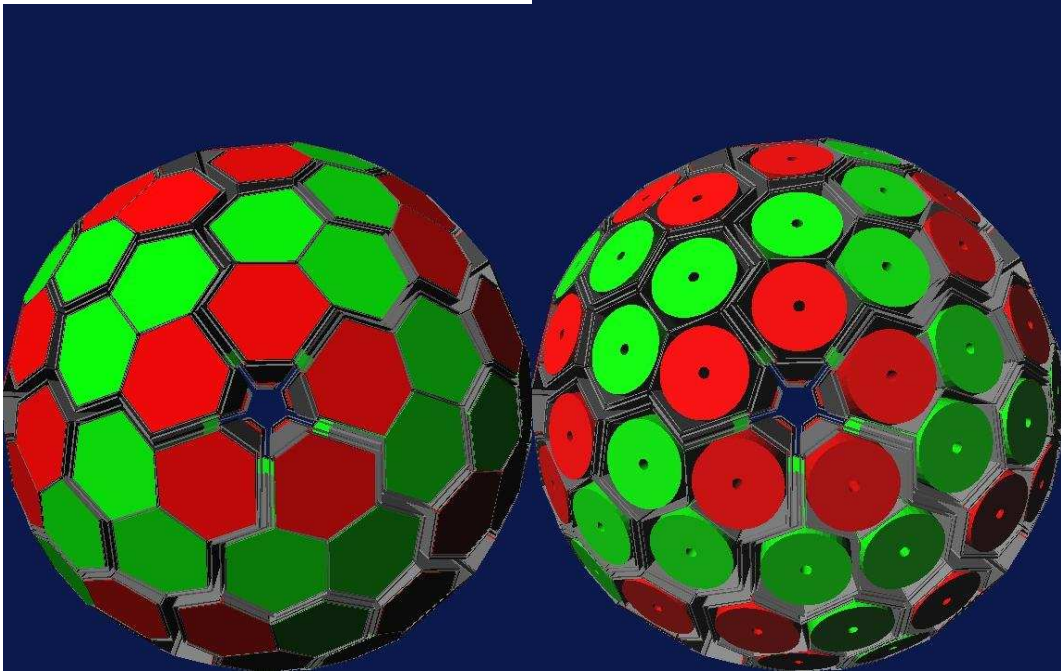
Figure 4.1: The 120 hexagonal detector geometry. Detectors are grouped into 40 triple clusters of two kinds (AAB and BBA). In the picture the red hexagons represent hex-A detectors, the green represent hex-B detectors. Each crystal is encapsulated.

Number of hexagons	Number of different of hexagonal shapes
80	2 (20, 60)
110	3 (20, 30, 60)
120	2 (60, 60)
150	3 (30, 60, 60)
180	3 (60, 60, 60)
200	4 (20, 60, 60, 60)

Table 4.1. Possible solutions for the total number of number of hexagons and the number of different hexagonal shapes required to tile a spherical surface. Each solution has 12 pentagons in addition to the stated number of hexagons.

Hexagon A

φ [Degree]	θ [Degree]	η [Degree]
57.96	61.83	60.20
61.50	59.41	59.07
67.30	55.79	56.91
61.23	59.83	58.92
57.96	60.21	61.83
54.02	62.99	62.99

Hexagon B

φ [Degree]	θ [Degree]	η [Degree]
52.63	63.68	63.68
61.50	59.08	59.42
61.24	58.93	59.84
58.66	61.83	59.50
58.66	59.50	61.84
67.30	56.91	55.79
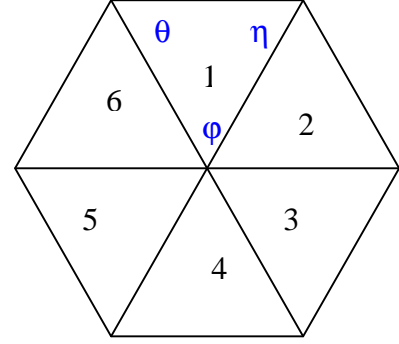
Table 4.2: Angles of the hexagonal crystals used in the 120 hexagon geometry. Two types of slightly irregular hexagons are required.

It is worthwhile noting that the 180 hexagonal detector solution, with slightly larger inner radius (16.8 cm) and solid angle coverage (77.2%), offers higher symmetry as well as a more natural way of packing three crystals in one cryostat. This design is being considered as a solution for the AGATA array (see section 4.7.1). Due to the higher number of detectors and the larger amount of Ge this solution is far more expensive than the solution described here.

The detectors are placed in cryostats, which maintain the germanium crystals at liquid nitrogen temperature and provide a clean environment to avoid contamination of the detector surface. Typically, there is a 4-5 mm space between the crystal and wall of the cryostat for thermal insulation. This makes the gap between crystals about 1 cm, which reduces the solid angle coverage. Currently, it is possible to pack multiple crystals in a single cryostat with a gap of 3.5 mm between the crystals. Packing 3 to 4 crystals per cryostat increases the solid angle coverage by 4-5% of 4π compared with 1 crystal per cryostat. The 120-hexagon configuration with two crystal shapes (A and B) can accommodate either 3 crystals per cryostat or 4 crystals per crystal. The three-crystal design requires six types of module, three of type AAB and three of type ABB. The four-crystal design has the advantage of using only one type of module AABB. Currently, we are pursuing the 3-crystal design (see figure 4.2). This decision is based on detector cost estimates and after consideration of the complexity and risk of fabrication. However, having only one type of module (AABB) is advantageous and reduces the total amount of space between crystals and cryostat, and we will continue to study the benefits and feasibility of the 4-crystal design.

Figure 4.2. Drawing of the 3-crystal module. Dimensions are in mm.
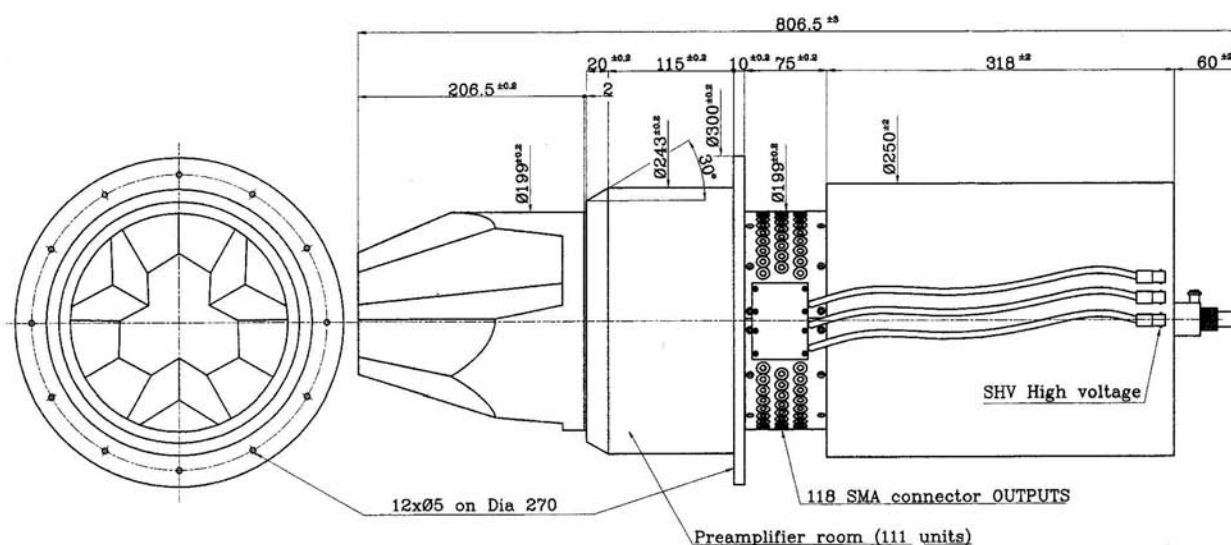
4.1.2. Detector arrangements

Gretina consists of 10 3-crystal modules described in the previous section. The 10 modules can be arranged in a number of ways depending on the physics requirements. Two proposed configurations for Gretina are shown in figure 4.3.

1. A symmetric arrangement clustered tightly around 0 or 180 degrees with respect to the beam, with an angular coverage of 17 degrees to 55 degrees.
2. An asymmetric arrangement, which extends the angular coverage from 17 to 101 degrees.

The first configuration offers a more compact solution with the minimum edge effect, while the second provides the capability to perform angular distribution measurements

4.1.3. Cryostat design

Three crystals are packed closely in one cryostat with minimal gamma-ray absorbing material. The distance between the crystals is 3.5 mm and the distance between the crystal and the cryostat wall is 4.5 mm. The cryostat walls on the side of the detector follow closely the tapered shape of the crystals and the taper continues until they intercept the cylindrical part of the cryostat. This ensures that there is no interference from the neighboring modules when a module is removed from the array. The detector modules are mounted on the support structure (see section 4.3.1) using a precision flange.

Each crystal provides 37 signals (36 segments and one central electrode). These signals pass through a feed-through on the encapsulation canister and are amplified by cold FET's (a total of 111 signals) mounted in the cryostat and go through another set of feed throughs to exit the cryostat. Additional feed throughs are provided for high voltage and pulser input. The Dewar design will provide means for annealing the crystal. These include internal heaters, thermometers, and pumping port.

The Dewar will have a liquid nitrogen holding time of at least 16 hours, and it is connected to an automated liquid nitrogen filling system (see section 4.3.2)
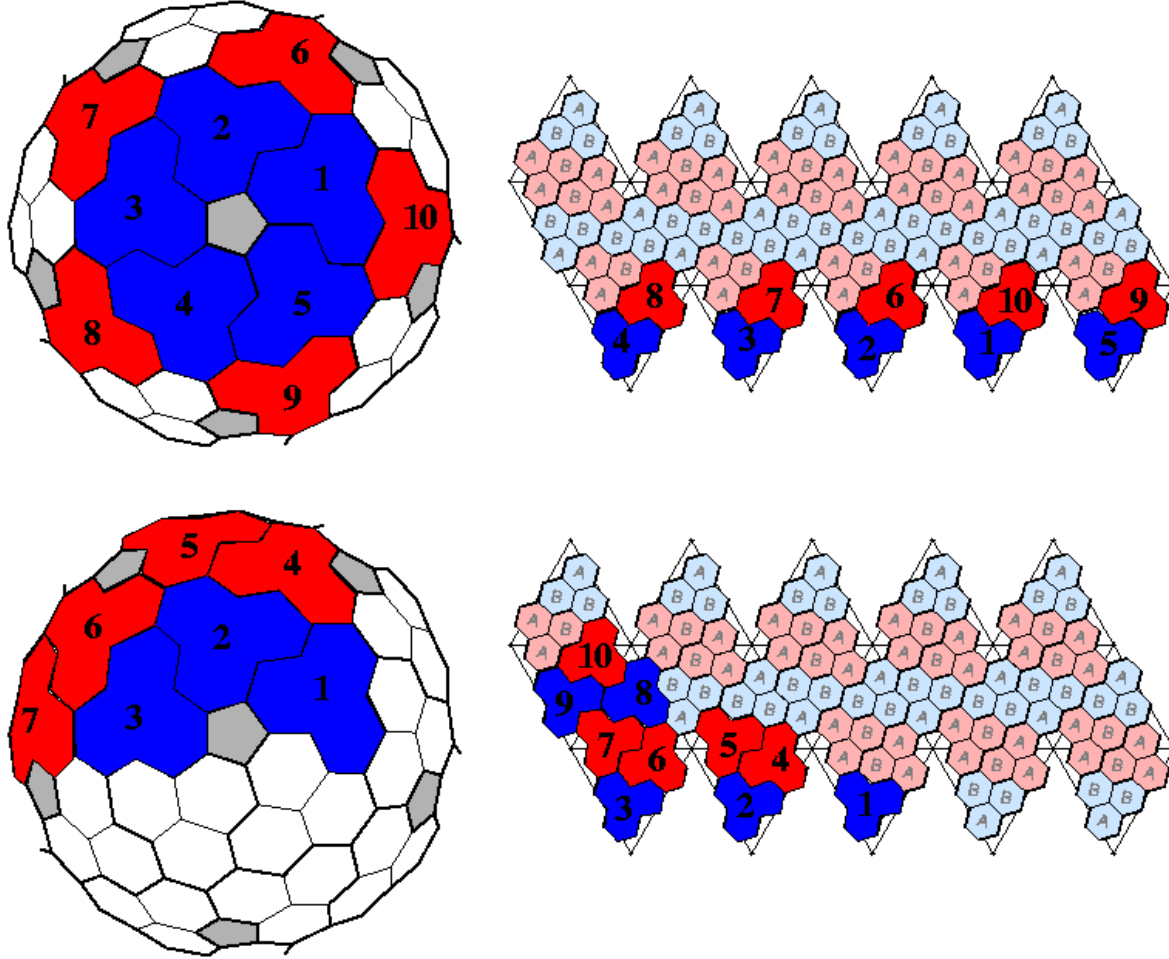
Figure 4.3: Two geometric configurations of Gretina. The first configuration (top) is a closed packed symmetric section of the sphere. The second configuration (bottom) is an asymmetric section of the sphere, consisting of the 10 neighboring clusters which better cover the angle between 17 and 101 degrees. On the right side of the picture, the planar projection of the sphere is shown.

4.1.4. Simulation results

Detailed Monte Carlo simulations have been performed using the code Geant 3.21. As well as presenting the results for Gretina, which has 30 detectors, we include results for the 120 detector system for comparison. The 120 detector system is referred to as GRETA.

Due to the complex geometry of the real array and the geometrical limitations imposed by the Geant 3.21 code, some simplifications have been used.

- The array is built from single detectors and not from triple cluster modules.

- An average inter-crystal gap and an average Al can thickness was used to take into account the different gap sizes between Ge crystals in the same cryostat (small gap = 4.5 mm) or between different cryostats (large gap = 10 mm), and the differences in the thickness of the Al can (0.8 mm) and that of the Al cryostat (1.1 mm). The following dimensions[4] were used: an average Ge-Ge gap of 7.8 mm, an average Ge-Al gap of 1.9 mm, an average Al-Al gap of 1.5 mm, and a total Al thickness of 3 mm.

Using the above approximations the total solid angle coverage was calculated to be ~80% of 4π for 120 detectors (GRETA) and ~19% for Gretina.
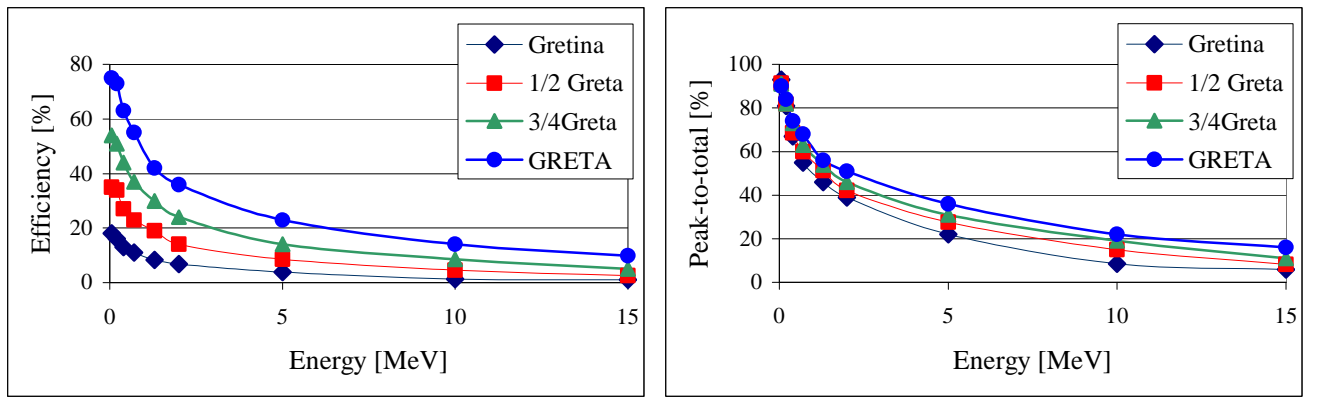
Figure **4.4**: Photo peak efficiency (left) and peak-to-total ratio (right) as a function of the gamma-ray energy for Gretina compared with that of the 60, 90, and 120 detector systems. The results have been obtained by summing all the interaction points produced by the Monte Carlo simulation for multiplicity $M\gamma$=1, i.e. they do not involve any tracking procedure.
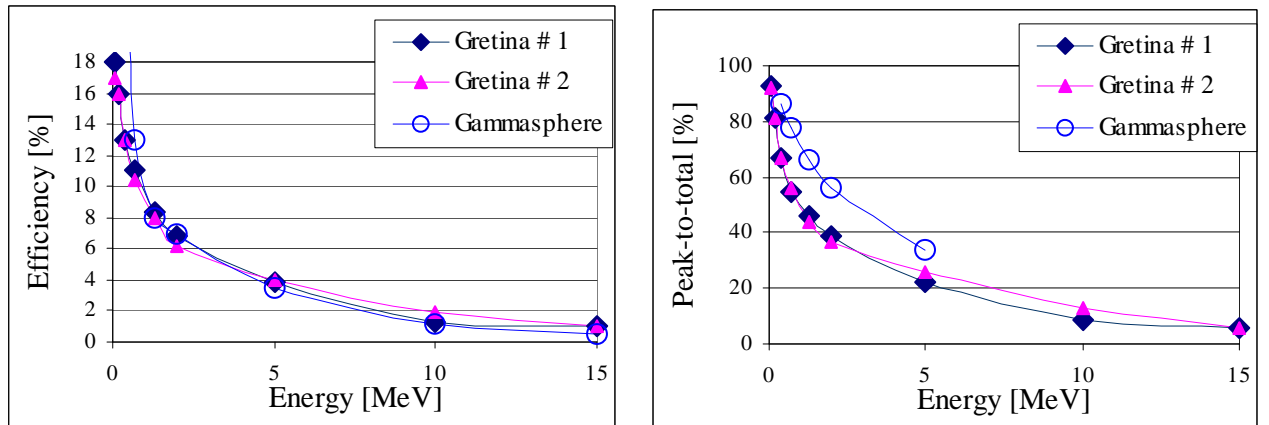
Figure **4.5**: Photo peak efficiency (left) and peak-to-total ratio (right) as a function of the gamma-ray energy for Gretina in the two possible configurations and Gammasphere. The results have been obtained by summing all the interaction points produced by the Monte Carlo simulation for multiplicity $M\gamma$=1.

---

[4] To simplify the Geant code, both the Ge crystals and the gaps are tapered to the center of the sphere. This means that the gaps are not constant along the Ge crystal, but are smaller at the front face and larger at the back. For this reason, the average gap and average Al thickness have been estimated in the middle of the Ge length.

The photo peak efficiency and peak-to-total ratio calculated as a function of the gamma-ray is given in figure 4.4 for Gretina (30 detectors). Also shown for comparison are the values for a 60, 90, and 120 detector system. In figure 4.5 the efficiency and peak-to-total for Gretina is compared to Gammasphere. These results have been used in the calculation of the resolving power reported in the following section. They were obtained by summing all the interaction points produced by the Monte Carlo simulation for multiplicity $M_\gamma=1$ and therefore they represent a maximum. For the physics case outlined in chapter 2, it is important to note that Gretina will have a higher resolving power compared with any existing array.

4.1.5. Performance

The performance of a gamma-ray detection system is determined by a number of parameters. Large full-energy efficiency (ε), good energy resolution (δE_γ), high peak-to-total ratio (P/T) and high position resolution are the most important. Therefore, our primary design goals are to maximize the efficiency and peak-to-total of the array and to preserve the energy resolution close to the intrinsic values, even in experiments involving fast-moving sources. In a K-fold γ-ray coincidence experiment, the sensitivity for detecting the weakest reaction channel or decay path increases as R^K, where $R=(\Delta E/\delta E_\gamma)(P/T)$ is the gain per fold, while the counting statistics improve as ε^K.

To compare the performance of different detector systems we use the resolving power (RP), which takes into account the parameters mentioned above and defines the weakest branch ($\alpha=1/RP$) that can be resolved by the array with a given sensitivity in peak-to-background. In typical high-multiplicity experiments this prescription determines an optimum fold and the $RP = R^{optimum\ fold}$. However, in applications involving low-multiplicity reactions, e.g. at a fragmentation facility, the event multiplicity could be less than the optimum fold and we define a figure of merit $\xi = N/\sigma$, where N is the number of counts in a given multi-dimensional peak and σ is the statistical fluctuations. Assuming a total of N_o events, the weakest branch that can be resolved is obtained by the solution of the equation:

$$\varepsilon^K X^2 - \xi^2 X - 2\xi^2 N_o/R^K = 0$$

where $X=\alpha N_o$. It can be shown that this approach agrees with the standard formulation of the resolving power, and corresponds to a 6-sigma peak (i.e. $\xi = 6$) at the optimum fold. For consistency, we have used that same figure of merit in the following estimates.

To evaluate the expected performance of Gretina we have considered several examples of experimental conditions that span a broad range of applications:

Slow-Beam Reactions: Coulomb excitation, transfer and fusion, as well as deep inelastic collisions are the most common reactions used to study single-particle and collective properties of nuclei. With stable beams and targets one generally has the choice of performing these reactions in either normal or inverse kinematics. Normal kinematics use lighter beams that are both easier to accelerate to the desired energies, and result in smaller Doppler corrections.

High γ-Ray Multiplicity Reactions: Many reactions between heavy ions and heavy targets at or above the Coulomb barrier produce residues at very high angular-momentum. Gamma-ray decays of these products may result in gamma-ray multiplicities in the range of $M_\gamma=15$-25, which increases the chance of multiple hits in a single crystal, or multiple interactions in a segment.

Fast-Beam Experiments: Nuclei from fragmentation reactions have very high velocities (v/c up to 50%) and low intensities. A tracking array provides an ideal detector for these experiments because of its large efficiency and, most importantly, its high angular resolution for Doppler correction.

Table 4.3 shows the resolving power expected under different experimental conditions covering most of the physics needs. The results are also presented in figure 4.6 where Gretina is compared to the full 120 detector GRETA array together with the performance of Gammasphere and SeGA. The numbers show that even for slow-beam reactions Gretina is comparable to Gammasphere, but it is for fast-beam applications that the impact of Gretina is more important due to the excellent position resolution combined with the large efficiency. The calculations assume that there is no contribution to the energy resolution from the uncertainty in the direction of the emitting fragment.

Table 4.3. The calculated resolving power of Gretina and GRETA for a variety of different reaction types ranging from β-decay (low multiplicity and v/c = 0) to fragmentation of fast beams, to very high-spin fusion evaporation reactions.

Type of Reaction	$<E_\gamma>$ (MeV)	v/c	M_γ	Resolving Power	
				GRETA	Gretina
1 Stopped	5.0	0.0	4	5×10^6	1×10^5
2 Stopped	1.5	0.0	4	2×10^7	6×10^5
3 High-spin Normal Kinematics	1.0	0.04	20	8×10^5	6×10^4
4 High-spin Inverse Kinematics	1.0	0.07	20	8×10^5	6×10^4
5 Coulex/transfer	1.5	0.1	15	9×10^5	9×10^4
6 Fragmentation	1.5	0.5	6	2×10^6	8×10^4
7 In beam Coulex	5.0	0.5	2	1.5×10^5	7×10^4
8 In beam Coulex	1.5	0.5	2	2×10^5	1.5×10^5
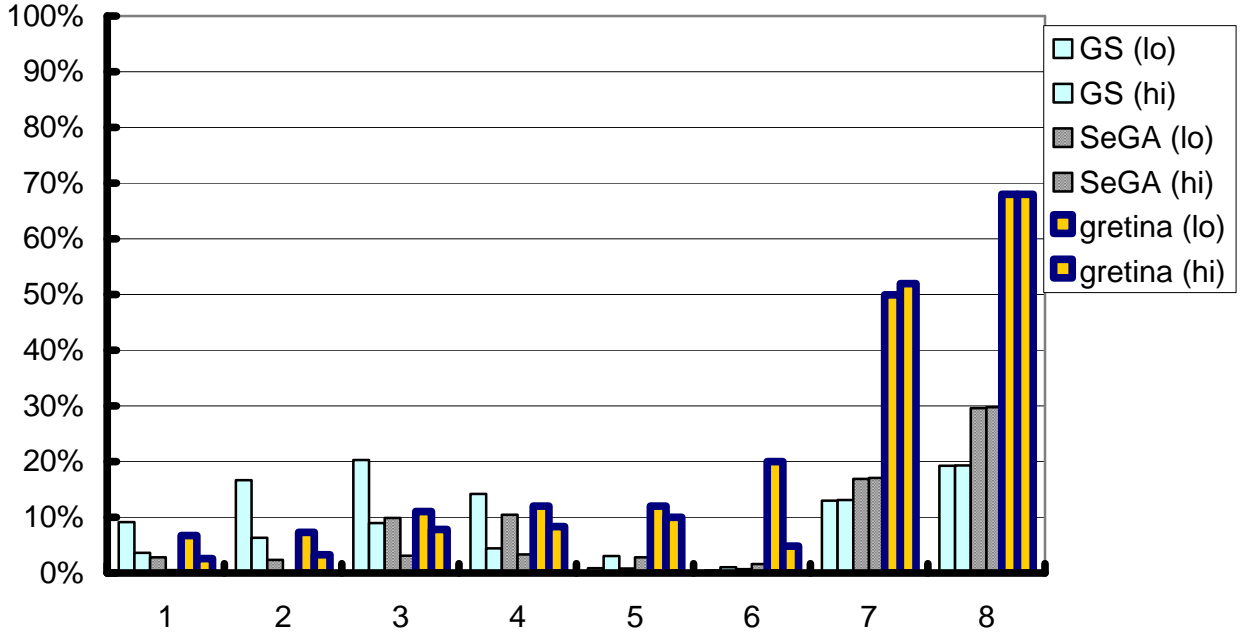
Fig 4.6. Resolving power (relative to a full 120 detector 4π tracking array) for Gretina, Gammasphere, and SeGA for the different reaction types given in Table 4.3. We have considered two cases per reaction: a high beam intensity limit (hi) of ~1pnA and a low intensity limit (lo) of ~10^6 pps.

4.2. Electronics and Data Acquisition

4.2.1. Pre-amplifiers

The Gretina germanium pre-amplifier consists of a charge sensitive first stage and a differentiating second stage. The input transistor, feed back capacitor, and resistor are mounted inside the sealed detector and are supplied by the detector manufacture. The input field effect transistor, InterFET IF1331, has approximately $2nVHz^{1/2}$ noise. Therefore the noise contributed by the preamplifier is negligible.

The rise time of the pre-amplifier will be determined by the wiring inside the detector. For the GRETA prototype detector the rise time is about 15 ns but the feed throughs required with the Gretina detector and the increase in wire length may result in slower rise time. The differentiating second stage produces a pulse with a decay time of 50 microseconds, which will allow a counting rate of 20 kHz per segments without appreciable pile up. The output signals have a gain of ~50 mV/MeV that matches the range of the input stage of the signal digitizer.

The pre-amplifiers and mounting structure shown in the photo in figure 4.7 correspond to a present design for a segmented detector. The Gretina pre-amplifier is similar, but the size is reduced and the board spacing is closer. Also, for ease of installation, the wiring for the input connects through the motherboard.
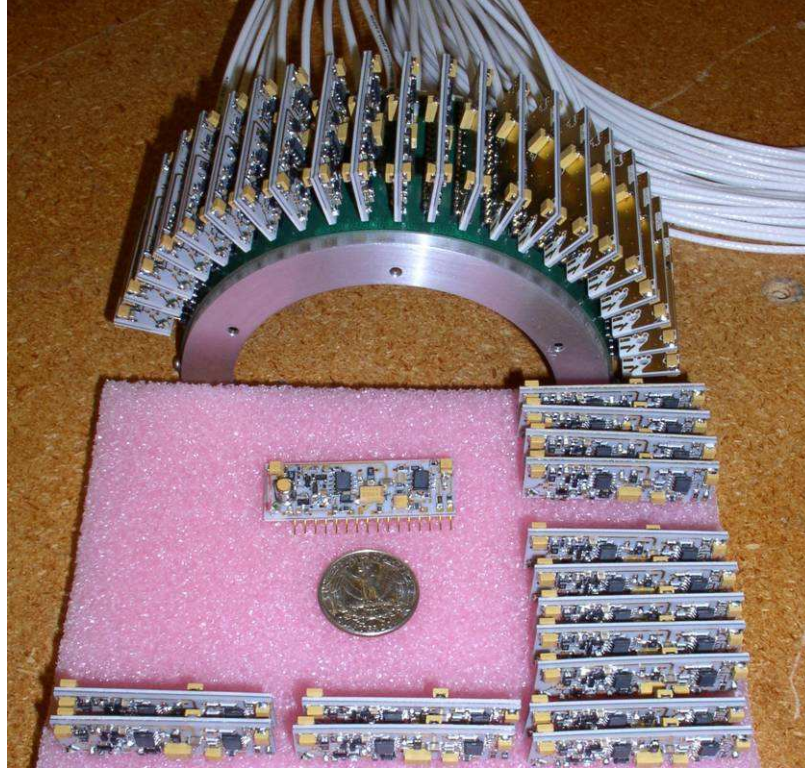
Figure 4.7. Pre-amplifiers and mounting structure used in an existing segmented detector.

4.2.2. Signal Digitization Board

The digital electronics module for Gretina is responsible for digitizing the induced current pulse from each segment, implementing a prompt first-level trigger, and carrying out simple algorithms on the data stream to reduce the data rate to the farm of signal decomposition processors. The need to perform detailed signal decomposition, combined with the variety of experiments Gretina will support places a number of requirements on the digital electronics module. First, the minimum sampling frequency of the digitizer is required to be 100 MHz to give a sufficient number of samples over the charge collection time (300 ns) to decompose multiple charge deposition sites within a segment and to provide the required time resolution. Second, the dynamic range of the digitizer must be 14 bits to give an energy resolution of 18 bits for reasonable integration times (< 6 μs). This large dynamic range is required in a tracking detector for experiments involving the simultaneous detection of low- and high-energy gamma-rays because having separate low- and high-gain channels is impractical. A third requirement is that the module is capable of processing a gamma-ray rate of 50 kHz per crystal and a readout rate (following the module level first level trigger) of at least 10 kHz. This implies a readout rate for each digital electronics module of 10 Mb/s (100 bytes/segment * 10 segments/gamma * 10^4 gammas/s). Finally, each signal within a Ge crystal is required to be associated with a global timestamp to allow gamma-rays from a given event within the detector to be reconstructed by a tracking procedure. Such a timestamp also allows an interface between Gretina and auxiliary detector systems.

The first level trigger for the module requires at least one segment to have a net charge deposition of > 10 keV, which is indicated by a net induced charge in the segment. This activates the readout of the segments where net charge is collected and also the readout of neighboring segments that may contain the image charge signals required by the decomposition algorithm. These prompt triggers are collected by an external, programmable trigger box which, in combination with triggers from auxiliary detectors, generates a validate signal to each digitizer module indicating the event should be read out. A readout latency of at least 20 μs is required by the digital electronics modules to allow for interface with slow auxiliary detectors.

A further reduction in data rate can be achieved by performing simple signal processing on the board. In order to extract energy at Ge resolution, integration of the signal over several μs is required. As only the signal trace during charge collection time (300 ns) is required by the decomposition algorithm, it is efficient to perform the energy integration on the board rather then on a downstream processor. Energy deposition is determined by applying a trapezoidal filter to the ADC signal that can be efficiently implemented in an FPGA. For rates greater then 10 kHz, an adaptive filter is required to maintain good energy resolution while avoiding pileup. Other algorithms are required to filter the signal, determine an event time from leading edge and constant fraction discriminators, and provide a windowing algorithm to capture the relevant part of the signal to be forwarded to the farm of processors performing signal decomposition.

A digitizer module is required for each Ge crystal and has 37 (36 segments + central contact) ADC channels. Given the heat load and component count for such a large number of digitizers, the module would likely be broken into 2-3 digitizer boards with a single trigger/readout board. As stated before, we expect to perform the trigger and other algorithms with FPGA's as was done on the 8 channel prototype board. These FPGA's will also format the data and possibly compress it before it is output to a FIFO for readout. The FPGA's should be programmable through the control system to allow changes to the algorithm. To simplify the design and reduce the cost of the digitizer module, data readout should be done using a high-speed commodity bus such as PCI. If PCI is chosen, it would be sensible to implement the card in a standard compact PCI form factor for which commercial crates, power supplies, and high-performance embedded processors are commercially available.

4.2.3. Signal Processing

A large amount of signal processing must be carried out to convert the raw signal traces output by the digitizer modules into gamma-ray energies and times. The three primary signal processing steps are signal decomposition, event building, and tracking following which the processed data is written to a storage system. A block diagram of the processing steps is shown in figure 4.8. The computational requirements of each step and hardware requirements for the system are given below.

Signal Decomposition

Signal decomposition is the process of extracting positions and energies of the gamma-ray scattering points within the Ge crystal from the signal traces collected by the digital electronics module. It is the most computational intensive part of Gretina data analysis and a description of algorithm developments for decomposition is presented in section 3.3. To achieve a 1-2 mm position resolution for a gamma-ray with multiple interaction points within a segment, the current algorithm requires 0.025s of CPU time with a 700 MHz PIII processor. Advances in microprocessor technology and improvements in the

current algorithms should provide at least an order of magnitude improvement. Given a minimum requirement that Gretina be able to decompose 25k gamma-rays/s at maximal position resolution (1-2 mm), roughly 120 CPU's are required. For experiments where maximum position resolution is not required (stopped, low multiplicity experiments), the data rates are limited by the Ge singles rate and the throughput of the acquisition system.

As the time required to perform signal decomposition currently limits the detector counting rate, a large R&D effort will be carried out during detector construction to develop new algorithms for decomposition. Currently we see several avenues for algorithm improvement. First, some segment signals may be amenable to analysis without resorting to the full decomposition algorithm. For example, in cases where a segment only has a single interaction point, signal decomposition reduces to a simple lookup table. Second, one may use techniques such as wavelet analysis that represent relevant signal information in a more compact form allowing the comparison stage of the fitting algorithm to be faster. Third, alternative algorithms may be pursued which make better use of the information at hand. For example, the decomposition fit routines could be constrained by the physics of Compton scattering to dramatically reduce the size of the search space.

Event Building

The decomposition algorithm provides the position and energy of one or more gamma-ray scattering points from a given crystal at a given time. An event in the detector, which produces several gamma-rays, will have its signals decomposed independently by several processors. The role of the event builder is to collect all interaction points from a given event in the detector with a unique timestamp and forward it to the processors running the tracking algorithm. At this point, time stamped data from auxiliary detectors may also be merged into the event.

Tracking

Tracking is the operation of taking all the interaction points assembled by the event builder from event decomposition, and grouping them into gamma-rays and assigning a scattering order. The algorithms used to carry this out are described in section 3.4. The CPU time for running this algorithm was ~10 ms per event and therefore the tracking algorithm will require 10% of the computational resources required by the decomposition algorithm. This fraction may increase with higher efficiency tracking algorithms.

Event Storage and Experimental Monitoring

Following tracking, reconstructed events are ready to be stored for later analysis. Prompt storage will be to a network attached disk array or large server with archival tape backup. The maximum rate of processed data to disk occurs in experiments where decomposition is minimal or not required and rates are high. For example, an experiment which generates a rate of 5 x 10^4 fold-6 events will produce a data rate of 5 Mb/s. Doubling this to safely accommodate data from auxiliary detectors gives a data rate of 10 Mb/s and this means that 4 Tb of data will need to be stored following ~5 days of continuous running at this rate. Facilities will be provided to copy experimental data to a wide variety of media to suit the needs of different experiment groups.

4.2.4. Hardware Implementation

Given the need for minimally 120 processors to carry out the decomposition algorithm as well as processors needed to carry out the tasks of event building and tracking, the only cost effective means to provide this processing power is with a farm of commodity processors using standard networking

hardware and protocols for communication. Commercial vendors are now introducing cost effective, high-density servers (blades) tailored to the needs of large computational farms. Each server node in such a computational farm is a card that includes one or two processors and are usually equipped with two network interfaces.

A possible implementation of such a system is given in figure 4.8. The 30 digitizer modules required for Gretina are placed in 10 compact PCI crates, with each crate equipped with a single embedded processor board. This embedded processor is responsible for reading out the 3 digitizer modules belonging to a given cluster, placing the data into IP packets and sending these packets to processors running the decomposition algorithm in the processing farm. These embedded processors dispatch events to each processor in the computational farm using a simple round-robin algorithm based on the events timestamp. This provides a simple form of load balancing for the processors performing the decomposition algorithm. As each crate is responsible for forwarding its own packets, there is no single node bottleneck that restricts data flow out of the digitizer modules. Additionally, these embedded processors will run the control software for configuring and monitoring the digitizer modules.

The embedded processors forward their data to the farm of processors for decomposition through two levels of IP switches. Data is first transferred from the embedded processors to a high capacity switch via gigabit Ethernet. The design requirement for readout is 10 Mb/s/card and the embedded processor must be capable of "packetizing" and dispatching data at a rate of 30 Mb/s. This also requires the primary switch to have a bandwidth of 300 Mb/s. Both requirements can be met with currently available commercial embedded processors and switches. The primary switch then fans out this data through gigabit Ethernet to a number of level 1 switches, which are directly connected to one port of each processor in the farm. For the 120 processors performing decomposition the data rate is only 2.5 Mb/s, which can be handled with standard 100Base/T networking.

While the bulk of the processors in the farm will be executing the decomposition algorithm, some processors will be allocated to event building and tracking. Communication between the decomposition processors and the processors executing the event building and tracking algorithm will be done on the second networking port on each processor card through a separate set of L1 switches. Following tracking, data is forwarded to a second L2 switch where it is forwarded to a one of more servers carrying performing data storage and online analysis.

Control Systems

Gretina will require two major control systems. The first is a standard slow control system for Gretina's electronic subsystems including the digitization modules, high-voltage power supplies and the LN filling system. It is required that the control system is scalable to 10^4 channels (10^3 ADC channels each with several parameters), operates across several platforms (embedded systems, Unix workstations) and provides a good operator interface. A unified control system that provides a consistent user interface to all detector subsystems is preferred. An example of such a system would be EPICs developed jointly by ANL and LANL. This system has been used successfully with Gammasphere and has been shown to scale to the required number of channels as demonstrated in several accelerator control systems.
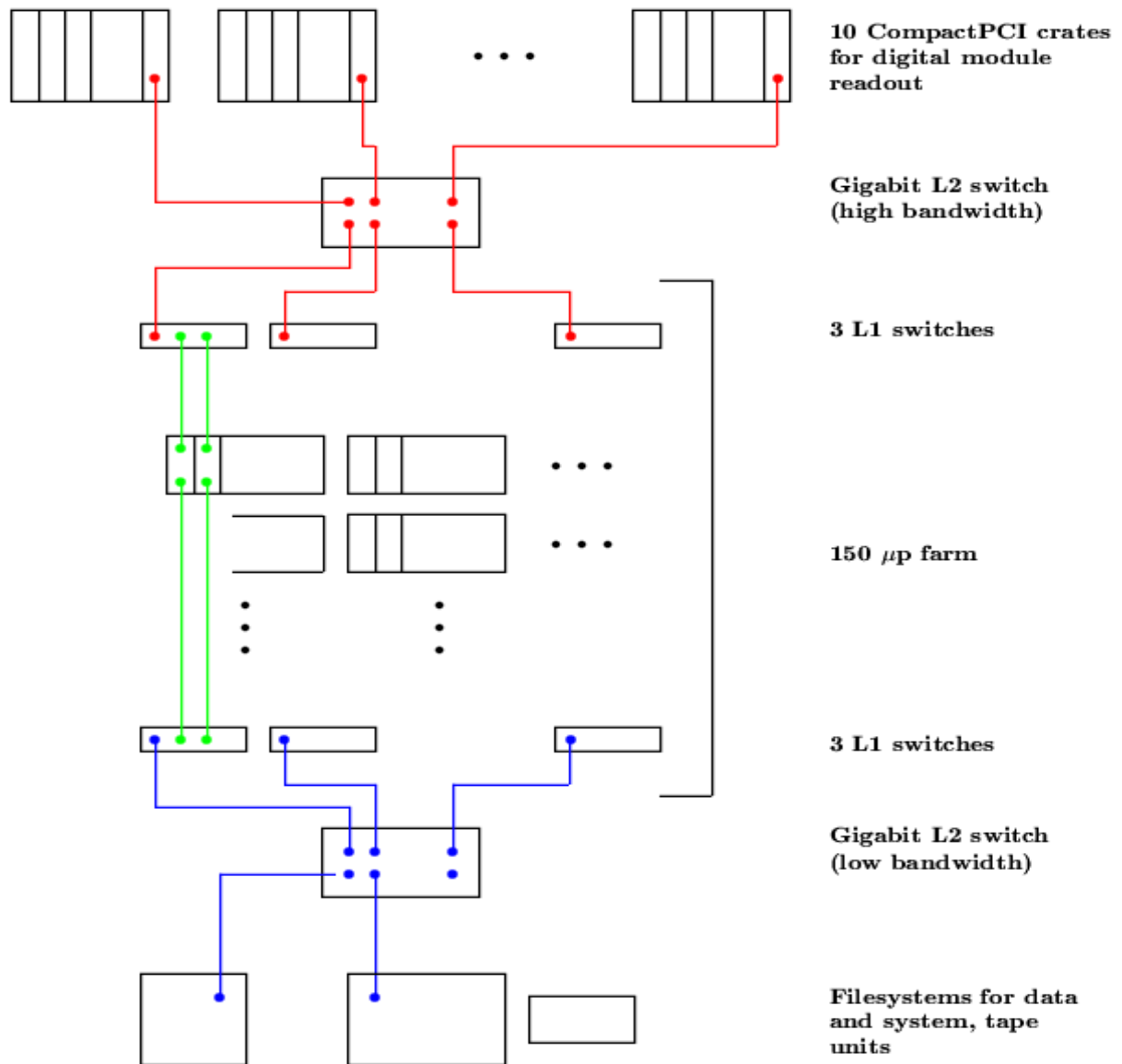
Figure 4.8. Schematic diagram of the computational hardware for Gretina

A second major control system is required for controlling the cluster of 150 CPU farm required for real-time signal analysis. Control software for large computational farms for functions such as partitioning, failover, and monitoring is rapidly evolving and we expect to use a commercial package for the control of the farm to increase reliability and reduce manpower requirements.

4.3. Gretina Mechanical System

4.3.1. Support structure for 3-Cluster detectors

The Gretina detector support system consists of a monolithic hemisphere that will have provision to mount 25 Gretina detector modules. The 48" diameter hemisphere will be custom machined from aluminum and will be approximately 2" thick and have precision features to accurately locate each detector module, thereby maintaining the absolute minimum clearances between the clusters. The detectors are electrically isolated from the hemisphere and from each other. The hemisphere is mounted to a custom, rigid, welded steel support structure. The support structure will allow the hemisphere to be installed orthogonal to the beam with the major axis of the hemisphere in the horizontal plane. The center of the hemisphere is coincident with the center of the target chamber. The support structure will be able to translate approximately 30" in the horizontal plane in a direction orthogonal to the beam, thus retracting the hemisphere to allow access to the target chamber. In addition, the support structure incorporates a mechanism that allows the hemisphere to rotate +/- 90 degrees to facilitate the installation or removal of detector modules. Depending upon the requirements of the specific application the primary support structure can also be used to mount the hemisphere with its major axis in the direction of the beam. The hemisphere with its complement of detector modules would then translate along the beam to allow access to the target chamber. Likewise, the hemisphere can be rotated +/- 90 degrees to install or remove detector modules. The requirements arising from different applications may warrant the fabrication of additional support structures incorporating unique features or capabilities to accommodate a specific application. Moreover, it may be advantageous to machine two different hemispheres for the two aforementioned applications. The hemisphere for fast beam experiments would mount detectors at forward angles and accommodate a 6 – 8 inch diameter beam pipe. Finally, consideration should be given to splitting the hemisphere into two segments or quarters. These quarter segments could be individually supported and mounted such that the major axis of the resultant hemisphere would be coincident with the beam. To access the target chamber, one or both of the segments could be retracted orthogonal to the beam.

4.3.2. Liquid nitrogen distribution

The Ge detectors will generally be maintained at liquid nitrogen temperature, except during shipment and repair. Gretina will comprise ten liquid nitrogen dewars, significantly fewer than Gammasphere. Each detector dewar will be periodically filled with liquid nitrogen using an automated system similar to that presently used for the ORNL CLARION array. It is essential that this system be highly reliable, and carefully interlocked with the temperature monitoring and high-voltage control system. Should a cluster of detectors warm significantly above liquid nitrogen temperatures while the detectors are biased the Field-Effect Transistors (FETs) of the preamplifiers are likely to be damaged necessitating a very costly repair.

The computer-controlled system will automatically initiate fill cycles at preset time intervals. Resistive temperature devices (RTDs) will be used to detect overflows of liquid nitrogen and thus determine that detectors have been successfully filled. The RTDs incorporated into the detector modules themselves will also be continually monitored; should a detector module begin to warm up, the bias voltages for those detectors will immediately shut off and an alarm generated. Alarms will also be generated as a result of unsuccessful fill cycles, and by non-nominal values of other monitored parameters (such as fill

line pressure, environmental temperatures, etc.) A watch-dog timer will be incorporated into the control system to generate an alarm, and could shut off voltages and disable fills should the monitor/control processor fail for any reason.

4.3.3. Target chamber

The target chamber consists of a 12" diameter aluminum sphere with a 0.065" thick wall. It will have the capability to mount internal auxiliary detector systems such as a smaller version of the Microball, a Si strip 4π detector system, etc. Easy access to such detector systems and suitable signal output paths will be included in the design. It should consist of a cylindrical vertical section enclosed by two near hemispheres. This provides large access paths to allow for the installation and maintenance of various targeting apparatus and auxiliary detector systems. It shall incorporate o-ring seals and will have 1-1/2" diameter opening at the upstream and downstream ports to accommodate the beam-tubes interface. A rigid arm, contained within a vertical plane coincident with the beam and occupying one of the pentagon vacancies, shall provide support for the hemisphere and targeting apparatus. The support arm could include a thru-vacuum linear actuator that would allow for target positioning or indexing without breaking vacuum.

4.4. Auxiliary Detector Systems in Gretina

Auxiliary detectors greatly increase the sensitivity of a gamma-ray detector array and will be an important addition to a gamma-ray tracking array. In this section we briefly describe several examples of auxiliary detectors that will be used with Gretina to address the physics discussed in Chapter 2. It is important that the mechanical design and data acquisition for Gretina do not preclude the efficient use of these auxiliary detectors.

4.4.1. Neutron detector shell
The existing shell of neutron detectors constructed at Washington University for Gammasphere is sufficient and should be used. It consists of up to 37 tapered hexagonal detectors that were designed to pack in a shell with an inner radius of 30 cm. For Gammasphere only 30 of these were used because it was not desirable to remove more than 30 Ge detector elements. For Gretina, one can place the detector modules at the backward angles and take advantage of a larger neutron-detection efficiency by using 48 neutron detectors (9 additional detectors are available at Washington University).

4.4.2 Charged-particle detector arrays

A high efficiency (4π) charged-particle array: For studies of the most neutron deficient nuclei it is essential that charged particle detectors have the maximum possible packing in 4π. Although the existing Microball detector could be reconfigured to fit in the Gretina scattering chamber, a significant improvement in energy resolution can be achieved by increasing the segmentation (number of CsI detectors per unit solid angle). This will define the recoil direction more accurately, and to a point where it does not compromise the excellent position resolution of Gretina (1-2 mm). It is suggested that a 4π device with 320 CsI detectors (named Nanoball) can satisfy this need and for some reactions it will

greatly improve the gamma-ray energy resolution. Table 4.4 gives the calculated resolving power for Gretina and Gretina+Nanoball in the reaction $^{24}Mg(^{24}Mg,2\alpha)^{40}Ca$. The uncertainty in the recoil direction due the emission of the two alpha particles results in poor gamma-ray energy resolution, which can be corrected using the charged-particle array. The resolution improves from ~55 keV to ~7 keV FWHM for a 3 MeV gamma-ray giving a large increase in resolving power. This new detector will also take advantage of digital processing to provide higher count rate capability.

Reaction	$<E_\gamma>$ (MeV)	v/c	M_γ	Relative Resolving Power	
				Gretina $\Delta E\gamma \sim 55$ keV	Gretina + Charged Particle Detector $\Delta E\gamma \sim 7$ keV
$^{24}Mg(^{24}Mg,2\alpha)^{40}Ca$	2.8	0.04	10	100	8×10^4

Table 4.4. Resolving power for Gretina and Gretina+Nanoball in the reaction $^{24}Mg(^{24}Mg,2\alpha)^{40}Ca$. The gain in resolving power is due to the improvement in the gamma-ray energy resolution from ~55 keV to ~7 keV for a 3 MeV gamma-ray. For comparison, Gammasphere's resolving power improves from 100 to 2.6×10^4 when coupled with Microball, for this reaction.

A high energy-resolution charged-particle array. Silicon-strip detectors are the appropriate devices for discrete line charged-particle spectroscopy. Given that the charged-particle energy resolution is very sensitive to the reaction kinematics, the target thickness, and the size of the beam spot on the target each particular class of experiments will likely need dedicated and perhaps perishable Silicon-strip detectors. Probably, this number will not exceed 1024. The readout of these devices will be done with the ASIC technology microchips, currently under development and production at Washington University.

4.4.3 Heavy ion detectors

A high-efficiency recoil detector: HERCULES (a High Efficiency Recoil Counter under Lots of Elastic Scattering) is ready for operation in conjunction with an array like Gretina. It has very high efficiency for (HI, αxn) reaction channels that are important for the very heavy systems. It is also conceivable to integrate HERCULES into a more complex and powerful setup, e.g. a combination coupling Gretina with a recoil separator and HERCULES.

A 4π position-sensitive parallel-plate heavy-ion detector: A new 4π position-sensitive parallel-plate heavy-ion detector like CHICO will be developed at Rochester for use with Gretina. It will have $\leq 1^o$ angular resolution in θ, φ, and 500ps time resolution providing 5% mass resolution for binary reactions. Like CHICO, this parallel-plate detector will have minimum mass to minimize degrading the performance of Gretina and it will handle high count rates plus intense heavy-ion fluxes with little radiation damage. It will detect products from binary reactions such as quasi-elastic scattering, fission etc, allowing complete kinematic reconstruction for each event, and enabling the simultaneous determination of the Q-value, masses, scattering angles θ, φ, and recoil velocities of the reaction products. When combined with Gretina, such a detector provides the capability for precise Doppler correction and simultaneous identification of the coincident de-excitation gamma-ray originating from each of the reaction products, as well as processes such as pre-fission gamma-ray decay.

5. MANAGEMENT ORGANIZATIONS

5.1. General

Gretina will be the premier national high-resolution gamma-ray detector array in the USA. Thus it is essential that the management plan encourages and facilitates involvement of all interested laboratories, university groups, and individuals in the design, construction and use of Gretina. This document provides the management organization for the Gretina project as defined for the research and development, plus construction phases. Specifically, the document defines the roles of the major project components: the Host Laboratory Management, the Management Advisory Committee, the Contract Project Manager, the Project Engineer, the Gretina Advisory Committee and the construction teams. The proposed plan closely follows the successful Gammasphere Management Plan. Figure 1 outlines the management structure proposed for the research and development, plus construction phases.
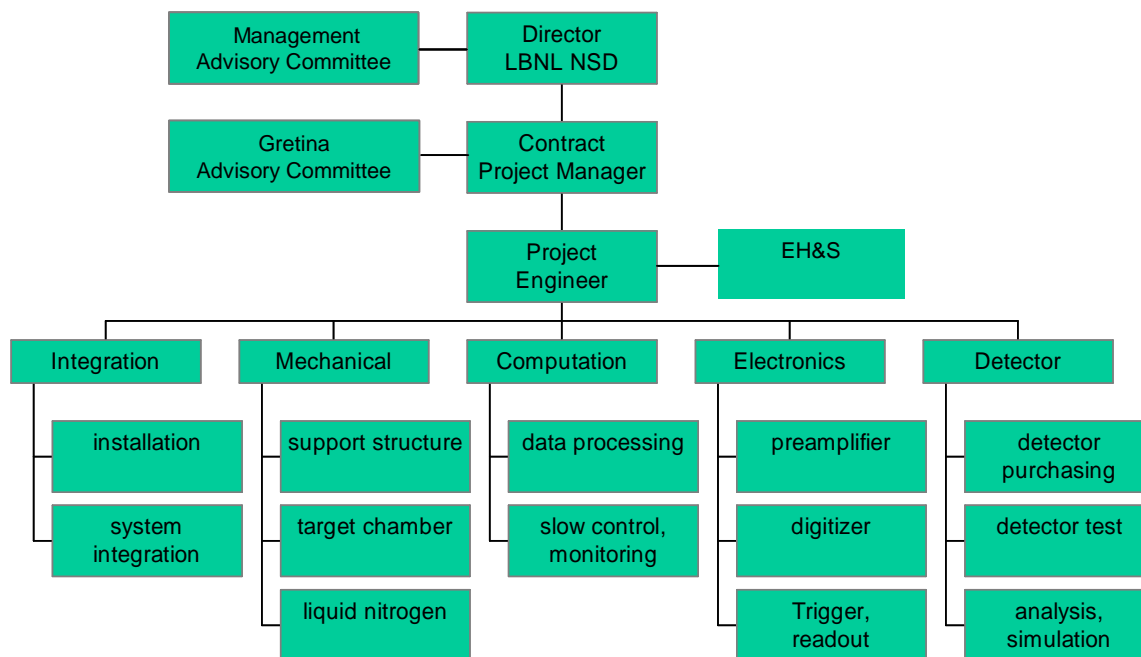
Figure 1.   Management Organization Chart for Construction of Gretina

5.2. Host Laboratory and Responsible Laboratory Management Official

Host Laboratory
The Host Laboratory is defined as the lead laboratory that is fully responsible for the construction of Gretina and assumes fiscal responsibility for the project. Lawrence Berkeley National Laboratory will be the Host Laboratory during the construction and commissioning phase of Gretina, and will be responsible for ensuring that the manpower and necessary infrastructure are provided for the R&D, construction, and commissioning of Gretina. The DOE office of NP is responsible for providing the funds to allow the host laboratory to fulfill its responsibilities. We expect semi-annual DOE review of the project

Responsible Laboratory Management Official
The Responsible Laboratory Management Official shall be the Director of the Nuclear Science Division of LBNL or a designate.

Responsibilities
- The Host Laboratory shall be administratively and fiscally responsible for the entire project. In particular it must provide the following:

- Provide overall management oversight for all aspects of the construction and commissioning phase of the project.

- Appoint the Contract Project Manager with the concurrence of the Gretina Advisory Committee.

- Approve personnel appointments made by the Contract Project Manager.

- Approve subcontracts recommended by the Contract Project Manager.

- Ensure that adequate staff and resources are available to complete the Gretina project in a timely and cost effective manner (within constraints of the budget provided by DOE).

- Set up external technical and project review committee.

- Ensure that Gretina is fully tested to demonstrate that it meets specifications, and that it is a reliable, and flexible system ready for installation at the first site.

- Provide documentation and access to information necessary for operation of Gretina at other sites.

5.3. Management Advisory Committee

Composition
The Management Advisory Committee shall be composed of the (Nuclear) Physics Division Directors of the DOE National Laboratories directly involved in the construction of Gretina (ANL, LBNL, and ORNL) or their designates, the Director of National Superconducting Cyclotron Laboratory at MSU or his designate, plus DOE representatives, and additional members if the existing members of Management Advisory Committee so choose. The LBNL NSD Division Director or his designate shall be the chairman.

Responsibilities

The Management Advisory Committee will serve as an oversight committee to the project. It will ensure that the different tasks of the project at the non-host sites are proceeding on schedule and on budget, as well as providing general oversight at the host site. It will arrange such reviews of the project, as it deems necessary to fulfill these responsibilities. It will be responsible for the appointment of the Gretina Advisory Committee.

5.4. Contract Project Manager

Appointment

The Contract Project Manager is to be appointed by the Responsible Laboratory Management Official with the concurrence of the Gretina Management Advisory Committee and the Gretina Advisory Committee.

Responsibilities

The Contract Project Manager shall report directly to the Responsible Laboratory Management Official and will be responsible for the overall direction of the Gretina Project. The Contract Project Manager shall appoint the staff needed for the project with the approval of the Responsible Laboratory Management Official and after discussion with the Gretina Advisory Committee. The Contract Project Manager also will have the following responsibilities:

- Shall be the spokesperson for the project to the DOE, the Host Laboratory, other participating institutions, and the scientific community.
- Appoint the Project Engineer in consultation with the Laboratory Management.
- Collaborate with the Gretina Advisory Committee and the Project Engineer to develop the performance requirements.
- Collaborate with the Responsible Laboratory Management Official and Project Engineer to develop the work plan, and assemble the staff and resources needed to complete the project.
- Oversee the design and verify that the design satisfies the performance requirements.
- Work with the Project Engineer to prepare a written design document for review by the Responsible Laboratory Management Official and the Gretina Advisory Committee. Written responses will be made to their recommendations. Major changes that affect the scientific capabilities of Gretina are to be made in concurrence with the Gretina Advisory Committee.
- Work with the Project Engineer to prepare for review by the external technical review committee, as well as DOE project review
- Recommend to the Responsible Laboratory Management Official, in consultation with the Project Engineer and the Gretina Advisory Committee, subcontractors for the construction teams.
- Organize workshops and arrange for a newsletter to keep the scientific (future user) community informed on the progress of the project.
- Consult regularly with the Gretina Advisory Committee on development of the project.
- Oversee the tests and commissioning to ensure that the system meets the performance requirements.
- Organize and coordinate the effort from other institutions participating in the project. Procedure for this will be discuss in the Management Plan.

5.5. Gretina Advisory Committee

The Gretina Advisory Committee represents the interests of the future Gretina community. Specifications for Gretina will be developed in concurrence between the Gretina Advisory Committee and the Contract Project Manager. The Gretina Advisory Committee will meet regularly with the Contract Project Manager, usually by phone conference, to discuss the scientific and technical issues. The Committee may meet by itself, or with consultants, if the occasion warrants. It may be consulted by the Management Advisory Committee on problems of review.

Composition
The Committee shall be composed of representatives from the three DOE national laboratories, ANL, LBNL, and ORNL, the NSCL at MSU (contingent upon these institutions continuing to play a major role in the Gretina project) and four university institutions engaged in Gretina. For reasons of continuity, the initial Committee will be the current Steering Committee. If necessary, replacement members will be appointed by the Host Laboratory Management subject to approval by the Management Advisory Committee. Efforts must be made to ensure that the composition of the Committee reflects the interests of the Gretina scientific community and no more than one member shall be from any one institution. The Contract Project Manager formally is not a member of the Advisory Committee but normally he will participate in Advisory Committee activities. The Committee shall elect its own chairman annually.

Responsibilities
- Discuss scientific and technical issues with the Contract Project Manager.
- Provide a mechanism for representation of the participants in the project.
- Concur with or voice concerns about the selection of the Contract Project Manager made by the Laboratory Management.
- Advise the Contract Project Manager on selection of personnel for the construction teams.
- Advise the Contract Project Manager on the selection of non-host-site construction teams, and of possible sub-contractors for approval by the Laboratory Management.
- Apprise Laboratory Management if there are major unresolved areas of concern.
- Maintain the Gretina Users Group and facilitate communication between the Project Management and the Users Group.

5.6. Project Engineer

The Project Engineer will have the responsibility for delivering the Gretina detector system in accordance with the performance requirements, schedule, and budget. The Project Engineer will report to and work closely with the Contract Project Manager. Together they will develop the work plan of the project.

Responsibility
- Collaborate with the Contract Project Manager and subsystem managers to prepare the work plan, and assemble the staff and resources needed to complete the project.
- Communicate the project requirements to the subsystem managers.
- Supervise the staff of the project.
- Ensure all subsystems function in a coherent system, and meet performance requirements.

- Execute the work plan in accordance with the scope, schedule and budget of the project.
- Set up guidelines for changes in scope, schedule, and budget, including the rules for releasing the contingency funds.
- Coordinate preparation of regular reports and project reviews as required by DOE, LBNL and other organizations.
- Ensure the work is performed safely and in compliance with LBNL and DOE regulations.

5.7. Subsystem Managers

Five subsystem managers are responsible for each of the five subsystems of Gretina, which are detector, electronics, computation, mechanical, and integration. They report to the Project Engineer and will be responsible for the design, construction, installation, and commissioning of the subsystem, in accordance with the performance requirements, schedule, and budget.

Responsibility
- Collaborate with the Project Engineer to development the work plan, and assemble the staff and resources needed to complete the subsystem.
- Communicate the subsystem requirements to the teams of staff.
- Ensure the subsystem meets the performance requirements.
- Execute the subsystem work plan in a manner consistent with the project scope, schedule and budget.
- Provide regular report of the status of the subsystem to the Project Engineer.
- Ensure the work is performed safely and in compliance with LBNL and DOE regulations.

5.8. Gretina User Group

The Gretina User's Group has been established by the Gretina Steering Committee. Membership is open to any interested scientist.

5.9. Operation Phase

GRETINA will be a national instrument, moveable between several major accelerators in the US and available to the entire nuclear science community, in order to capitalize on the broad variety of scientific opportunities this significant detector system can bring. Upon delivery of Gretina (initially from LBNL) to a new location then the site laboratory will assume the responsibility of being the Host Laboratory. As has proved successful with Gammasphere, the specific order of rotation and duration at any particular laboratory will be based on scientific merit and will be decided at the appropriate time by the community of users and funding agencies. Details of the operational management should be developed during the construction phase by the Laboratory Management, the Management Advisory Committee, Contract Project Manager, and the Gretina Advisory Committee.

References

[Ag03] "AGATA Technical Proposal", ftp://ftp.gsi.de/pub/agata/prop/Agata-pub-proposal.pdf

[Au00] T.Aumann, et al., Phys. Rev. Lett. **84, 35** (2000).

[Au99] T. Aumann, et al., Nucl. Phys. A **649,** 297c (1999)

[Be89] J. R. Beene, et al., Phys. Rev. C **39**, 1307 (1989).

[Br75] F. Briggs et al., Atomic Data Nuclear Data Tables **16**, 201 (1975).

[De99] M.A. Deleplanque et al., Nucl. Instr. and Meth. A **430**, 292 (1999).

[Do96] J. Dobaczewski et al., Phys. Rev. C **53** 2809 (1996)

[En02] J. Enders, et al., Phys. Rev. C**65** 034318 (2002).

[Gl97] T. Glasmacher, et al., Phys. Lett. B **395** 163 (1997).

[Gl98] T. Glasmacher, Ann. Rev. Nucl. Part. Sci. **48**, 1 (1998).

[GRTCC02] "A National Plan for Development of Gamma-Ray Tracking Detectors in Nuclear Science", Gamma-Ray Tracking Coordinating Committee (GRTCC), July 2002, http://www.pas.rochester.edu/~cline/GRTCC-report.pdf

[Ha01] P. G. Hansen and B. M. Sherrill, Nucl. Phys. A 693, 133 (2001). P.G. Hansen and J.A. Tostevin, Ann. Rev. Nucl. Part. Sci., **53** (2003) in print.

[Ho89] P. Hoff,. et al., Z. Phys., A **322**, 407 (1989).

[Ku02] "Advanced Pulse-Shape Analysis and Implementation of Gamma-ray Tracking in a Position Sensitive HpGe Detector", A. Kuhn PhD Thesis, UC Berkeley, LBL publication 51726

[LRP02] "The 2002 NSAC Long Range Plan". http://www.er.doe.gov/production/henp/np/nsac/LRP_5547_FINAL.pdf

[Ma01] V. Maddalena, et al., Phys. Rev. **C 63** 024613 (2001).

[Mi83] D.J. Millener, J.W. Olness, E.K. Warburton, S.S. Hanna, Phys. Rev. C **28** (1983) 497.

[Mo95] T. Motobayashi et al., Phys. Lett. B **346** 9 (1995).

[Mu76] T. Mukoyama, Nucl. Instr. and Meth. A **134** 125 (1976).

[Mu01] W.F. Mueller et al., Nucl. Instr. Meth. A **466** 492 (2001).

[Na00] A. Navin, et al., Phys. Rev. Lett. **85** 266 (2000)

[Ol03] H. Olliver, T. Glasmacher, A. Stuchbery, submitted to Phys. Rev. **C** (2003)

[Pr01] B.V. Pritychenko, et al., Phys. Rev. **C 63** 011305(R) (2001).

[Ra01] S. Raman, C.W. Nestor, and P. Tikkanen, Atomic Data and Nuclear Data Tables, **78**, 1 (2001).

[Ra02] D.C. Radford et al., Phys. Rev. Lett., **88**, 222501 (2002).

[Ra39] S. Ramo, Proc. IRE **27**, 584 (1939).

[Re99] P. Reiter et. al. Phys. Rev. Lett. **82**, 509 (1999), Phys. Rev. Lett. **84**, 3542 (2000).

[Bu02] P.A. Butler et al., Phys. Rev. Lett. **89**, 202501 (2002)

[He02] R.D. Herzberg et al., Phys. Rev. **C 65**, 014303, (2002).

[Le99] M. Leino et al., Eur. Phys. J. A **6,** 63, (1999)

[Ca98] F. Camera, et al., Eur. Phys. J. A **2**, 1 (1998)

[Sc99a] G.J. Schmid et al., Nucl. Instr. and Meth. A **430** 69 (1999) .

[Sc99b] G.J. Schmid et al.,Nucl. Instr. and Meth. A **422** 368 (1999).

[Va99] R. L. Varner, et al., Proceedings of the International Workshop on Collective Excitations in Fermi and Bose Systems, edited by C. Bertulani, World Scientific p.264 (1999).

[Ve00a] K. Vetter et al., Nucl. Instr. and Meth. A **452** 105 (2000).

[Ve00b] K. Vetter et al., Nucl. Instr. and Meth. A **452** 223 (2000).

[Yo01] K. Yoneda et al, Physics Letters B **499**, 233 (2001).

APPENDIX A: Principles of Gamma-ray Tracking.

Localizing the Interaction Point(s)

Tracking relies on the ability to accurately locate the individual gamma-ray interactions and to disentangle "tracks" belonging to different gamma-rays. This requires a three-dimensional position resolution of 1-2 mm. Currently, it is not possible to produce detectors with a pixelation of 1 mm x 1mm x 1mm to achieve this resolution. Instead, by using induced signals and charge drift time, it is possible to achieve this position resolution with a two-dimensional segmented detector having a segment size of 1-2 cm.

In a Ge detector, charge signals are produced when electrons and holes (charge carriers), formed by the slowing down of the primary electrons (from e.g., photo- or Compton-event) and positrons (from pair-production), induce an image charge on the electrodes. Only the segment that is reached by the charge carriers has a net charge. All other segments exhibit transient image signals, which vanish when the charge carriers are collected. These transient pulses can be either positive of negative. The size and shape of the induced transient pulses are sensitive to the distance between the charge carriers and the segments. Since the two-dimensional segmentation is perpendicular to the radial electric field lines (approximately the direction of drift velocity), position in these two transverse dimensions (e.g. the length, z, and azimuthal angle, ϕ) can be obtained. The radial component (r) of the position will be derived from the drift time of charges.

The Tracking Principle

The combination of segmentation and pulse-shape analysis provides the energies and positions of the multiple gamma-ray interaction points. Tracking algorithms are then used to identify and separate individual gamma rays, to reconstruct their full energy, and to determine the time sequence of the interactions. The principle of tracking is based on the physics of gamma-ray interactions (i.e., the photo absorption, the Compton scattering, and the pair-production). The absorption of a γ ray in matter is a statistical process, which usually consists of several individual interaction steps, often several centimeter apart, depending on the initial γ-ray energy. At each interaction point, part of the gamma-ray energy is transferred to the detector. For a fully absorbed gamma ray, the last interaction is a photo absorption event. The goal of tracking is to identify the interaction points that belong to the same γ-event and to reconstruct their scattering sequence.

Compton scattering

Compton scattering is the scattering of photons from electrons. It is the predominant interaction mechanism between ~200 keV and 5-6 MeV. As sketched below, the incoming γ ray transfers a fraction of its initial energy to a electron, which is ejected by the atom (recoil electron), and the scattered γ ray is

deflected through an angle θ that ranges between 0° and 180°. Assuming that at the instant of scattering the electron is unbound and at rest, the energy of the scattered photon, $E_{\gamma'}$, is derivable from energy and momentum conservation,

$$E_{\gamma'} = \frac{E_\gamma}{1 + \frac{E_\gamma}{mc^2}(1 - \cos\theta)} \qquad (1)$$

where m_0c^2 is the rest-mass energy of the electron (511 keV). The energy ranges from E_γ to a minimum value of approximately $m_0c^2/2$. If the energies E_γ and $E_{\gamma'}$ are measured, the scattering angle can be calculated from eq. (1).

If, the positions of the gamma-ray interaction points are known, the scattering angle θ^C can be obtained from the coordinates of the three points involved (as illustrated below):

$$\cos\theta^C = \frac{\vec{p}_\gamma \cdot \vec{p}_{\gamma'}}{|\vec{p}_\gamma||\vec{p}_{\gamma'}|} \qquad (2)$$

Equations (1) and (2) are the foundations of the tracking concept, since they provide two independent determinations of the angle involved in the same scattering process. For a correct Compton scattering event, they should have the same value.
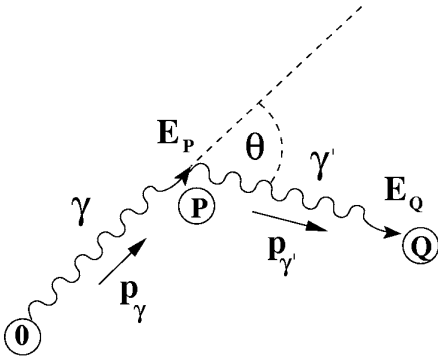
By comparing the two values of the angle at each of the interaction points the correct scattering sequence can be determined. For a gamma ray with N interaction points, there are N! possible scattering sequences. The most likely scattering sequence is determined by means of a least-squares minimization of the angle differences. To check the validity of a given interaction sequence, we calculate the quantity

$$\chi^2 = \sum_{n=1}^{N-1} \left(\frac{\theta - \theta^C}{\sigma_\theta}\right)^2 \qquad (3)$$

where σ_ϑ is the uncertainty of the angle measurement which takes into account the uncertainty of the position determination and the distance traveled by the γ ray between the two points. The calculation starts at the first interaction point, assuming the gamma ray is emitted at the target position, and the gamma ray energy is the sum of energy deposited at all the interaction points (a peak event). The sum includes all the vertices, up to the last Compton scattering point. Ideally, among the N! possible permutations of the points, the correct sequence, whose energies add to a peak event, should have a zero value of χ^2. In practice, due to the finite energy and position resolution of the detector, the χ^2 is finite even for the correct sequence. This represents an unavoidable limitation to the reconstruction efficiency of the tracking algorithm. Since the absolute value of χ^2 does not carry any physical meaning, an acceptance threshold on its distribution is set depending on the quality of the reconstructed spectra. The reconstruction efficiency of a tracking algorithm at a given γ-ray energy is measured as a percentage of correctly identified events, i.e. those in the photopeak. Typically, a higher χ^2 threshold would give higher efficiency to the detriment of the peak-to-total. The reconstruction efficiency of tracking algorithm strongly depends on the position resolution; for efficient γ-ray tracking algorithms a position resolution of ~1-2 mm is required

Pair production

For gamma-ray energies above a few MeV (threshold energy equal to $2m_0c^2$) pair production can occur. This process is characterized by the disappearance of the photon in the Coulomb field of the nucleus and by the creation of an electron-positron pair. Pair production events are easily recognized from their characteristic signature: a point with energy E_γ-1.022 MeV and two 0.511 MeV γ rays emitted back-to-back. The tracking of the 0.511 MeV gamma rays is the same as the Compton event discussed above.

APPENDIX B. Expected Gretina Performance

Detector module	
Number of Ge crystal	30
Size of Ge crystal	8 cm Dia x 9 cm L (before shaping)
Number of segments	6 x 6
Energy resolution[1]	2.1 keV average, 2.3 keV max. at 1.33 MeV 1.15 keV average, 1.4 keV max. at 0.122 MeV
Time resolution	~ 7 nsec at 1.33 MeV
Array peak efficiency[2]	~ 8.3% at 1.33 MeV
Array peak-to-total ratio[2]	~ 46% at 1.33 MeV
Support structure	
Distance from target to Ge crystal	15 cm
Translation range	30 inches
Rotation range	±90°
Target Chamber	
Target positioning	Remote
Accommodate auxiliary detectors	
Signal Digitizer	
Sampling rate	80-100 MHz
Resolution	14 bits
Integral nonlinearity in energy	0.1%
Differential nonlinearity in energy	1%
Output	ID, Energy, LE time, CFD time, signal trace
Trigger and Readout	
Readout speed	10 MB/s/crystal
Accommodate auxiliary detectors	
Computation	
Data processing rate	25,000 gamma/s
Data storage rate	10 MB/s
Performance[3]	
Position resolution	1-2 mm
Efficiency[4]	6.2% at 1.33 MeV
Peak-to-total	60% at 1.33 MeV

[1] Based on manufacturer agreed prototype specification
[2] For other energies see Figure 4.5
[3] Based on existing algorithms
[4] With signal decomposition efficiency of 85%, and tracking efficiency of 88%

APPENDIX F: Working Groups

Software Working Group			
Appelbe	Duncan E	d.appelbe@dl.ac.uk	CLRC Daresbury Lab
Beyer	C.J.	cj@tempusmud.com	Vanderbilt
Carpenter	Mike	carpente@sun0.phy.anl.gov	Argonne National Laboratory
Chowdhury	Partha	Partha_Chowdhury@uml.edu	Univ. Massachusetts Lowell
Cromaz*	**Mario**	MCromaz@lbl.gov	Lawrence Berkeley National Laboratory
Daniel	Andrei	daniel@jinr.ru	Joint Institute for Nuclear Research
Kulp	Wm. David	david@nuclear.physics.gatech.edu	Georgia Institute of Technology
Lauritsen	Torben	torben@anl.gov	Argonne National Laboratory
Lee	I-Yang	iylee@lbl.gov	Lawrence Berkeley National Laboratory
Nyberg	Johan	nyberg@tsl.uu.se	Uppsala University
Radford	David	radfordD@mail.phy.ornl.gov	Oak Ridge National Laboratory
Rainovski	Georgi I.	rig@ns.ph.liv.ac.uk	The University of Liverpool
Smith	John F.	jfs@mags.ph.man.ac.uk	University of Manchester
Starosta	Kris	Starosta@nuclear.physics.sunysb.edu	SUNY at Stony Brook
Tabor	Samuel L	tabor@nucmar.physics.fsu.edu	Florida State University
Vetter	Kai	kvetter@llnl.gov	LLNL

Physics Working Group			
Baktash	Cyrus	baktashc@ornl.gov	Oak Ridge National Laboratory
Beene	Jim	BEENE@orph01.phy.ornl.gov	Oak Ridge National Laboratory
Bernstein	Lee A	bernstein2@llnl.gov	LLNL
Beyer	C.J.	cj@tempusmud.com	Vanderbilt
Calderin	Ivo J.	calderin@nucmar.physics.fsu.edu	Florida State University
Carpenter	Mike	carpente@sun0.phy.anl.gov	Argonne National Laboratory
Casten	Richard	rick@riviera.physics.yale.edu	Yale
Chapman	Robert	chap-ph0@wpmail.paisley.ac.uk	University of Paisley
Cline	Doug	cline@nsrl.rochester.edu	Univ. of Rochester
Cullen	David	dmc@mags.ph.man.ac.uk	University of Manchester
Daniel	Andrei	daniel@jinr.ru	Joint Institute for Nuclear Research
Fallon	Paul	PFallon@lbl.gov	Lawrence Berkeley National Laboratory
Fossan	David B.	david.fossan@sunysb.edu	SUNY at Stony Brook
Freedman	Stuart	Stuart J Freedman	Lawrence Berkeley National Laboratory
Garg	Umesh	garg@nd.edu	University of Notre dame
Glasmacher	Thomas	glasmacher@nscl.msu.edu	MSU
Greene	John P.	greene@anl.gov	Argonne National Laboratory
Hammond	Neil J	hammond@phy.anl.gov	Argonne National Laboratory
Kaye	Robert A.	kaye@calumet.purdue.edu	Purdue University Calumet
Khoo	Teng Lek	khoo@anl.gov	Argonne National Lab
Kondev	Filip G	kondev@anl.gov	Argonne National Laboratory
Labiche	Marc	labi-ph0@paisley.ac.uk	University of Paisley
Lister	Kim	Lister@anlphy.phy.anl.gov	Argonne National Laboratory
Ma	Wenchao	mawc@ra.msstate.edu	Mississippi State University
Macchiavelli	Augusto	AOMacchiavelli@lbl.gov	Lawrence Berkeley National Lab
Nazarewicz	Witold	witek@utk.edu	UT/ORNL
Nolan	Paul J	nolan@ns.ph.liv.ac.uk	University Of Liverpool
Nyberg	Johan	nyberg@tsl.uu.se	Uppsala University
Rainovski	Georgi I.	rig@ns.ph.liv.ac.uk	The University of Liverpool

Regan	Patrick H	p.regan@surrey.ac.uk	University of Surrey
Riley*	**Mark**	mriley@nucmar.physics.fsu.edu	Florida State University
Roux	David G	roux@ph.msstate.edu	Mississippi State University
Shengjiang	Zhu	zhushj@mail.tsinghua.edu.cn	Tsinghua University
Simpson	John	j.simpson@dl.ac.uk	Daresbury Laboratory
Smith	John F.	jfs@mags.ph.man.ac.uk	University of Manchester
Stuchbery	Andrew E	stuchbery@nscl.msu.edu	Australian National University
Tandel	Sujit	sujit_tandel@uml.edu	University of Massachusetts
Wang	Xiaofeng	xwang3@nd.edu	University of Notre Dame
Ward	David	dward@lbl.gov	Lawrence Berkeley National Lab
Wiedenhoever	Ingo	iwiedenhover@physics.fsu.edu	Florida State University
Wood	John L.	jw20@prism.gatech.edu	Georgia Institute of Technology
Wyss	Ramon	wyss@nuclear.kth.se	KTH
Yu	Chang-Hong	chy@mail.phy.ornl.gov	Oak Ridge National Laboratory

Detector Working Group

Beausang	Con	cwb@galileo.physics.yale.edu	Yale University
Cline	Doug	cline@nsrl.rochester.edu	Univ. of Rochester
Cullen	David M.	dmc@mags.ph.man.ac.uk	University of Manchester
Glasmacher	Thomas	glasmacher@nscl.msu.edu	MSU
Khoo	Teng Lek	khoo@anl.gov	Argonne National Laboratory
Kondev	Filip G	kondev@anl.gov	Argonne National Laboratory
Kreiner	Andrs J.	kreiner@tandar.cnea.gov.ar	CNEA-UNSAM
Lee	I-Yang	iylee@lbl.gov	Lawrence Berkeley National Laboratory
Lister	Kim	Lister@anlphy.phy.anl.gov	Argonne National Laboratory
Macchiavelli*	**Augusto**	AOMacchiavelli@lbl.gov	Lawrence Berkeley National Lab
Nolan	Paul J	nolan@ns.ph.liv.ac.uk	University Of Liverpool
Nyberg	Johan	nyberg@tsl.uu.se	Uppsala University
Phlips	Bernard	phlips@osse.nrl.navy.mil	NRL
Podolyak	Zsolt	Z.Podolyak@surrey.ac.uk	University of Surrey
Radford	David	radfordD@mail.phy.ornl.gov	Oak Ridge National Laboratory
Regan	Patrick H	p.regan@surrey.ac.uk	University of Surrey U.K.
Simpson	John	j.simpson@dl.ac.uk	Daresbury Laboratory
Vetter	Kai	kvetter@llnl.gov	LLNL

Auxiliary Detector Working Group

Baktash	Cyrus	baktashc@ornl.gov	Oak Ridge National Laboratory
Bernstein	Lee A	bernstein2@llnl.gov	LLNL
Cline	Doug	cline@nsrl.rochester.edu	Univ. of Rochester
Galindo-Uribarri	Alfredo	uribarri@mail.phy.ornl.gov	Oak Ridge National Laboratory
Garg	Umesh	garg@nd.edu	University of Notre Dame
Macchiavelli	Augusto	AOMacchiavelli@lbl.gov	Lawrence Berkeley National Lab
Nyberg	Johan	nyberg@tsl.uu.se	Uppsala University
Reviol	Walter	reviol@wuchem.wustl.edu	Washington University
Sarantites*	**Demetrios**	dgs@wuchem.wustl.edu	Washington University
Shapira	Dan	shapira@lbl.gov	Oak Ridge National Laboratory
Skulski	Wojtek	skulski@pas.rochester.edu	Univ. of Rochester
Wu	Ching-Yen	Wu@NSRL.rochester.edu	University of Rochester

Electronics Working Group

Beyer	C.J.	cj@tempusmud.com	Vanderbilt

Cline	Doug	cline@nsrl.rochester.edu	Univ. of Rochester
Devlin	Matt	devlin@lanl.gov	LANL
Garrett	Paul E.	pgarrett@llnl.gov	LLNL
Glasmacher	Thomas	glasmacher@nscl.msu.edu	Michigan State University
Macchiavelli	Augusto	AOMacchiavelli@lbl.gov	Lawrence Berkeley National Lab
Maier	Michael R	mrmaier@lbl.gov	Lawrence Berkeley National Lab
Naday	Steve	snaday@anl.gov	Argonne National Laboratory
Ngijoi	Emmanuel	Emmanuel_Ngijoi-Yogo@student.uml.edu	UMass Lowell
Nyberg	Johan	nyberg@tsl.uu.se	Uppsala University
Pauly	Steven W.	spauly@ris-corp.com	RIS Corp.
Radford*	**David**	radfordD@mail.phy.ornl.gov	Oak Ridge National Laboratory
Skulski	Wojtek	skulski@pas.rochester.edu	Univ. of Rochester
Vetter	Kai	kvetter@llnl.gov	LLNL
Weizeorick	John	jtweizeorick@anl.gov	Argonne National Laboratory
Wiedenhoever	Ingo	iwiedenhover@physics.fsu.edu	Florida State University

* Chair of working group